Contents lists available at ScienceDirect

Chemical Engineering Research and Design

journal homepage: www.elsevier.com/locate/cherd

Bubble column reactors for high pressures and high temperatures operation

C. Leonard[a,b], J.-H. Ferrasse[a,*], O. Boutin[a], S. Lefevre[b], A. Viand[b]

[a] Aix-Marseille Université, CNRS, Centrale Marseille; M2P2 UMR 7340, 13541, Marseille, France
[b] S.A.R.L A3I, 255, rue Gustave Eiffel, ZAC des Eoliennes, 26290, Donzere, France

ARTICLE INFO

Article history:
Received 1 December 2014
Received in revised form 14 April 2015
Accepted 10 May 2015
Available online 16 May 2015

Keywords:
Bubble columns
Gas holdup
Volumetric mass transfer coefficient
Axial dispersion coefficient
Interfacial area
Flow regimes

ABSTRACT

Bubble column reactors are multiphase contactors based on the dispersion of a gas phase in the form of bubbles inside a cylindrical vessel where a liquid or a suspension circulates. Those reactors present many advantages such as good heat and mass transfer rates, no moving parts, compactness, easy operating and low maintenance and operating costs. Their main drawback is the significant backmixing which can affect selectivity and conversion of reaction products. They have gained particular attention in the field of wastewater treatment for Wet Air Oxidation (WAO) processes application. Those processes are operated at high pressures (up to 30 MPa) and temperatures (up to 573 K). In order to efficiently operate those processes, conversion, heat and mass transfer must be optimised. Those parameters depend themselves on operating conditions such as pressure, temperature, superficial gas and liquid velocities and on design parameters such as sparger and column design. This review is aimed to find the relevant parameters for operating bubble column at high pressures and temperatures in continuous mode. The main mechanisms governing the bubble column will be described. The influence of the different parameters on gas holdup, mass transfer properties and on liquid axial dispersion coefficient will be extensively studied.

Contents

* Corresponding author. Tel.: +33 442908505; fax: +33442908515.
E-mail address: jean-henry.ferrasse@univ-amu.fr (J.-H. Ferrasse).
http://dx.doi.org/10.1016/j.cherd.2015.05.013
0263-8762/

1. Introduction

Bubble column reactors are multiphase gas–liquid–solid contactors in which the dispersed phase is a gas and the continuous phase is a liquid or a suspension. The gas phase is dispersed into the liquid or suspension in the form of bubbles by means of a gas sparger generally placed at the bottom of the column. The column can be designed to work in semi-batch mode (batch for liquid) or in continuous mode. Few studies deal with co-current bubble columns (Biń et al., 2001; Chaumat et al., 2005; Choi and Wiesmann, 2004; De Bruijn et al., 1988; Fukuma et al., 1987; Gopal and Sharma, 1983; Holcombe et al., 1983; Ishibashi et al., 2001; Jin et al., 2007b; Kumar et al., 2012a,b; Majumder et al., 2006; Muroyama et al., 2013; Onozaki et al., 2000; Pjontek et al., 2014; Pohorecki et al., 1999; Pohorecki et al., 2001; Sangnimnuan et al., 1984; Shawaqfeh, 2003; Simonnet et al., 2007; Tarmy et al., 1984; Voyer and Miller, 1968; Yang and Fan, 2003) and fewer with counter-current bubble columns (Biń et al., 2001; Hikita et al., 1981; Jin et al., 2010; Maalej et al., 2003; Shah et al., 2012; Smith et al., 1996; Stegeman et al., 1996).

Bubble column reactors are generally used as reactors in chemical, biochemical, petroleum and metallurgical industries. In particular, among the different types of chemical reactions, oxidation, chlorination, alkylation, polymerisation, esterification (see Stacy et al., 2014 for a recent application) and hydrogenation can be implemented in bubble columns. They can also be used to operate other processes such as gas conversion to produce fuels or fermentation and biological wastewater treatment in the field of biochemical processes. The Fischer–Tropsch synthesis, which is the coal liquefaction to produce fuels, is carried on bubble columns and is widely studied in the literature (Behkish et al., 2002; Deckwer et al., 1980; Gandhi et al., 1999; Hulet et al., 2009; Krishna and Sie, 2000).

Among the different processes that can be operated in bubble columns, Wet Air Oxidation (WAO) has received particular interest in the field of wastewater treatment (Boutin et al., 2011; Debellefontaine et al., 1996; García-Molina et al., 2007; Kolaczkowski et al., 1999; Lefèvre, 2010; Lefèvre et al., 2011). This process is aimed to treat wastewater (organic effluents, sludge from wastewater treatment plant...) by putting it in contact with an oxidizer (such as oxygen). The process can be catalysed or not. WAO processes are operated to work at high pressures and high temperatures. Pressure conditions are typically set between 2 and 18 MPa for catalysed processes and between 2 and 30 MPa for non-catalyzed processes. Temperature conditions are generally set between 373 and 593 K. Working at those conditions is necessary to increase partial pressure and solubility of oxygen in the liquid phase and increase the kinetic rate of the oxidation reaction. Those WAO processes are typically operated in bubble columns as it provides a high liquid holdup necessary to achieve high mass transfer efficiency for slow reactions.

Several parameters influence the operating of bubble columns. Among them, it can be distinguished between operating parameters such as gas–liquid system studied, pressure, temperature, gas and liquid superficial velocities, operating mode (semi-batch, co-current or counter-current) and design parameters: column height and diameter and sparger design. Many studies focus on the effect of several of these parameters on the performance of the bubble column in terms of heat transfer, mass transfer (Table 1), gas holdup (Table 1) or bubble diameter (Table 1) and on the flow regimes (Chilekar, 2007, 2010; Cui, 2005; Gourich et al., 2006; Grover et al., 1986; Hashemi et al., 2009; Jin et al., 2007b; Kang et al., 2000; Kemoun et al., 2001; Krishna et al., 1994, 2000; Krishna et al., 1991; Letzel et al., 1997; Lin et al., 2001; Passos et al., 2015; Reilly et al., 1994; Ruzicka et al., 2001; Şal et al., 2013; Shaikh and Al-Dahhan, 2005; Tarmy et al., 1984; Thorat and Joshi, 2004; Vial

Table 1 – Literature database for the bubble column parametric study.

Authors	System studied	Conditions	Gas sparger	Column design	Parameters studied	Working mode	Available correlation(s)
Akita and Yoshida (1973)	**Gas** : Air, O_2 ; **Liquid** : Water, Glycol, Methanol, Glycerol, Aqueous solution of Na_2SO_3, CCl_4 ; **Solid** : none	**P** : 0.1 MPa ; **T** : 283-313 K; u_G : 0.004 - 0.3 $m.s^{-1}$; u_L : 0 $m.s^{-1}$; **Cv** : 0%	Perforated plate, Porous plate, Single orifice-nozzle	H_C: 2.5 m; **Dc** : 0.077, 0.15, 0.3 m	ε_G, k_La	SB	$\frac{k_L a D_C^2}{D_{m,i,j}} = 0.6\left(\frac{\vartheta_L}{D_{m,i,j}}\right)^{1/2}\left(\frac{gD_C^2\rho_L}{\sigma_L}\right)^{0.62}\left(\frac{gD_C^3}{\vartheta_L^2}\right)^{0.31}\varepsilon_G^{1.1}$
Akita and Yoshida (1974)	**Gas** : Air, O_2 ; **Liquid** : Water, Glycol, Methanol, Glycerol, Aqueous solution of Na_2SO_3, CCl_4 ; **Solid** : none	**P** : 0.1 MPa ; **T** : 283-313 K; u_G : 0.004 - 0.3 $m.s^{-1}$; u_L : 0 $m.s^{-1}$; **Cv** : 0%	Perforated plate, Porous plate, Single orifice-nozzle	H_C: 2.5 m; **Dc** : 0.077, 0.15, 0.3 m	d_B, a, k_La	SB	$\frac{\varepsilon_G}{(1-\varepsilon_G)^4} = \beta\left(\frac{gD_C^2\rho_L}{\sigma_L}\right)^{\frac{1}{8}}\left(\frac{gD_C^3}{\vartheta_L^2}\right)^{\frac{1}{12}}\left(\frac{u_G}{\sqrt{gD_C}}\right)$ $\beta = 0.2$ *for pure liquids, 0.25 for salt solutions*
Baz-Rodriguez et al. (2014)	**Gas** : Air ; **Liquid** : Water, Aqueous solutions of salts (NaCl, $CaCl_2$, $MgCl_2$) ; **Solid** : none	**P** : 0.1 MPa ; **T** : 303 K; u_G : 0.0005 - 0.0197 $m.s^{-1}$; u_L : 0 $m.s^{-1}$; C_v : 0%	Porous plate (d_0 = 160-250 µm)	H_C: 1.2 m; **Dc** : 0.095 m	ε_G, d_B, k_L, a, k_La	SB	None
Behkish et al. (2002)	**Gas** : H_2, CO, N_2, CH_4 ; **Liquid** : Isopar-M, Hexanes mixture ; **Solid** : Iron oxides, glass beads	**P** : 0.17 - 0.8 MPa ; **T** : 298 K; u_G : 0.08 - 0.2 $m.s^{-1}$; u_L : 0 $m.s^{-1}$; **Cv** : 0 - 36%	Unknown	H_C: 2.8 m; **Dc** : 0.316 m	ε_G, d_B, k_La	SB	$k_La = 0.18\left(\frac{\vartheta_L}{D_{m,i,j}}\right)^{-0.6}\left(\frac{\rho_L v_{m,i}}{M_j}\right)^{-2.84}(\rho_G u_G)^{0.49}e^{-2.66.C_v}$
Behkish et al. (2007)	**Gas** : N_2 - He ; **Liquid** : Isopar-M ; **Solid** :Aluminia powder	**P** : 0.67 - 3 MPa ; **T** : 298-473 K; u_G : 0.07 - 0.39 $m.s^{-1}$; u_L : 0 $m.s^{-1}$; **Cv** : 0 - 20%	Spider-type (6 legs, 108 orifices, d_0 = 5 mm)	H_C: 3 m; **Dc** : 0.29 m	ε_G, d_B	SB	None
Bín et al. (2001)	**Gas** : Air-O_3 mixture ; **Liquid** : Water ; **Solid** : none	**P** : 0.1 MPa ; **T** : 293 - 296 K; u_G : 0 - 0.045 $m.s^{-1}$; u_L : 0 .0016 - 0.0071 $m.s^{-1}$; **Cv** : 0 %	Porous plate (d_0 = 100-150 µm)	H_C: 5.5 m; **Dc** : 0.15 m	ε_G, k_La, $D_{ax,L}$	Co-C/Coun-C	None
Bouaifi et al. (2001)	**Gas** : Air ; **Liquid** : Water ; **Solid** : none	**P** : 0.1 MPa ; **T** : 298 K; u_G : 0.0025 - 0.04 $m.s^{-1}$; u_L : 0 $m.s^{-1}$; **Cv** : 0 %	Perforated plate (d_0 = 2.5 mm), Membrane sparger (d_0 = 5 mm), Porous plate (porosity : 0.3)	H_C: 2 m; **Dc** : 0.15, 0.2 m	ε_G, d_B, k_L, a, k_La, $D_{ax,L}$	SB	$\varepsilon_G = C\left(\frac{u_G(\rho_L g H_C + \Delta P_0)}{H_C}\right)^{0.85}$, $a = C'\left(\frac{u_G(\rho_L g H_C + \Delta P_0)}{H_C}\right)^{1.08}$ *C and C' depend on sparger* $k_L = 1.13\sqrt{\frac{D_{m,i,j}}{d_{32}}}u_S^{1/2}$
Chaumat et al. (2005)	**Gas** :N_2, CO_2 ; **Liquid** : Water, Cyclohexane ; **Solid** : none	**P** : 0.1 MPa ; **T** : 293 K; u_G : 0 - 0.14 $m.s^{-1}$; u_L : 0-0.08 $m.s^{-1}$; **Cv** : 0 %	Toroidal sparger (0.8 % free area, d_0 = 1, 0.5 mm)	H_C: 1.6 m; **Dc** : 0.2 m	ε_G, d_B, k_L, a, k_La	Co-C	None
Chilekar (2007)	**Gas** :N_2, Air ; **Liquid** : Water, Aqueous solution of sodium gluconate, Isopar-M ; **Solid** : Carbon (30 µm), Silica (44 µm)	**P** : 0.1 - 1.3 MPa ; **T** : 292 - 296 K; u_G : 0 - 0.4 $m.s^{-1}$; u_L : 0 $m.s^{-1}$; **Cv** : 0-3 %	Perforated plate (d_0 = 0.5 mm, 200 holes)	H_C: 1.4 - 1.7 m; **Dc** : 0.11 - 0.29 m	ε_G, d_B, k_La, a, k_L	SB	$\frac{k_L a_L}{\varepsilon_G} = 3.0\sqrt{\frac{D_{m,i,j}u_{b,0}}{d_{b,0}}}$
Chilekar et al. (2010)	**Gas** :N_2, Air ; **Liquid** : Water, Aqueous solution of sodium gluconate, Isopar-M ; **Solid** : Carbon (30 µm), Silica (44 µm)	**P** : 0.1 - 1.3 MPa ; **T** : 292 - 296 K; u_G : 0 - 0.4 $m.s^{-1}$; u_L : 0 $m.s^{-1}$; **Cv** : 0-3 %	Perforated plate (d_0 = 0.5 mm, 200 holes)	H_C: 1.4 m; **Dc** : 0.15 m	ε_G, d_B, k_La	SB	$\frac{k_L a_L}{\varepsilon_G} = 3.0\sqrt{\frac{D_{m,i,j}u_{b,0}}{d_{b,0}}}$
Choi and Wiesmann (2004)	**Gas**: O_2-O_3 mixture ; **Liquid**: Water + Dyes (RB 5 & RO 96); **Solid**: none	**P** : 0.1 MPa ; **T** : 294.5 K; u_G : 0 - 0.0024 $m.s^{-1}$; u_L : 0.00081 $m.s^{-1}$; **Cv** : 0 %	No sparger	H_C: 1 m; **Dc** : 0.059 m	k_La	Co-C	None
Clark (1990)	**Gas**: N_2, H_2; **Liquid**: Water, Methanol; **Solid**: Glass powder (45-63 µm)	**P**: 2.5 - 10 MPa ; **T**: 293 - 453 K; u_G: 0 - 0.6 $m.s^{-1}$; u_L: 0 $m.s^{-1}$; **Cv**: 0 - 10%	Porous plate (d_0 = 60 µm)	H_C: 1.6 m; **Dc** : 0.075 m	ε_G	SB	None
Cui (2005)	**Gas**: Air; **Liquid**: Water, Norpar 15; **Solid**: Glass beads (120 µm), Acetate (500 - 2000 µm)	**P**: 0.1 - 1.5 MPa ; **T**: 298 K; u_G: 0 - 0.201 $m.s^{-1}$; u_L: 0 $m.s^{-1}$; **Cv**: 0 - 4%	Perforated plate (d_0 = 1.5 mm, 120 holes), Single nozzle (d_0 = 6 mm)	H_C: 0.15 - 1.37 m; **Dc** : 0.0508 - 0.1016 m	ε_G	SB	None
De Bruijn et al. (1988)	**Gas**: H_2, CH_4-H_2 mixture; **Liquid**: Zerice Oil; **Solid**: none	**P**: 5.57 - 13.89 MPa ; **T**: 573 K; u_G: 0.007 - 0.020 $m.s^{-1}$; u_L: 0.0004 - 0.001 $m.s^{-1}$; **Cv**: 0 %	Unknown	H_C: 2.4 m; **Dc** : 0.0508 m	ε_G	Co-C	None
Deckwer et al. (1980)	**Gas**: N_2; **Liquid**: Molten paraffin; **Solid**: Aluminia powder (5 µm)	**P**: 0.4 - 1.1 MPa ; **T**: 416 - 533 K; u_G: 0 - 0.035 $m.s^{-1}$; u_L: 0 $m.s^{-1}$; **Cv**: 0 - 16%	Perforated plate (d_0 = 75 µm)	H_C: Unknown; **Dc** : 0.041, 0.1 m	ε_G	SB	None
De Swart and Krishna (1995)	**Gas**: Air; **Liquid**: Mineral Oil, Ethanol, Octanol, Water, Aqueous solutions of NaOH; **Solid**: Glass beads (40 µm)	**P**: 0.1 MPa ; **T**: 298 K; u_G: 0 - 0.5 $m.s^{-1}$; u_L: 0 $m.s^{-1}$; **Cv**: 0 - 20%	Porous plate (d_0 = 0.2 mm), Bronze sintered plate (d_0 = 50 µm)	H_C: 3 - 4.5 m; **Dc** : 0.05 - 0.174 m	ε_G	SB	None
Dewes et al. (1995)	**Gas**: Air; **Liquid**: Water- 0.8 M sodium sulfate solution; **Solid**: Glass beads	**P**: 0.1 - 0.8 MPa ; **T**: 298 K; u_G: 0.01 - 0.08 $m.s^{-1}$; u_L: 0 $m.s^{-1}$; **Cv**: 0 - 2%	Perforated plate (d_0 = 1 mm, 7 holes)	H_C: 1.37 m; **Dc** : 0.115 m	ε_G, k_L, a, k_La	SB	None
Dewes and Schumpe (1997)	**Gas**: He, N_2, Air, SF_6; **Liquid**: Water- 0.8 M sodium sulfate solution; **Solid**: Xanthan gum, kieselguhr (22 µm), Alumina (7 µm)	**P**: 0.1 - 1 MPa ; **T**: 298 K; u_G: 0.01 - 0.08 $m.s^{-1}$; u_L: 0 $m.s^{-1}$; **Cv**: 0 - 18%	Perforated plate (d_0 = 1 mm, 7 holes)	H_C: 1.37 m; **Dc** : 0.115 m	ε_G, k_La	SB	$k_L a_L \propto u_G^{0.90}\mu_{SL}^{-0.55}\rho_G^{0.46}$
Fan et al. (1999)	**Gas**: N_2; **Liquid**: Paratherm NF; **Solid**: Glass beads	**P**: 0.1 - 15.6 MPa ; **T**: 299.5 - 360.5 K; u_G: 0.05 - 0.69 $m.s^{-1}$; u_L: 0 $m.s^{-1}$; **Cv**: 0%	Perforated plate, Bubble cap, Sparger	H_C: > 3.05 m; **Dc** : 0.1 - 0.61 m	ε_G, d_B	SB	$\frac{\varepsilon_G}{1-\varepsilon_G} = \frac{2.9\left(\frac{u_G^4\rho_G}{\sigma_L g}\right)^{0.21}Mo_m^{0.0079}\left(\frac{\rho_G}{\rho_{GL}}\right)^{0.096Mo_m^{-0.011}}}{[cosh(Mo_m^{0.054})]^{4.1}}$, *with* $Mo_m = \frac{g(\rho_{GL}-\rho_G)\mu_{GL}^4}{\rho_{GL}^2\sigma_L^3}$
Ferreira et al. (2013)	**Gas**: Air; **Liquid**: Water, Aqueous solutions of HCl, KOH, H_3PO_4; **Solid**: none	**P**: 0.1 MPa ; **T**: 298 K; u_G: 0 - 0.014 $m.s^{-1}$; u_L: 0 $m.s^{-1}$; **Cv**: 0%	Perforated plate (Open Area = 0.05%, d_0 = 0.5 mm)	H_C: 0.65 m; **Dc** : 0.14 m	ε_G, d_B, k_L, a, k_La	SB	None
Forret et al. (2003)	**Gas**: Air; **Liquid**: Water; **Solid**: none	**P**: 0.1 MPa ; **T**: 298 K; u_G: 0.05 - 0.2 $m.s^{-1}$; u_L: 0 $m.s^{-1}$; **Cv**: 0%	Unknown	H_C > 0.6 m; **Dc** : 0.15 - 1 m	ε_G, $D_{ax,L}$	SB	none
Fukuma et al. (1987)	**Gas**: Air; **Liquid**: Water, Aqueous solutions of glycerol; **Solid**: Glass beads (56 - 460 µm)	**P**: 0.1 MPa ; **T**: 293.05 K; u_G: 0.01 - 0.08 $m.s^{-1}$; u_L: 0.001 - 0.05 $m.s^{-1}$; **Cv**: 0 -50 %	Multi-nozzle (8 tubes, d_0 = 2.6 mm)	H_C: 1.2 - 3.2 m; **Dc** : 0.15 m	d_B	Co-C	$d_{32} = \frac{0.59\left(\frac{q_G}{\varepsilon_G}\right)^2}{g}$
Gandhi et al. (1999)	**Gas**: Air; **Liquid**: Water; **Solid**: Glass beads (35 µm)	**P**: 0.1 MPa ; **T**: 293.5 K; u_G: 0.05 - 0.28 $m.s^{-1}$; u_L: 0 $m.s^{-1}$; **Cv**: 0 -40 %	Four-armed sparger (20 orifices, d_0 = 1.5 mm)	H_C: 2.5 m; **Dc** : 0.15 m	ε_G	SB	None
García-Abuín et al. (2010)	**Gas**: CO_2; **Liquid**: Water, Aqueous solutions of GA; **Solid**: none	**P**: 0.1 MPa ; **T**: 298 K; u_G: 0 - 0.0031 $m.s^{-1}$; u_L: 0 $m.s^{-1}$; **Cv**: 0 %	Glass capillary (1 hole)	H_C: 1.03 m; **Dc** : 0.06 m (rectangular)	ε_G, d_B, k_L, a	SB	None
García-Abuín et al. (2012)	**Gas**: Air; **Liquid**: Water, Aqueous solutions of polymer with and without surfactant; **Solid**: none	**P**: 0.1 MPa ; **T**: 298 K; u_G: 0 - 0.009 $m.s^{-1}$; u_L: 0 $m.s^{-1}$; **Cv**: 0 %	5 hole sparger	H_C: 0.65 m; **Dc** : 0.04 m (rectangular)	ε_G, d_B, a	SB	None
Gopal and Sharma (1983)	**Gas**: Air; **Liquid**: Water, Aqueous solutions; **Solid**: none	**P**: 0.1 MPa ; **T**: 298 K; u_G: 0.01 - 0.08 $m.s^{-1}$; u_L: Unknown ; **Cv**: 0 %	Different spargers	H_C: 0.12 - 4 m; **Dc** : 0.2, 0.6, 1.0 m	ε_G, k_L, a, k_La	Co-C	None
Gourich et al. (2006)	**Gas**: Air; **Liquid**: Water, Aqueous solutions of propanol (0.05%v/v); **Solid**: none	**P**: 0.1 MPa ; **T**: 298 K; u_G: 0.006 - 0.1 $m.s^{-1}$; u_L: 0 $m.s^{-1}$; **Cv**: 0 %	Multi-orifice nozzle (76 holes, d_0 = 0.5 mm)	H_C: 1.66 m; **Dc** : 0.1 m	ε_G	SB	None
Gourich et al. (2008)	**Gas**: Air; **Liquid**: Water, Aqueous solutions of ethanol; **Solid**: none	**P**: 0.1 MPa ; **T**: 298 K; u_G: 0.006 - 0.1 $m.s^{-1}$; u_L: 0 $m.s^{-1}$; **Cv**: 0 %	Multi-orifice nozzle (76 holes, d_0 = 0.5 mm)	H_C: 3 m; **Dc** : 0.1 m	ε_G	SB	None
Grover et al. (1986)	**Gas**: Air; **Liquid**: Water, Aqueous solution of NaCl, $CuCl_2$; **Solid**: none	**P**: 0.1 MPa ; **T**: 303 - 353 K; u_G: 0.001 - 0.045 $m.s^{-1}$; u_L: 0 $m.s^{-1}$; **Cv**: 0 %	Sintered glass disc	H_C: 1.5 m; **Dc** : 0.1 m	ε_G	SB	$\varepsilon_G = \left(\frac{1+1.1.10^{-4}E_R}{5.10^{-4}E_R}\right)\left(\frac{u_G\mu_L}{\sigma_L}\right)^{0.76}\left(\frac{g\mu_L^4}{\sigma_L^3\rho_L}\right)^{-0.27}\left(\frac{\rho_G}{\rho_L}\right)^{-0.09}\left(\frac{\mu_G}{\mu_L}\right)^{0.35}$
Han and Al-Dahhan (2007)	**Gas**: Air; **Liquid**: Water; **Solid**: none	**P**: 0.1 - 1.0 MPa ; **T**: 298 K; u_G: 0 - 0.6 $m.s^{-1}$; u_L: 0 $m.s^{-1}$; **Cv**: 0 %	Peforated plates (163 holes, d_0 = 0.5 & 1.32 mm, 0.156 & 1.09 % free area), Cross sparger (4 holes, d_0 = 2.54 mm, 0.1% free area)	H_C: 1.81 m; **Dc** : 0.162 m	ε_G, k_L, a, k_La	SB	None
Hashemi et al. (2009)	**Gas**: N_2/O_2 mixture; **Liquid**: Water; **Solid**: Ion-exchange resin (84.8 µm)	**P**: 0.1 - 4.0 MPa ; **T**: 277 - 295 K; u_G: 0 - 0.2 $m.s^{-1}$; u_L: 0 $m.s^{-1}$; **Cv**: 0 - 10%	Peforated plate (34 holes, d_0 = 3.175 mm)	H_C: 0.6 - 0.7 m; **Dc** : 0.1 m	ε_G, k_La	SB	None
Hikita and Kikukawa (1974)	**Gas**: Air; **Liquid**: Water, Aqueous solutions of methanol and cane sugar; **Solid**: none	**P**: 0.1 MPa ; **T**: 298 K; u_G: 0.043 - 0.338 m.s-1 ; u_L: 0 m.s-1 ; C_v: 0%	4 Single orifice-nozzles (d0 = 1.30, 1.31, 2.06, 3.62 mm)	H_C: 1.33 - 2.2 m; D_c : 0.10 - 0.19 m	ε_G, $D_{ax,L}$	SB	$\varepsilon_G = 0.505u_G^{0.47}\left(\frac{72}{\sigma_L}\right)^{\frac{2}{3}}\left(\frac{1}{\mu_L}\right)^{0.05}$ $D_{ax,L} = (0.15 + 0.69\,u_G^{0.77})D_C^{1.25}\left(\frac{1}{\mu_L}\right)^{0.12}$
Hikita et al. (1980)	**Gas**: Air, CO_2, CH_4, C_3H_8, H_2-Air mixtures; **Liquid**: Water, Aqueous solution of methanol, n, i-butanol, aniline, sucrose and electrolytes; **Solid**: none	**P**: 0.1 MPa ; **T**: 298 K; u_G: 0.042 - 0.38 $m.s^{-1}$; u_L: 0 $m.s^{-1}$; **Cv**: 0%	Single orifice-nozzle (d_0 = 1.1 mm)	H_C: 1.5 m; **Dc** : 0.1 m	ε_G	SB	$\varepsilon_G = 0.672\left(\frac{u_G\mu_L}{\sigma_L}\right)^{0.578}\left(\frac{g\mu_L^4}{\sigma_L^3\rho_L}\right)^{-0.131}\left(\frac{\rho_G}{\rho_L}\right)^{0.062}\left(\frac{\mu_G}{\mu_L}\right)^{0.107}$
Hikita et al. (1981)	**Gas**: Air, CO_2, CH_4, O_2; **Liquid**: Water, Aqueous solution of methanol, n-butanol, sucrose and electrolytes; **Solid**: none	**P**: 0.1 MPa ; **T**: 298 K; u_G: 0.042 - 0.38 $m.s^{-1}$; u_L: 0 $m.s^{-1}$; **Cv**: 0%	5 Single orifice-nozzles (d_0 = 0.9, 1.30, 1.31, 2.06, 3.62 mm)	H_C: 1.5 - 2.4 m; **Dc** : 0.1 - 0.19 m	k_La	SB / Coun-C	$\frac{k_L a_L u_G}{g} = 14.9\left(\frac{u_G\mu_L}{\sigma_L}\right)^{1.76}\left(\frac{g\mu_L^4}{\sigma_L^3\rho_L}\right)^{-0.248}\left(\frac{\vartheta_L}{D_{m,i,j}}\right)^{-0.604}\left(\frac{\mu_G}{\mu_L}\right)^{0.243}$
Holcombe et al. (1983)	**Gas**: N_2; **Liquid**: Water; **Solid**: none	**P**: 0.3 -0.71 MPa ; **T**: 298 K; u_G: 0 - 0.6 $m.s^{-1}$; u_L: 0 - 0.02 $m.s^{-1}$; **Cv**: 0%	Unknown	H_C: Unknown; **Dc** : 0.078 m	$D_{ax,L}$	Co-C	$D_{ax,L} = 1.26\,u_G^{0.46}D_C^{\frac{4}{3}}$

Table 1 – (*Continued*)

Houzelot et al. (1983)	**Gas**: Air; **Liquid**: Water; **Solid**: none	**P**: 0.1 - 0.3 MPa ; **T**: 298 K; u_G: 0 - 0.006 $m.s^{-1}$; u_L: 0 $m.s^{-1}$; **Cv**: 0%	Unknown	H_C: Unknown; **Dc** : 0.05 m	$D_{ax,L}$	SB	None
Idogawa et al. (1986)	**Gas**: Air; **Liquid**: Water; **Solid**: none	**P**: 0.1 - 15 MPa ; **T**: 284 - 293 K; u_G: 0.005 - 0.05 $m.s^{-1}$; u_L: 0 $m.s^{-1}$; **Cv**: 0%	Different spargers	H_C: Unknown; **Dc** : 0.05 m	ε_G, d_B	SB	None
Idogawa et al. (1987)	**Gas**: H_2, He, Air; **Liquid**: Water, Methanol, Ethanol, Acetone, aqueous solutions; **Solid**: none	**P**: 0.1 - 5 MPa ; **T**: 284 - 293 K; u_G: 0.005 - 0.05 $m.s^{-1}$; u_L: 0 $m.s^{-1}$; **Cv**: 0%	Perforated plate (d_0 = 1 mm)	H_C: Unknown; **Dc** : 0.05 m	ε_G, d_B	SB	$\frac{\varepsilon_G}{1-\varepsilon_G} = 0.059\, u_G^{0.8} \rho_G^{0.17} \left(\frac{\sigma_L}{72}\right)^{-0.22\exp(-P)}$ $\sigma_L[mN.m^{-1}], u_G\,[cm.s^{-1}]$
Ishibashi et al. (2001)	**Gas**: H_2; **Liquid**: Oil slurry; **Solid**: Coal + catalyst	**P**: 16.8 - 18.6 MPa ; **T**: 505 - 738 K; u_G: 0.01 - 0.09 $m.s^{-1}$; u_L: 0.002 - 0.004 $m.s^{-1}$; **Cv**: Unknown	Unknown	H_C: 11 m; **Dc** : 1 m	ε_G	Co-C	None
Ishiyama et al. (2001)	**Gas**: N_2, CO_2; **Liquid**: Water; **Solid**: none	**P**: 0.1 - 1.1 MPa ; **T**: 293 - 308 K; u_G: 0.008 - 0.12 $m.s^{-1}$; u_L: 0 $m.s^{-1}$; **Cv**: 0%	2 Single orifice-nozzles (d_0 = 1.0, 4.0 mm)	H_C: 1.15-1.6 m; **Dc** : 0.045 m	ε_G, d_B	SB	None
Jiang et al. (1995)	**Gas**: N_2; **Liquid**: Paratherm NF; **Solid**: none	**P**: 0.1 - 21 MPa ; **T**: 298 K; u_G: 0 - 0.4 $m.s^{-1}$; u_L: 0 $m.s^{-1}$; **Cv**: 0 %	Unknown	H_C: Unknown m; **Dc** : 0.0508 m	ε_G, d_B	SB	None
Jin et al. (2004)	**Gas**: Air; **Liquid**: Water; **Solid**: Quartz sand	**P**: 1 - 3 MPa ; **T**: 298 - 473 K; u_G: 0.03 - 0.1 $m.s^{-1}$; u_L: 0 $m.s^{-1}$; **Cv**: 0 -20%	4 Nozzles (d_0 = 8 mm)	H_C: 0.4 - 0.6 m; **Dc** : 0.06 - 0.1 m	k_La	SB	$k_La = C_1\left(1-\frac{C_V}{0.70}\right)^{0.802} \mu_L^{-0.244} u_G^{0.721} \rho_P^{0.143}$
Jin et al. (2007a)	**Gas**: N_2; **Liquid**: Water; **Solid**: none	**P**: 0.1 MPa ; **T**: 295 K; u_G: 0 - 0.13 $m.s^{-1}$; u_L: 0 $m.s^{-1}$; **Cv**: 0%	Perforated plates (d_0 = 1, 3 mm, 5 holes)	H_C: 1.2 m; **Dc** : 0.056 m	ε_G	SB	None
Jin et al. (2007b)	**Gas**: Air; **Liquid**: Water; **Solid**: none	**P**: 0.1 MPa ; **T**: 295 K; u_G: 0.02 - 0.25 $m.s^{-1}$; u_L: 0 - 0.011 $m.s^{-1}$; **Cv**: 0%	Perforated plate (d_0 = 1 mm, 55 holes)	H_C: 2.5 m; **Dc** : 0.16 m	ε_G	Co-C	$\varepsilon_G = 1.042 u_G^{0.523} \left(\frac{H_C}{D_C}\right)^{-0.096}$
Jin et al. (2010)	**Gas**: Air; **Liquid**: Water; **Solid**: none	**P**: 0.1 MPa ; **T**: 295 K; u_G: 0.02 - 0.25 $m.s^{-1}$; u_L: 0 - 0.011 $m.s^{-1}$; **Cv**: 0%	Perforated plate (d_0 = 1 mm, 55 holes)	H_C: 2.5 m; **Dc** : 0.16 m	ε_G	Coun-C	$\varepsilon_G = 0.900 u_G^{0.503} \left(\frac{H_C}{D_C}\right)^{-0.047} + 0.050\, u_L^{0.289}$
Jin et al. (2014)	**Gas**: H_2, CO, CO_2; **Liquid**: Paraffin; **Solid**: Quartz sand (150-200 µm)	**P**: 1 - 3 MPa ; **T**: 298 - 423 K; u_G: 0.03 - 0.1 $m.s^{-1}$; u_L: 0 $m.s^{-1}$; **Cv**: 0 -20%	Perforated plate (d_0 = 8 mm, 2.56% open area)	H_C: 0.4 - 0.6 m; **Dc** : 0.10 m	k_L, a, k_La	SB	$k_La = 3.051\left(\frac{\rho_L \vartheta_{m,G}}{M}\right)^{-1.193}\left(\frac{\vartheta_L}{D}\right)^{-0.734}(\rho_G u_G)^{0.524}\left(1-\frac{C_V}{0\,85}\right)^{2.303}$
Jordan and Schumpe (2001)	**Gas**: He, H_2; **Liquid**: Ethanol, Butanol, Decalin, Toluene; **Solid**: none	**P**: 0.1 - 4 MPa ; **T**: 293 - 343 K; u_G: 0.01 - 0.21 $m.s^{-1}$; u_L: 0 $m.s^{-1}$; **Cv**: 0%	Perforated plates (d_0 = 4.3, 1 mm; 1, 19 holes)	H_C: 1.3 m; **Dc** : 0.10 m	ε_G, k_La	SB	$\frac{k_La_L d_B^2}{D_{m,i,j}} = B_1\left(\frac{\vartheta_L}{D_{m,i,j}}\right)^{1/2}\left(\frac{gd_B^2\rho_L}{\sigma_L}\right)^{0.34}\left(\frac{gd_B^3}{\vartheta_L^2}\right)^{0.27}\left(\frac{u_G}{\sqrt{gd_B}}\right)^{0.72}\left(1+13.2\left(\frac{u_G}{\sqrt{gd_B}}\right)^{0.37}\left(\frac{\rho_G}{\rho_L}\right)^{0.49}\right)$ $\frac{\varepsilon_G}{1-\varepsilon_G} = B_2\left(\frac{gd_B^2\rho_L}{\sigma_L}\right)^{0.16}\left(\frac{gd_B^3}{\vartheta_L^2}\right)^{0.04}\left(\frac{u_G}{\sqrt{gd_B}}\right)^{0.70}\left(1+27.0\left(\frac{u_G}{\sqrt{gd_B}}\right)^{0.52}\left(\frac{\rho_G}{\rho_L}\right)^{0.58}\right)$
Kang et al. (1999)	**Gas**: Air; **Liquid**: Aqueous solutions of CMC; **Solid**: none	**P**: 0.1 - 0.6 MPa ; **T**: 298 K; u_G: 0.02 - 0.20 $m.s^{-1}$; u_L: 0 $m.s^{-1}$; **Cv**: 0%	4 Perforated pipes (d_0 = 1 mm; 12 holes)	H_C: 2.0 m; **Dc** : 0.152 m	ε_G, k_La	SB	None
Kang et al. (2000)	**Gas**: Air; **Liquid**: Water; **Solid**: none	**P**: 0.1 - 0.6 MPa ; **T**: 298 K; u_G: 0.02 - 0.25 $m.s^{-1}$; u_L: 0 $m.s^{-1}$; **Cv**: 0%	4 Perforated pipes (d_0 = 1 mm; 12 holes)	H_C: 1.5 m; **Dc** : 0.058 m	d_B	SB	None
Kantarci et al. (2005)	**Gas**: Air; **Liquid**: Water; **Solid**: Yeast cells (10 µm), Bacteria cells (0.2 - 0.7 µm)	**P**: 0.1 MPa ; **T**: 298 K; u_G: 0.03 - 0.20 $m.s^{-1}$; u_L: 0 $m.s^{-1}$; **Cv**: 0%	Spider-type (6 arms, 24 holes, d_0 = 2mm)	H_C: 0.6 m; **Dc** : 0.17 m	ε_G, d_B	SB	None
Kemoun et al. (2001)	**Gas**: Air; **Liquid**: Water; **Solid**: none	**P**: 0.1 - 0.7 MPa ; **T**: 293 K; u_G: 0.02 - 0.18 $m.s^{-1}$; u_L: 0 $m.s^{-1}$; **Cv**: 0%	Perforated plate (d_0 = 0.4 mm, 61 holes, 0.04% open area)	H_C: 1.8 - 2.0 m; **Dc** : 0.162 m	ε_G	SB	None
Kluytmans et al. (2003)	**Gas**: Air, O_2, N_2; **Liquid**: Water, Sodium gluconate aqueous solution; **Solid**: Carbon (30 µm)	**P**: 0.1 MPa ; **T**: 298 K; u_G: 0 - 0.4 $m.s^{-1}$; u_L: 0 $m.s^{-1}$; **Cv**: Unknown	Unknown	H_C: 2.0 m; **Dc** : 0.3 m	ε_G, d_B, k_L, a, k_La	SB	None
Kojima et al. (1997)	**Gas**: O_2-N_2 mixture; **Liquid**: Water, $Na_2H_2PO_4$ solution, enzyme aqueous solution; **Solid**: none	**P**: 0.1 - 1.1 MPa ; **T**: 290 - 300 K; u_G: 0.005 - 0.15 $m.s^{-1}$; u_L: 0 $m.s^{-1}$; **Cv**: 0%	Single nozzle (d_0 = 1.38, 2.10, 2.90, 4.03 mm)	H_C: 0.9 - 1.2 m; **Dc** : 0.045 m	ε_G, k_La	SB	$\varepsilon_G = 1.18\, u_G^{0.679}\left(\frac{\sigma_L}{0.076}\right)^{-0.546}\exp\left\{l_1\left(\frac{\rho_L Q_G^2}{d_0^3\sigma_L}\right)\left(\frac{P}{0.1013}\right)^{l_2}\right\}$ $k_La_L = l_3\varepsilon_G{}^{l_4}\left(\frac{\rho_L Q_G^2}{d_0^3\sigma_L}\right)^{l_5}\left(\frac{P}{0.1013}\right)^{l_6}$
Kölbel et al. (1971)	**Gas**: H_2, ethylene; **Liquid**: $C_{13\text{-}18}$ mixture; **Solid**: catalyst particles	**P**: 0.1 - 0.588 MPa ; **T**: 298 - 353 K; u_G: 0 - 0.17 $m.s^{-1}$; u_L: 0 $m.s^{-1}$; **Cv**: 3%	Porous plate (d_0 = 10 µm)	H_C: 4 m; **Dc** : 0.0418 m	ε_G, $D_{ax,L}$	SB	None
Krishna et al. (1991)	**Gas**: N_2, CO_2, Ar, He, SO_2; **Liquid**: Water, turpentine, n-butanol, monoethylene glycol; **Solid**: none	**P**: 0.1 - 2.0 MPa ; **T**: 298 K; u_G: 0 - 0.35 $m.s^{-1}$; u_L: 0 $m.s^{-1}$; **Cv**: 0%	Unknown	H_C: 1.2 - 4 m; **Dc** : 0.16 - 0.19 m	ε_G	SB	$\varepsilon_G = 4u_G, homogeneous\ regime$ $\varepsilon_G = 4u_{G,trans} + A\left(u_G - u_{G,trans}\right)^B, heterogeneous\ regime$
Krishna et al. (1994)	**Gas**: Air, Ar, He, SF_6; **Liquid**: Water; **Solid**: none	**P**: 0.1 MPa ; **T**: 298 K; u_G: 0 - 0.4 $m.s^{-1}$; u_L: 0 $m.s^{-1}$; **Cv**: 0%	Sintered glass plate	H_C: 0.6 - 2.4 m; **Dc** : 0.05 - 0.1 m	ε_G	SB	$\varepsilon_G = \frac{u_G}{u_{B,\infty}(1-\varepsilon_G)^{B-1}}, homogeneous\ regime$ $\varepsilon_G = \varepsilon_{G,trans} + A\left(u_G - u_{G,trans}\right)^B, heterogeneous\ regime$
Krishna and Ellenberger (1996)	**Gas**: Air, Ar, He, SF_6; **Liquid**: Water, Oil paraffins, tetradecane; **Solid**: none	**P**: 0.1 MPa ; **T**: 298 K; u_G: 0 - 0.866 $m.s^{-1}$; u_L: 0 $m.s^{-1}$; **Cv**: 0%	2 Porous plates (d_0 = 50, 175 µm), Spider-type (d_0 = 2.5 mm), Sieve plate (d_0 = 2.5 mm)	H_C: 0.3 - 2.2 m; **Dc** : 0.1 - 0.63 m	ε_G	SB	See reference
Krishna et al. (1999)	**Gas**: Air; **Liquid**: Water; **Solid**: none	**P**: 0.1 MPa ; **T**: 298 K; u_G: 0 - 0.4 $m.s^{-1}$; u_L: 0 $m.s^{-1}$; **Cv**: 0%	Porous plate (d_0 = 50 µm), Spider-type	H_C: 4 m; **Dc** : 0.174, 0.38, 0.63 m	$D_{ax,L}$	SB	$\varepsilon_G = \frac{u_G}{u_{BS}}, homogeneous\ regime$ $\varepsilon_G = \frac{\left(u_G - u_{G,trans}\right)}{u_{BL}} + \varepsilon_{G,trans}\left[1 - \frac{\left(u_G - u_{G,trans}\right)}{u_{BL}}\right], heterogeneous\ regime$
Krishna et al. (2000)	**Gas**: Air; **Liquid**: Aqueous solutions of ethanol; **Solid**: none	**P**: 0.1 MPa ; **T**: 298 K; u_G: 0 - 0.5 $m.s^{-1}$; u_L: 0 $m.s^{-1}$; **Cv**: 0%	Perforated plate (d_0 = 0.5 mm, 625 holes)	H_C: 4 m; **Dc** : 0.15 m	ε_G	SB	Same as above
Krishna et al. (2001)	**Gas**: Air; **Liquid**: Water; **Solid**: none	**P**: 0.1 MPa ; **T**: 298 K; u_G: 0 - 0.04 $m.s^{-1}$; u_L: 0 $m.s^{-1}$; **Cv**: 0%	Perforated plates (d_0 = 0.5 mm)	H_C: 1 m; **Dc** : 0.1, 0.15, 0.38 m	ε_G	SB	None
Kulkarni (2007)	**Gas**: Air; **Liquid**: Sodium sulfite and $CoSO_4$ aqueous solution; **Solid**: none	**P**: 0.1 MPa ; **T**: 297 K; u_G: 0.024 $m.s^{-1}$; u_L: 0 $m.s^{-1}$; **Cv**: 0%	Sieve plate sparger (d_0 = 0.8 mm, Open area = 0.347 %)	H_C: 0.9 m; **Dc** : 0.15 m	d_B, k_L, k_La	SB	None
Kumar et al. (2012a)	**Gas**: Air; **Liquid**: Water; **Solid**: Glass beads (35 µm)	**P**: 0.1 MPa ; **T**: 298 K; u_G: 0.01 - 0.1628 $m.s^{-1}$; u_L: 0 - 0.1226 $m.s^{-1}$; **Cv**: 0-9%	Perforated plate (d_0 unknown)	H_C: 1 - 1.8 m; **Dc** : 0.15 m	ε_G	Co-C	None
Kumar et al. (2012b)	**Gas**: Air; **Liquid**: Water; **Solid**: none	**P**: 0.1 - 0.7 MPa ; **T**: 298 K; u_G: 0.01 - 0.1628 $m.s^{-1}$; u_L: 0 - 0.1226 $m.s^{-1}$; **Cv**: 0%	Spider-type (120 holes, d_0 = 1mm)	H_C: 2.72 m; **Dc** : 0.154 m	ε_G	Co-C	None
La Rubia et al. (2010)	**Gas**: CO_2; **Liquid**: Aqueous solutions of TEA; **Solid**: none	**P**: 0.1 MPa ; **T**: 298 K; u_G: 0 - 0.0024 $m.s^{-1}$; u_L: 0 $m.s^{-1}$; **Cv**: 0%	Capillary sparger (3 capillaries, d_0 = 3 mm)	H_C: 1.03 m; **Dc** : 0.06 m (rectangular)	ε_G, d_B, k_L, a, k_La	SB	None
Lau et al. (2004)	**Gas**: Air, N_2; **Liquid**: Water, Paratherm NF; **Solid**: none	**P**: 0.1 - 4.24 MPa ; **T**: 293 -385 K; u_G: 0 - 0.108 $m.s^{-1}$; u_L: 0 $m.s^{-1}$; **Cv**: 0%	Unknown	H_C: Unknown; **Dc** : 0.0508, 0.1016 m	ε_G, k_La	SB	$k_La_L = 1.77\,\varepsilon_G^{1.2}\sigma_L^{-0.22} exp(1.65\,u_L - 65.3\,\mu_L)$
Lau et al. (2012)	**Gas**: Air, N_2; **Liquid**: Water; **Solid**: none	**P**: 0.1 MPa ; **T**: 298 K; u_G: 0 - 0.108 $m.s^{-1}$; u_L: 0 $m.s^{-1}$; **Cv**: 0%	Perforated plate (211 holes, d_0 = 3 mm), Porous plate (d_0 = 0.6 mm), Single orifice-nozzle (d_0 = 5.5 mm)	H_C: 0.28 - 1.008 m; **Dc**: 0.14 m	ε_G, d_B, k_L, a, k_La	SB	None
Lemoine et al. (2004)	**Gas**: Air, N_2; **Liquid**: Toluene, mixtures of toluene, benzoic acid, benzaldehyde; **Solid**: none	**P**: 0.2 - 0.8 MPa ; **T**: 298 K; u_G: 0.06 - 0.14 $m.s^{-1}$; u_L: 0 $m.s^{-1}$; **Cv**: 0%	Unknown	H_C: 2.8 m; **Dc** : 0.316 m	ε_G, d_B, k_L, a, k_La	SB	None
Letzel et al. (1997)	**Gas**: N_2; **Liquid**: Water; **Solid**: none	**P**: 0.1 - 1.3 MPa ; **T**: 298 K; u_G: 0 - 0.5 $m.s^{-1}$; u_L: 0 $m.s^{-1}$; **Cv**: 0%	Perforated plate (d_0 = 0.5 mm, 200 holes)	H_C: 1.2 m; **Dc** : 0.15 m	ε_G	SB	None
Letzel et al. (1998)	**Gas**: N_2; **Liquid**: Water; **Solid**: none	**P**: 0.1 - 1.3 MPa ; **T**: 298 K; u_G: 0 - 0.5 $m.s^{-1}$; u_L: 0 $m.s^{-1}$; **Cv**: 0%	Perforated plate (d_0 = 0.5 mm, 200 holes)	H_C: 1.2 m; **Dc** : 0.15 m	ε_G	SB	None
Letzel et al. (1999)	**Gas**: N_2; **Liquid**: Water; **Solid**: none	**P**: 0.1 - 1.3 MPa ; **T**: 298 K; u_G: 0 - 0.5 $m.s^{-1}$; u_L: 0 $m.s^{-1}$; **Cv**: 0%	Perforated plate (d_0 = 0.5 mm, 200 holes)	H_C: 1.2 m; **Dc** : 0.15 m	ε_G, k_La	SB	None
Lin et al. (1998)	**Gas**: N_2; **Liquid**: Paratherm NF; **Solid**: none	**P**: 0.1 - 19.4 MPa ; **T**: 290 - 351 K; u_G: 0 - 0.3 $m.s^{-1}$; u_L: 0 $m.s^{-1}$; **Cv**: 0%	Multiorifice sparger (d_0 = 3 mm)	H_C: 0.8, 1.58 m; **Dc** : 0.0508, 0.1016 m	ε_G, d_B	SB	None
Lin and Fan (1999)	**Gas**: N_2; **Liquid**: Paratherm NF; **Solid**: none	**P**: 0.1 - 15.2 MPa ; **T**: 290 K; u_G: 0 - 1.2 $m.s^{-1}$; u_L: 0 $m.s^{-1}$; **Cv**: 0%	Single orifice-nozzle (d_0 = 1.5875 mm)	H_C: 0.8; **Dc** : 0.0508 m	d_B	SB	None
Lin et al. (2001)	**Gas**: N_2; **Liquid**: Paratherm NF; **Solid**: none	**P**: 0.1 - 15 MPa ; **T**: 290 K; u_G: 0 - 0.24 $m.s^{-1}$; u_L: 0 $m.s^{-1}$; **Cv**: 0%	Perforated plate (d_0 = 2.5 mm)	H_C: 0.8; **Dc** : 0.0508 m	ε_G	SB	None

Table 1 – (*Continued*)

Lorenz et al. (2005)	**Gas**: N_2; **Liquid**: Water, Ethanol, 1-Butanol; **Solid**: none	**P**: 0.1 - 0.5 MPa ; **T**: 298 - 323 K; u_G: 0.01 - 0.21 $m.s^{-1}$; u_L: 0 $m.s^{-1}$; **Cv**: 0%	Unknown	H_C: 2.1 m; **Dc** : 0.1 m	ε_G, $D_{ax,L}$	SB	None
Luo et al. (1999)	**Gas**: N_2; **Liquid**: Paratherm NF; **Solid**: Alumina (100 µm)	**P**: 0.1 - 5.6 MPa ; **T**: 301 - 351 K; u_G: 0 - 0.045 $m.s^{-1}$; u_L: 0 $m.s^{-1}$; **Cv**: 0 - 19.1%	Perforated plate (120 holes, d_0 = 1.5 mm)	H_C: 1.37 m; **Dc** : 0.102 m	ε_G, d_B	SB	$\frac{\varepsilon_G}{1-\varepsilon_G}=\frac{2.9\left(\frac{u_G^4\rho_G}{\sigma_L g}\right)^{0.21Mo_m^{-0.1079}}\left(\frac{\rho_G}{\rho_{SL}}\right)^{0.096Mo_m^{-0.011}}}{\left\lvert cosh\left(Mo_m^{0.054}\right)\right\rvert^{4.1}}, with\ Mo_m=\frac{g(\rho_{SL}-\rho_G)\mu_L^4}{\rho_L^2\sigma_L^3}$
Maalej et al. (2003)	**Gas**: N_2/CO_2; **Liquid**: Aqueous solution of Na_2CO_3, $NaHCO_3$ and NaOH; **Solid**: none	**P**: 0.1 - 5.0 MPa ; **T**: 293 K; u_G: 0 - 0.03 $m.s^{-1}$; u_L: Unknown; **Cv**: 0 %	Unknown	H_C: 0.25 m; **Dc** : 0.046 m	k_L, a, k_La	Coun-C	None
Maceiras et al. (2010)	**Gas**: CO_2; **Liquid**: DEA aqueous solution; **Solid**: none	**P**: 0.1 MPa ; **T**: 298 K; u_G: 0.00077 - 0.00190 $m.s^{-1}$; u_L: 0 $m.s^{-1}$; **Cv**: 0 %	Porous plate (d_0 = 4 mm)	H_C: 1.03 m; **Dc** : 0.06 m (rectangular)	ε_G, d_B, a	SB	$\varepsilon_G = 1.85.10^{-9}\left(\frac{u_G}{\sqrt{gD_C}}\right)^{0.45}\left(\frac{gD_C^3}{\vartheta_L^2}\right)^{0.62}\left(\frac{gD_C^2\rho_L}{\sigma_L}\right)^{0.7}\left(\frac{d_{32}}{D_C}\right)^{-1.3}$
Majumder et al. (2006)	**Gas**: Air; **Liquid**: Water; **Solid**: none	**P**: 0.1 MPa ; **T**: 302 K; u_G: 0.0017 - 0.01358 $m.s^{-1}$; u_L: 0.0707 - 0.1414 $m.s^{-1}$; **Cv**: 0 %	Single orifice-nozzles (d_0 = 4, 5, 6, 7 mm)	H_C: 1.6 m; **Dc** : 0.05 m	ε_G, d_B, a	Co-C	$\frac{d_{32}}{d_0}=1.48.10^{-2}\left(\frac{z}{d_0}\right)^{1.09}V_B^{-1.388}\left(\frac{d_0 g}{u_G^2}\right)^{-0.759}\left(\frac{d_0 u_G \rho_L}{\mu_L}\right)^{0.449}\left(\frac{d_0\rho_L\sigma_L}{\mu_L^2}\right)^{-0.303}$
Mena et al. (2011)	**Gas**: Air; **Liquid**: Water; **Solid**: EPS (1100, 770, 591 µm), Glass beads (9.6 µm)	**P**: 0.1 MPa ; **T**: 298 K; u_G: 0 - 0.0027 $m.s^{-1}$; u_L: 0 $m.s^{-1}$; **Cv**: 0-30 %	Multi-nozzle sparger (13 needles, d_0 = 0.3 mm)	H_C: 0.2 m; **Dc** : 0.084 m	k_La	SB	$k_La = D_1 u_G^{D_2}(1+d_P)^{D_3}\left(1-\frac{C_V}{100}\right)^{D_4}, D_i\ depend\ on\ solid\ phase$
Mouza et al. (2005)	**Gas**: Air; **Liquid**: Water, Aqueous solutions of glycerin and ethanol; **Solid**: none	**P**: 0.1 MPa ; **T**: 298 K; u_G: 0 - 0.008 $m.s^{-1}$; u_L: 0 $m.s^{-1}$; **Cv**: 0 %	Porous plates (d_0 = 20, 40 µm)	H_C: 1.5 m; **Dc** : 0.10 m (rectangular)	ε_G, d_B	SB	$\varepsilon_G = 0.001\left[\left(\frac{u_G^2}{gD_C}\right)^{0.5}\left(\frac{gD_C^3}{\vartheta_L^2}\right)^{0.1}\left(\frac{gD_C^2\rho_L}{\sigma_L}\right)^{2.2}\left(\frac{d_{32}}{D_C}\right)\right]^{2/3}$
Muroyama et al. (2013)	**Gas**: O_2, N_2; **Liquid**: Water; **Solid**: none	**P**: 0.1 MPa ; **T**: 298 K; u_G: 0 - 0.000664 $m.s^{-1}$; u_L: 0.00472 - 0.01415 $m.s^{-1}$; **Cv**: 0 %	Single orifice pipe (d_0 = 16 mm), G3 glass filter	H_C: 0.5 - 1.85 m; **Dc** : 0.15 m	ε_G, d_B, k_La	Co-C	None
Neubauer (1977)	**Gas**: Air, N_2; **Liquid**: Water, n-octanol, n-propanol; **Solid**: none	**P**: 0.1 -30 MPa ; **T**: 298 K; u_G: Unknown; u_L: 0 $m.s^{-1}$; **Cv**: 0 %	Perforated plates (d_0 = 0.5 - 5 mm)	H_C: 1.2 m; **Dc** : 0.036 - 0.24 m	d_B	SB	None
Ohki and Inoue (1970)	**Gas**: Air; **Liquid**: Water, Aqueous solution of potassium chloride; **Solid**: none	**P**: 0.1 MPa ; **T**: 298 K; u_G: 0.02 - 0.25 m.s-1; u_L: 0 $m.s^{-1}$; **Cv**: 0 %	10 Perforated plates (d_0 = 0.4 - 3 mm, 2 - 91 holes)	H_C: 2 - 3 m; **Dc** : 0.04 - 0.16 m	ε_G, $D_{ax,L}$	SB	$D_{ax,L} = 0.3\,u_G^{1.2}D_C^2 + 170 d_0\ \ homogeneous\ regime$ $D_{ax,L} = \frac{14D_c}{(1-\varepsilon_G)^2}\ \ slug-flow\ regime$
Olivieri et al. (2011)	**Gas**: Air; **Liquid**: Water, Aqueous solutions of glycerol, alginate; **Solid**: none	**P**: 0.1 MPa ; **T**: 303 K; u_G: 0 - 0.10 $m.s^{-1}$; u_L: 0 $m.s^{-1}$; **Cv**: 0 %	Perforated plate (128 needles 2 cm long, d_0 = 0.4 mm)	H_C: 2 m; **Dc** : 0.12 m	ε_G	SB	None
Onozaki et al. (2000)	**Gas**: H_2; **Liquid**: Oil slurry; **Solid**: Coal + catalyst	**P**: 16.6 - 16.8 MPa ; **T**: 313 - 733 K; u_G: 0.01 - 0.09 $m.s^{-1}$; u_L: 0.002 - 0.004 $m.s^{-1}$; **Cv**: 0 - 51.5 %wt	Unknown	H_C: 11 m; **Dc** : 1 m	ε_G	Co-C	None
Oyevaar et al. (1991)	**Gas**: N_2, N_2 + 1%vol CO_2; **Liquid**: Water, Aqueous solutions of DEA + antifoam; **Solid**: none	**P**: 0.1 - 8.0 MPa ; **T**: 298 K; u_G: 0.01 - 0.10 $m.s^{-1}$; u_L: 0 $m.s^{-1}$; **Cv**: 0 %	Perforated plate (d_0 = 0.4 mm, 21 holes), Porous plates (d_0 = 30 & 100 µm)	H_C: 0.81 m; **Dc** : 0.081 m	ε_G, d_B, a	SB	None
Öztürk (1987)	**Gas**: Air; **Liquid**: Water, Ligroin, Tetralin, Aqueous solution Na_2SO_4 (0.8 M); **Solid**: PE (24.6 & 106 µm), PVC (82 µm), Activated carbon (5.4 µm), Kieselguhr (6.6 µm), Al_2O_3 (10.5 µm)	**P**: 0.1 MPa ; **T**: 293 K; u_G: 0 - 0.08 $m.s^{-1}$; u_L: 0 $m.s^{-1}$; **Cv**: 0 %	2 Single orifice tubes (d_0 = 3 & 0.9 mm)	H_C: 0.85 m; **Dc** : 0.095 m	ε_G, k_La	SB	$\varepsilon_G = K_1 u_G^{0.77}\,\mu_{SL}^{-0.21}$ $k_La = K_2 u_G^{0.75}\,\mu_{SL}^{-0.42}$ $\quad K_i\ depend\ on\ liquid\ phase$
Öztürk et al. (1987)	**Gas**: Air, N_2, CO_2, He, H_2; **Liquid**: Water, 17 organic liquids, 22 mixtures; **Solid**: none	**P**: 0.1 MPa ; **T**: 293 K; u_G: 0 - 0.1 $m.s^{-1}$; u_L: 0 $m.s^{-1}$; **Cv**: 0 %	Single orifice tube (d_0 = 3 mm)	H_C: 0.85 m; **Dc** : 0.095 m	ε_G, k_La	SB	$\frac{k_L a_i d_B^2}{D_{m,i,j}} = 0.62\left(\frac{\vartheta_L}{D_{m,i,j}}\right)^{1/2}\left(\frac{gd_B^2\rho_L}{\sigma_L}\right)^{0.33}\left(\frac{gd_B^3}{\vartheta_L^2}\right)^{0.29}\left(\frac{u_G}{\sqrt{gd_B}}\right)^{0.68}\left(\frac{\rho_G}{\rho_L}\right)^{0.04}$
Parasu Veera and Joshi (2000)	**Gas**: Air; **Liquid**: Water, Aqueous solutions of butanol and CMC; **Solid**: none	**P**: 0.1 MPa ; **T**: 298 K; u_G: 0.063 - 0.29 $m.s^{-1}$; u_L: 0 $m.s^{-1}$; **Cv**: 0 %	3 Perforated plates (d_0 = 1, 3, 25 mm, 623, 71, 1 holes, 0.42 % open area)	H_C: 0.85 - 2.31 m; **Dc** : 0.095 m	ε_G	SB	$\varepsilon_G = z_1 u_G^{z_2}\left(\frac{H_C}{D_C}\right)^{z_3}, z_1, z_2, z_3\ depend\ on\ liquid\ system$
Passos et al. (2015)	**Gas**: Air; **Liquid**: Water, Aqueous solutions of glucerin, Xanthan gum with various surfactants; **Solid**: none	**P**: 0.1 MPa ; **T**: 298 K; u_G: 0 - 0.035 $m.s^{-1}$; u_L: 0 $m.s^{-1}$; **Cv**: 0 %	Porous plates (d_0 = 40 µm)	H_C: 0.4 m; **Dc** : 0.09 m (rectangular)	ε_G, d_B	SB	$\varepsilon_G = 15.64\left[\left(\frac{u_G^2}{gD_C}\right)^{1.77}\left(\frac{gD_C^3}{\vartheta_L^2}\right)^{0.85}\left(\frac{gD_C^2\rho_L}{\sigma_L}\right)^{0.64}\left(\frac{D_0}{D_C}\right)^{4.27}\left(\frac{d_0}{D_0}\right)^{0.02}\right]^{0.19}$ $\frac{d_{32}}{D_0} = 0.58\left[\left(\frac{u_G^2\rho_L D_0}{\sigma_L}\right)^{-1.17}\left(\frac{u_G^2}{gD_C}\right)^{1.8}\left(\frac{u_G\rho_L D_0}{\mu_L}\right)^{0.1}\left(\frac{d_0}{D_0}\right)^{1.7}\right]^{0.2}$
Pjontek et al. (2014)	**Gas**: Air; **Liquid**: Water, Aqueous solution of ethanol (0.5%wt); **Solid**: none	**P**: 0.1 - 9.0 MPa ; **T**: 297 K; u_G: 0 - 0.15 $m.s^{-1}$; u_L: 0 - 0.091 $m.s^{-1}$; **Cv**: 0 %	Perforated plate (d_0 = 3.175 mm, 23 holes)	H_C: 0.385 - m; **Dc** : 0.385 m	ε_G	Co-C	None
Pohorecki et al. (1999)	**Gas**: N_2; **Liquid**: Water; **Solid**: none	**P**: 0.1 - 1.1 MPa ; **T**: 303 - 433 K; u_G: 0.002 - 0.020 $m.s^{-1}$; u_L: 0.0014 $m.s^{-1}$; **Cv**: 0 %	Perforated plates (1 - 27 orifices, d_0 = 1 - 5 mm)	H_C: 3.9 m; **Dc** : 0.304 m	ε_G, d_B, a	Co-C	$\varepsilon_G = 1.25\,u_G^{0.63} \qquad a = 1120\,u_G^{0.63}$
Pohorecki et al. (2001)	**Gas**: N_2; **Liquid**: Cyclohexane; **Solid**: none	**P**: 0.2 - 1.1 MPa ; **T**: 303 - 433 K; u_G: 0.002 - 0.055 $m.s^{-1}$; u_L: 0.0014 $m.s^{-1}$; **Cv**: 0 %	Perforated plates (1 - 27 orifices, d_0 = 1 - 5 mm)	H_C: 3.9 m; **Dc** : 0.304 m	ε_G, d_B, a	Co-C	$\varepsilon_G = 0.383\,u_G^{0.65}\,\sigma_L^{-0.52}$
Reilly et al. (1986)	**Gas**: Air, Ar, He; **Liquid**: Water, Varsol, Varsol + antifoam, trichloroethylene; **Solid**: Glass beads (71 - 745 µm)	**P**: 0.1 MPa ; **T**: 283 - 323 K; u_G: 0 - 0.35 $m.s^{-1}$; u_L: 0 $m.s^{-1}$; **Cv**: 0 - 25%	Perforated plate (293 orifices, d_0 = 1.5 mm), Single orifice pipe (d_0 = 25.4 mm), Spider sparger (6 orifices, d_0 = 13.4 mm)	H_C: 5 m; **Dc** : 0.30 m	ε_G	SB	$\varepsilon_G = 296\,u_G^{0.44}\,\sigma_L^{-0.16}\,\rho_L^{-0.98}\,\rho_G^{0.19} + 0.009$
Reilly et al. (1994)	**Gas**: Air, He, Ar, CO_2, N_2; **Liquid**: Water, Isopar-G, Isopar-M, trichloroethylene, Varsol; **Solid**: none	**P**: 0.1 - 1.1 MPa ; **T**: 298 K; u_G: 0.006 - 0.23 $m.s^{-1}$; u_L: 0 $m.s^{-1}$; **Cv**: 0%	Spider-type (4 arms, 16 holes, d_0 = 0.5 mm)	H_C: 2.7 m; **Dc** : 0.15 m	ε_G	SB	$\varepsilon_G = Z_1 M, homogeneous\ regime$ $\varepsilon_G = Z_1 M^{1/3}, heterogeneous\ regime$ $Z_i depend\ on\ gas\ and\ liquid\ properties$
Ruzicka et al. (2001)	**Gas**: Air; **Liquid**: Water; **Solid**: none	**P**: 0.1 MPa ; **T**: 298 K; u_G: 0 - 0.18 $m.s^{-1}$; u_L: 0 $m.s^{-1}$; **Cv**: 0 %	Perforated plate (0.2% open area, d_0 = 0.5 mm)	H_C: 0.1 - 1.2 m; **Dc** : 0.14, 0.29, 0.40 m	ε_G	SB	None
Şal et al. (2013)	**Gas**: Air; **Liquid**: Water; **Solid**: none	**P**: 0.1 MPa ; **T**: 296 K; u_G: 0 - 0.145 $m.s^{-1}$; u_L: 0 $m.s^{-1}$; **Cv**: 0 %	3 Perforated plates (Open Area = 1%, d_0 = 1,2,3 mm, 817, 217, 91 holes)	H_C: 1.5 m; **Dc** : 0.33 m	ε_G	SB	$\varepsilon_G = 0.2278\left(\frac{u_G^2}{gd_0}\right)^{0.7767}\left(\frac{gd_0^3}{\vartheta_L^2}\right)^{0.3649}\left(\frac{gd_0^2\rho_L}{\sigma_L}\right)^{-0.3916}\left(\frac{d_0}{D_C}\right)^{0.4780}\left(\frac{D_C^2 u_G^2\rho_L}{d_0^3\sigma_L N_0^2}\right)^{-0.2402}$
Sangnimnuan et al. (1984)	**Gas**: Air; **Liquid**: Tetralin; **Solid**: Coal	**P**: 4.5 - 15 MPa ; **T**: 437 - 657 K; u_G: 0.012 - 0.02 $m.s^{-1}$; u_L: 0.001 - 0.003 $m.s^{-1}$; **Cv**: Unknown	Unknown	$H_C/D_C > 5$; **Dc** : 0.019 m	ε_G, $D_{ax,L}$	Co-C	$D_{ax,L} = 15.4\,u_G^{1.53}$
Schäfer et al. (2002)	**Gas**: N_2; **Liquid**: Water, Cyclohexane, Ethanol, Cyclohexanone, Cyclohexanol; **Solid**: none	**P**: 0.1 - 5.0 MPa ; **T**: 298 - 448 K; u_G: 0 - 0.39 $m.s^{-1}$; u_L: 0 $m.s^{-1}$; **Cv**: 0 %	Capillary sparger (19 capillaries, 2,5 cm long, d_0 = 150 µm), Porous plate (d_0 = 11, 32 and 70 µm), Ring sparger	H_C: Unknown; **Dc** : 0.054 m	d_B	SB	None
Shah et al. (2012)	**Gas**: Air, N_2; **Liquid**: Water, Aqueous solutions of PEG; **Solid**: none	**P**: 0.1 MPa ; **T**: 298 K; u_G: 0.021 - 0.1052 $m.s^{-1}$; u_L: 0.0005 - 0.0020 $m.s^{-1}$; **Cv**: 0 %	Perforated plate (d_0 = 0.5 mm)	H_C: 2 m; **Dc** : 0.29 m	ε_G, k_La, $D_{ax,L}$	Coun-C	$\varepsilon_G = 0.072\left(\frac{u_G^2}{gD_C}\right)^{0.5}\left(\frac{u_L^2}{gD_C}\right)^{-0.018}\left(\frac{gD_C^3}{\vartheta_L^2}\right)^{0.087}$ $\frac{u_L D_C}{(1-\varepsilon_G)D_{ax,L}} = 1.5\left(\frac{u_G^2}{gD_C}\right)^{-0.740}\left(\frac{u_L^2}{gD_C}\right)^{0.560}\left(\frac{gD_C^3}{\vartheta_L^2}\right)^{-0.016}$ $\frac{k_L a D_C}{u_L} = 0.0029\left(\frac{u_G^2}{gD_C}\right)^{0.301}\left(\frac{u_L^2}{gD_C}\right)^{-0.511}\left(\frac{gD_C^3}{\vartheta_L^2}\right)^{0.120}$
Shaikh and Al-Dahhan (2005)	**Gas**: Air; **Liquid**: Therminol LT; **Solid**: none	**P**: 0.1 - 1 MPa ; **T**: 298 K; u_G: 0.01 - 0.20 $m.s^{-1}$; u_L: 0 $m.s^{-1}$; **Cv**: 0 %	Unknown	H_C: 2.5 m; **Dc** : 0.162 m	ε_G	SB	None
Shawaqfeh (2003)	**Gas**: Air; **Liquid**: Water; **Solid**: none	**P**: 0.1 MPa ; **T**: 298 K; u_G: 0.094 - 0.41 $m.s^{-1}$; u_L: 0 - 0.0116 $m.s^{-1}$; **Cv**: 0 %	Single orifice-nozzle, d_0 = 2 cm	H_C: 0.63 m; **Dc** : 0.074 m	ε_G, $D_{ax,L}$	Co-C	$\varepsilon_G = \frac{u_G}{0.472 + 1.243 u_G} \qquad D_{ax,L} = 0.014\,u_G^{0.43}\exp(-48.85 u_L)$
Simonnet et al. (2007)	**Gas**: Air; **Liquid**: Water; **Solid**: none	**P**: 0.1 MPa ; **T**: 298 K; u_G: 0- 0.08 $m.s^{-1}$; u_L: 0 - 0.10 $m.s^{-1}$; **Cv**: 0 %	Capillary sparger (133 capillaries, d_0 = 0.44 mm)	H_C: 1.0 m; **Dc** : 0.1 m (rectangular)	ε_G, d_B	Co-C	None
Smith et al. (1996)	**Gas**: Air; **Liquid**: Water, Mineral Oil; **Solid**: none	**P**: 0.1 MPa ; **T**: 298 K; u_G: 0 - 0.05 $m.s^{-1}$; u_L: 0 - 0.017 $m.s^{-1}$; **Cv**: 0 %	Porous plate (d_0 = 1.7 µm), 2 Annular shear spargers (d_0 = 2 µm, porous area = 92.9 & 46.5 cm^2), Membrane sparger	H_C: 1.5, 2.1 m; **Dc** : 0.1, 0.14 m	ε_G, d_B, a, $D_{ax,L}$	Coun-C	None
Soong et al. (1997)	**Gas**: N_2; **Liquid**: Drakeol-10; **Solid**: none	**P**: 0.1 - 1.36 MPa ; **T**: 293 - 538 K; u_G: 0 - 0.09 $m.s^{-1}$; u_L: 0 $m.s^{-1}$; **Cv**: 0 %	Perforated plate (d_0 = 1 mm, 5 holes)	H_C: 2.44 m; **Dc** : 0.10 m	ε_G, d_B	SB	None
Stegeman et al. (1996)	**Gas**: N_2, N_2/CO_2 mixture; **Liquid**: Water, Aqueous solutions of DEA + ETG; **Solid**: none	**P**: 0.1 - 7.0 MPa ; **T**: 298 K; u_G: 0 - 0.06 $m.s^{-1}$; u_L: Unknown; **Cv**: 0 %	Perforated plate (d_0 = 0.4 mm, 284 holes)	H_C: 0.64 m; **Dc** : 0.156 m	ε_G, a	Coun-C	None
Tarmy et al. (1984)	**Gas**: H_2; **Liquid**: n-Heptane; **Solid**: coal	**P**: 0.12 - 0.62 MPa ; **T**: 298 K; u_G: 0 - 0.12 $m.s^{-1}$; u_L: Unknown; **Cv**: Unknown	Single orifice nozzle (d_0 = 7.0 mm)	H_C: Unknown; **Dc** : 0.024- 0.61 m	ε_G, $D_{ax,L}$	Co-C	None
Therning and Rasmuson (2001)	**Gas**: Air; **Liquid**: Water; **Solid**: Plastic ball rings packing	**P**: 0.1 - 0.66 MPa ; **T**: 293 K; u_G: 0.03 - 0.17 $m.s^{-1}$; u_L: 0 $cm.s^{-1}$; **Cv**: 0 %	Perforated plate (d_0 = 1.5 mm, 0.2% open area)	H_C: 3.2 m; **Dc** : 0.154 - 0.2 m	ε_G, $D_{ax,L}$	SB	None

Table 1 – (*Continued*)

Thorat and Joshi (2004)	**Gas**: Air; **Liquid**: Water, Aqueous solutions (0.2 M NaCl, Carboxymethyl cellulose 1%w); **Solid**: none	**P**: 0.1 MPa ; **T**: 298 K; u_G: 0 - 0.3 $m.s^{-1}$; u_L: 0 $m.s^{-1}$; **Cv**: 0 %	22 Perforated plates (Open area = 0.13 - 1.68 %, d_0 = 0.8 - 50 mm)	H_C: 0.385 - 3.08 m; **Dc** : 0.385 m	ε_G	SB	None
Urseanu et al. (2003)	**Gas**: N_2; **Liquid**: Water, Aqueous solutions of glucose, Tellus Oil; **Solid**: none	**P**: 0.1 - 1.0 MPa ; **T**: 298 K; u_G: 0 - 0.4 $m.s^{-1}$; u_L: 0 $m.s^{-1}$; **Cv**: 0 %	Perforated plate (d_0 = 0.5 mm, 200 holes), Ring sparger (d_0 = 1.5 mm, 16 holes)	H_C: 1.22 m; **Dc** : 0.15 - 0.23 m	ε_G	SB	$\varepsilon_G = 0.21\, u_G^{0.58} \mu_L^{-0.12} D_C^{-0.18} \rho_G^{0.3exp(-9\mu_L)}$
Vandu et al. (2004)	**Gas**: Air; **Liquid**: Paraffin Oil; **Solid**: Alumina based-catalyst	**P**: 0.1 MPa ; **T**: 298 K; u_G: 0 - 0.4 $m.s^{-1}$; u_L: 0 $m.s^{-1}$; **Cv**: 0 - 25%	Perforated plate (199 holes, d_0 = 0.5 mm)	H_C: 1.34 - 1.36 m; **Dc** : 0.1 m	ε_G, k_La	SB	None
Vázquez et al. (2000a)	**Gas**: CO_2, O_2; **Liquid**: Aqueous solution of Na_2CO_3 (0.5 M) & $NaHCO_3$ (0.5 M), Aqueous solution of sodium sulfite (0.6 M) + cobalt sulfate (3.5.10-5 mol/L), Aqueous solution of sodium dithionite (0.1 M) + sodium hydroxide (1 M), ; **Additives**: $AsNaO_2$ (0 - 10-2 mol/L) + Sodium Lauryl sulfate (0 - 5.10-4%w) + Sucrose (0 - 85.7 g/L)	**P**: 0.1 MPa ; **T**: 298 K; u_G: 0 - 0.0012 $m.s^{-1}$; u_L: 0 $m.s^{-1}$; **Cv**: 0 %	3 Porous plates (d_0 = 40 - 200 µm)	H_C: 1.086 m; **Dc** : 0.113 m	a	SB	$a = K_0 \left(\frac{D_C u_G \rho_L}{\mu_L}\right)^{0.98} \left(\frac{u_G^2}{gD_C}\right)^{0.09} \left(\frac{gD_C{}^2\rho_L}{\sigma_L}\right)^{-0.70} \left(\frac{\vartheta_L}{D_{m,i,j}}\right)^{0.57} \left(\frac{d_P}{D_C}\right)^{-0.19}$ K_0 *is an adjustment parameter depending on the measurement method*
Vial et al. (2001)	**Gas**: Air; **Liquid**: Water; **Solid**: none	**P**: 0.1 MPa ; **T**: 298 K; u_G: 0 - 0.15 $m.s^{-1}$; u_L: 0 $m.s^{-1}$; **Cv**: 0 %	Multi-orifice nozzle (62 holes, d_0 = 1 mm), Single orifice-nozzle (d_0 = 5 mm)	H_C: 2 m; **Dc** : 0.1 m	ε_G	SB	None
Voyer and Miller (1968)	**Gas**: Air, CO_2; **Liquid**: Water, Aqueous solution of NaOH; **Solid**: none	**P**: 0.1 MPa ; **T**: 298 K; u_G: 0.09 - 0.63 $m.s^{-1}$; u_L: 0.015 $m.s^{-1}$; **Cv**: 0 %	Perforated plate (50 holes, d_0 = 3,81 mm)	H_C: 1.026 m; **Dc** : 0.14 m	k_L, a	Co-C	None
Wilkinson and Van Dierendonck (1990)	**Gas**: N_2, Ar, He, CO_2, SF_6; **Liquid**: Water; **Solid**: none	**P**: 0.1 - 2.0 MPa ; **T**: 293 K; u_G: 0 - 0.17 $m.s^{-1}$; u_L: 0 $m.s^{-1}$; **Cv**: 0 %	Ring spargers (19 - 37 holes, d_0 = 10 - 2 mm)	H_C: 1.5, 2.0 m; **Dc** : 0.16 m	ε_G	SB	None
Wilkinson et al. (1992)	**Gas**: N_2; **Liquid**: N-heptane, Water, Monoethylene glycol; **Solid**: none	**P**: 0.1 - 2.0 MPa ; **T**: 293 - 313 K; u_G: 0 - 0.28 $m.s^{-1}$; u_L: 0 $m.s^{-1}$; **Cv**: 0 %	Ring sparger (4 holes, d_0 = 7 mm)	H_C: 1.5 m; **Dc** : 0.15, 0.23 m	ε_G	SB	$\varepsilon_G = \frac{u_G}{u_{BS}}$, *homogeneous regime* $\varepsilon_G = \frac{u_{G,trans}}{u_{BS}} + \frac{(u_G - u_{G,trans})}{u_{BL}}$, *transition and heterogeneous regime*
Wilkinson et al. (1993)	**Gas**: N_2; **Liquid**: N-heptane, Water, Monoethylene glycol; **Solid**: none	**P**: 0.1 - 1.5 MPa ; **T**: 298 K; u_G: 0 - 0.3 $m.s^{-1}$; u_L: 0 $m.s^{-1}$; **Cv**: 0 %	Ring sparger	H_C: 1.5 m; **Dc** : 0.158 m	$D_{ax,L}$	SB	None
Wilkinson et al. (1994)	**Gas**: N_2; **Liquid**: N-heptane, Water, Monoethylene glycol, Aqueous solution of sodium sulfite (0.8 M); **Solid**: none	**P**: 0.1 - 2.0 MPa ; **T**: 298 K; u_G: 0 - 0.28 $m.s^{-1}$; u_L: 0 $m.s^{-1}$; **Cv**: 0 %	Ring sparger (19 holes, d_0 = 10 mm)	H_C: 1.5 m; **Dc** : 0.15, 0.158, 0.23 m	ε_G, d_B, k_La	SB	$\frac{gd_{32}{}^2\rho_L}{\sigma_L} = 8.8\left(\frac{u_G\mu_L}{\sigma_L}\right)^{-0.04}\left(\frac{g\mu_L{}^4}{\sigma_L{}^3\rho_L}\right)^{0.12}\left(\frac{\rho_G}{\rho_L}\right)^{-0.22}$
Xue et al. (2008)	**Gas**: Air; **Liquid**: Water; **Solid**: none	**P**: 0.1 - 1.0 MPa ; **T**: 293 K; u_G: 0.02 - 0.60 $m.s^{-1}$; u_L: 0 $m.s^{-1}$; **Cv**: 0 %	Perforated plate (Open Area = 0.15%, d_0 = 0.5 mm, 163 holes), Perforated plate (Open Area = 1.0%, d_0 = 1.32 mm, 163 holes), Cross sparger (4 holes, d_0 = 2.54 mm, Open Area = 0.1%)	H_C: 1.8 m; **Dc** : 0.1626 m	ε_G, d_B, a	SB	None
Yang et al. (2001)	**Gas**: CO-H_2-N_2; **Liquid**: Liquid paraffin; **Solid**: Silica gel powder (134 µm)	**P**: 1 - 5 MPa ; **T**: 293 - 523 K; u_G: 0 - 0.025 $m.s^{-1}$; u_L: 0 $m.s^{-1}$; **Cv**: 0 -20 %	Unknown	H_C: 0.48 m; **Dc** : 0.037 m	k_L, a	SB	$aD_C = 1.271.10^{-4}\left(\frac{P}{\rho_{SL}u_G{}^2}\right)^{0.204}\left(\frac{D_C u_G \rho_{SL}}{\mu_{SL}}\right)^{0.638}\left(\frac{\vartheta_{SL}}{D_{m,i,j}}\right)^{0.826}$ $\frac{k_L D_C}{D_{m,i,j}} = H_1\left(\frac{P}{\rho_{SL}u_G{}^2}\right)^{H_2}\left(\frac{D_C u_G \rho_{SL}}{\mu_{SL}}\right)^{H_3}\left(\frac{\vartheta_{SL}}{D_{m,i,j}}\right)^{H_4}$, H_i *depend on gas studied*
Yang and Fan (2003)	**Gas**: N_2; **Liquid**: Water, Paratherm NF; **Solid**: none	**P**: 0.1 - 10.3 MPa ; **T**: 300 K; u_G: 0 - 0.4 $m.s^{-1}$; u_L: 0 - 0.01 $m.s^{-1}$; **Cv**: 0 %	2 Perforated plates (45 & 120, d_0 = 1.6 mm), Porous plate (d_0 = 200 µm), Multi-orifice nozzle (13 holes, d_0 = 3.2 mm)	H_C: 0.4572 - 1.1176 m; **Dc** : 0.0508, 0.1016 m	ε_G, $D_{ax,L}$	Co-C	None
Zahradník et al. (1997)	**Gas**: Air, Helium; **Liquid**: Water, Aqueous solutions (electrolytes, aliphatic alcohols, saccharose); **Solid**: none	**P**: 0.1 MPa; **T**: 298 K; u_G: 0-0.3 $m.s^{-1}$; u_L: 0 $m.s^{-1}$; C_x: 0%	Perforated plates (Open Area: 0.2 - 2%, d_0 = 0.5 -1.6 mm), Sintered metal/glass plates (d_0 = 100-250 µm), Perforated rubber plates (d_0 = 2 - 10 mm)	H_C: 0.25 - 1.5 m; D_C: 0.14, 0.15, 0.29m	ε_G, k_La, $D_{ax,L}$	SB	$\varepsilon_G(1-\varepsilon_G) = 0.79\frac{u_G}{u_{B,\infty}}$, *homogeneous regime* $\varepsilon_G = \frac{u_G}{2.02\,u_G + u_{B,\infty}}$, *heterogeneous regime*

et al., 2001; Zahradník et al., 1997). The hydrodynamic of the bubble column is actually not well-known and difficult to predict because most of these studies only focus on two to four parameters and are system-dependant.

In order to design and optimise WAO processes, it is then necessary to predict the mass transfer efficiency of the bubble column. However, operating WAO processes in bubble columns has never been studied in the literature. Moreover only few studies have been conducted at pressures over 3 MPa (for high pressure studies see Behkish et al., 2007; Clark, 1990; De Bruijn et al., 1988; Fan et al., 1999; Hashemi et al., 2009; Idogawa et al., 1985; 1986; Ishibashi et al., 2001; Jiang et al., 1995; Jin et al., 2004; Jordan and Schumpe, 2001; Lau et al., 2004; Lin and Fan, 1999; Lin et al., 2001, 1998; Luo et al., 1999; Maalej et al., 2003; Neubauer, 1977; Onozaki et al., 2000; Oyevaar et al., 1991; Pjontek et al., 2014; Sangnimnuan et al., 1984; Schäfer et al., 2002; Yang and Fan, 2003; Yang et al., 2001) or at temperatures over 373 K (for high temperature studies see Behkish et al., 2007; Clark, 1990; De Bruijn et al., 1988; Deckwer et al., 1980; Ishibashi et al., 2001; Jin et al., 2004, 2014; Onozaki et al., 2000; Pohorecki et al., 1999, 2001; Sangnimnuan et al., 1984; Schäfer et al., 2002; Soong et al., 1997; Yang et al., 2001) and seldom in the air-water or oxygen-water systems (Table 1). It is then necessary to collect and to synthesize the results obtained on the operating of bubble columns at lower conditions of pressure and temperature. Many studies are operated in semi-batch mode (batch for liquid, continuous for gas phase) and only few studies deals with continuous mode (see above). The degree of mixing in bubble columns is rarely studied and the determination of liquid or gas axial dispersion coefficient is rarely performed (Bouaifi et al., 2001; Chilekar, 2007; Forret et al., 2003; Hikita and Kikukawa, 1974; Holcombe et al., 1983; Houzelot et al., 1983; Kölbel et al., 1971; Krishna et al., 1999a; Lorenz et al., 2005; Ohki and Inoue, 1970; Onozaki et al., 2000; Sangnimnuan et al., 1984; Shah et al., 2012; Shawaqfeh, 2003; Smith et al., 1996; Tarmy et al., 1984; Therning and Rasmuson, 2001; Wilkinson et al., 1993; Yang and Fan, 2003; Zahradník et al., 1997). The main objective of this review is to find the relevant parameters for the design of WAO processes and to provide bases for operating bubble columns in continuous mode at high pressures and temperatures. Thus, the effect of pressure, temperature and superficial liquid velocity on gas holdup, mass transfer coefficient, interfacial area, volumetric mass transfer coefficient and liquid axial dispersion coefficient will be extensively studied. The effect of other parameters such as superficial gas velocity, sparger and column design and working mode (semi-batch, co- or counter-current), which have been largely discussed before in literature, will be summarized in the light of WAO processes. In the first part, the different mechanisms that govern bubble columns will be detailed. The second part deals with the parametric study of gas holdup, mass transfer properties and liquid axial dispersion coefficient. The results presented will be linked to the different mechanisms and the tendencies for high pressure processes will be reported. Heat transfer coefficient and correlations available for the estimation of bubble column properties (such as mass transfer coefficients, gas and liquid holdup and heat transfer coefficient) are not studied in this review as they have already been the subject of recent articles (Hulet et al., 2009; Jhawar and Prakash, 2011; Rollbusch et al., 2015; Shaikh and Al-Dahhan, 2013).

2. Bubble columns governing mechanisms

2.1. Hydrodynamic studies

In literature, the study of the hydrodynamic of bubble columns at high pressures and/or at high temperatures is limited (Chilekar, 2007, 2010; Cui, 2005; Han and Al-Dahhan, 2007; Hashemi et al., 2009; Kang et al., 2000; Kemoun et al., 2001; Krishna et al., 1991; Letzel et al., 1997; Lin et al., 2001, 1998; Reilly et al., 1994; Shaikh and Al-Dahhan, 2005; Tarmy et al., 1984). In order to characterise and discuss the flow in bubble columns, the tendencies at atmospheric pressure and temperature will be reported. Authors commonly accept that four different flow regimes exist in the column whose limit depends on operating conditions. Those four regimes are schematically represented on Fig. 1.

Fig. 1 shows that two main flow regimes can be identified: the homogeneous regime also called 'bubbly flow regime' and the heterogeneous regime. The homogeneous regime is characterized by a narrowed bubble size distribution. Two sub-regimes can be distinguished, depending on the span of the bubble size distribution. In the case of a narrow bubble size distribution, the flow is called 'perfect bubbly'. The 'imperfect bubbly' flow is characterized by a larger bubble size distribution (Joshi et al., 1998; Kantarci et al., 2005). In the homogeneous regime, breakage and coalescence phenomenon do not control the flow which is mainly determined by the primary bubble size at the gas distributor. This kind of regime is usually observed at small superficial gas velocity. The turbulence is mainly attributed to bubble drag, resulting in a liquid microcirculation. Between the homogeneous and heterogeneous regimes, a transition regime where a macrocirculation appears could be observed. The heterogeneous regime is, on the contrary, characterised by a larger bubble size distribution where small and large bubbles coexist. In this regime, breakage and coalescence phenomenon control the flow which is usually not controlled by the primary bubble at the gas distributor (Kantarci et al., 2005). The first heterogeneous regime (also called "churn-turbulent" regime) is characterized by the existence of a liquid macro-circulation due to the non homogeneous radial profile of gas distribution: the liquid is rising in the centre of the column and is getting down near the wall (Forret et al., 2003; Kantarci et al., 2005; Smith et al., 1996; Xue et al., 2008; Yang and Fan, 2003; Zahradník et al., 1997). This movement is the main cause of turbulence in the heterogeneous flow. The turbulence attributed to drag force from bubbles still exists but is not predominant. The slug flow presented on Fig. 1 is a specific regime which can be observed at high superficial gas velocity and small column diameter (typically less than 15 cm (Kantarci et al., 2005; Shawaqfeh, 2003)). In this regime, bubble plugs can appear due to the stabilisation of bubbles at the wall.

As the mechanisms governing the homogeneous and heterogeneous regimes are different, effects of the parameters could be different from one regime to the other. It is then important to know precisely the hydrodynamic regime in order to determine the main parameter. The transition between the two regimes is then an important factor to take into account.

2.2. Transition between homogeneous and heterogeneous regime

The transition between the two different regimes in bubble columns has mostly been studied at ambient pressure and temperature. Diagrams are often used to find the adequate operating conditions to reach a certain regime and are presented in Fig. 2.

For an air/water system, the transition superficial gas velocity at ambient pressure and temperature is around 4 cm s^{-1}, depending on gas sparger and column design. This is shown by many authors (Kantarci et al., 2005; Rollbusch et al., 2015; Simonnet et al., 2007; Zahradník et al., 1997).

Two transitions are typically studied in literature: the transition between the homogeneous and the transition regime and the transition between the transition regime and the heterogeneous regime. However some authors do not mention the transition regime and a global transition between homogeneous and heterogeneous is studied.

Among the different methods used in literature to study transition velocity, the simplest and most commonly used in literature is the drift-flux method which is based on a graphical determination of the transition. The drift-flux (q_D) is defined by Eq. (1):

$$q_D = \varepsilon_G(1-\varepsilon_G)\left(\frac{u_G}{\varepsilon_G} \pm \frac{u_L}{1-\varepsilon_G}\right) \quad (1)$$

In Eq. (1) the sign is + for co-current mode and − for counter-current mode. Two methods of drift-flux have been reported by Gourich et al. (2006): the Wallis method which is based on the drawing of q_D versus gas holdup (ε_G) and the Zuber and Findlay method which is based on the drawing of u_G/ε_G versus u_s. The determination of the transition velocity is then simply done by measuring gas holdup and by finding the changes in slope on the curves. Gourich et al. (2006) reported that these methods are efficient to study the transition between homogeneous and transition regime. Nevertheless these methods can be difficult to use in the case of the transition between transition and heterogeneous regime. Experimental results indicate that Zuber and Findlay method can be more efficient than Wallis method in the case of viscous fluids. Gourich et al. (2006) reported that the most efficient method to study the transition is the spectral analysis of pressure fluctuations. It consists in the analysis of pressure fluctuations measured by pressure sensors on the column, calculating the PSDF (Power Spectral Density Function) and observing its variation versus frequency. The different regimes are characterised by different peak at specified frequency (a peak at 0.1 Hz is reported to be characteristic of the homogeneous regime in semi-batch mode). This method has been successfully used to determine transition by different authors (Chilekar, 2007; Gourich et al., 2006; Kang et al., 1999; Vial et al., 2001), in the case of semi-batch operated column but never in continuous mode where the 0.1 Hz peak could not appear.

Regime transition depends on operating conditions. The influence of pressure and temperature has been studied at pressure up to 15.2 MPa and temperature up to 351 K. Lin et al. (1999), show that transition velocity between homogeneous and heterogeneous regime increases quickly while increasing pressure and temperature. They used satistic analysis of pressure fluctuations and Wallis plot to study the transition. While the effect of temperature is linear under their conditions, a plateau is observed at pressures over 10 MPa, this plateau being more pronounced at high temperatures. It can be deduced that under those conditions (same velocities) and at higher pressure (up to 30 MPa) and temperature (up to 573 K) many processes will work mainly in homogeneous regime. The effect of pressure on transition velocity

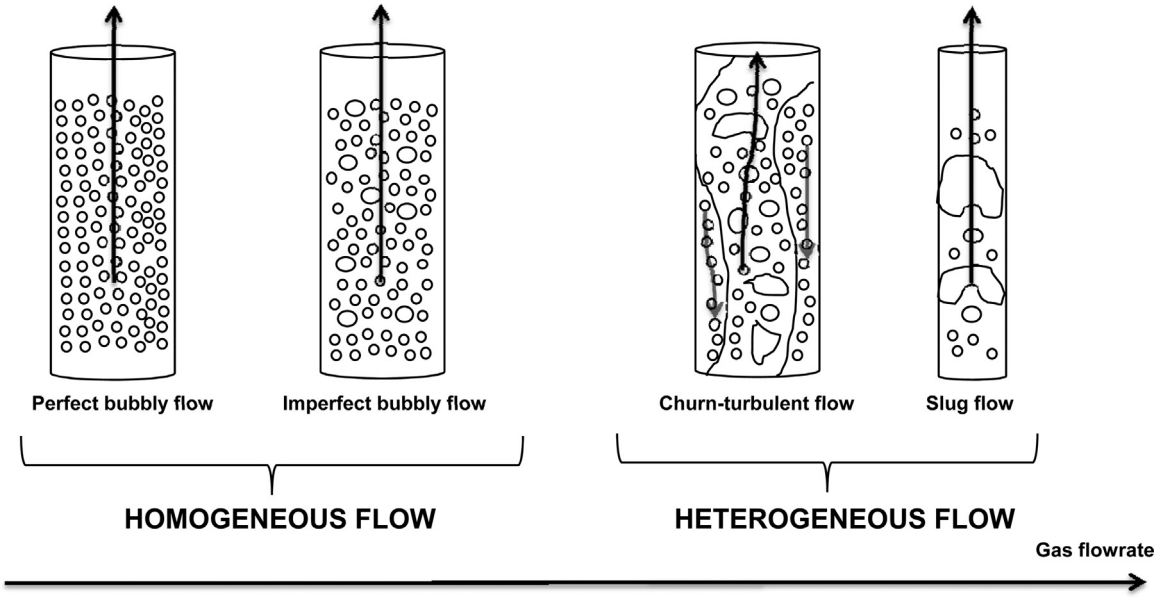

Fig. 1 – Main flow regimes in bubble columns.

has also been reported more recently by Han and Al-Dahhan (2007) who observed an increase of regime transition velocity for pressure up to 1 MPa for an air–water system. The increase is faster for their conditions as they reported a transition velocity of 15 cm s^{-1} at 298 K instead of 1 cm s^{-1} for Lin et al. (1999) under the same conditions of pressure and temperature. Shaikh and Al-Dahhan (2005) also observed transition velocity at 1 MPa between 9 and 14 cm s^{-1} for the air/Therminol LT system. The differences could be attributed to the effect of other parameters: gas sparger, column design and system studied (Table 1). In fact, the differences could be mainly attributed to the viscosity of the liquid phase: Paratherm NF is more viscous than water and Therminol LT (22 mPa s for Paratherm NF and 0.88 mPa s for Therminol LT at ambient conditions), which can results in an increase of bubble size. Pressure and temperature would have attenuated effects. These points will be discussed in Section 3.1.4. Other authors also report an increase of the transition velocity while increasing pressure (Chilekar, 2007, 2010; Clark, 1990; Cui, 2005; Hashemi et al., 2009; Kang et al., 2000; Kemoun et al., 2001; Krishna and Sie, 2000; Krishna et al., 1991; Kumar et al., 2012b; Letzel et al., 1997, 1998; Lin et al., 2001; Reilly et al., 1994; Tarmy et al., 1984; Wilkinson et al., 1992). Chilekar et al. (2007, 2010) and Krishna et al. (1991, 1994) report that the increase of gas density is the phenomenon responsible for this increase (effect of pressure on gas holdup in Section 3.1.3).

Şal et al. (2013), Vial et al. (2001), Thorat and Joshi (2005) and Ohki and Inoue (1970) report an increase of the transition velocity while changing the sparger properties (i.e., decreasing orifice diameter and increasing open area, see Section 3.1.7). Şal et al. (2013) report that decreasing the sparger orifice diameter leads to a decrease of the bubble size (Section 3.1.7)

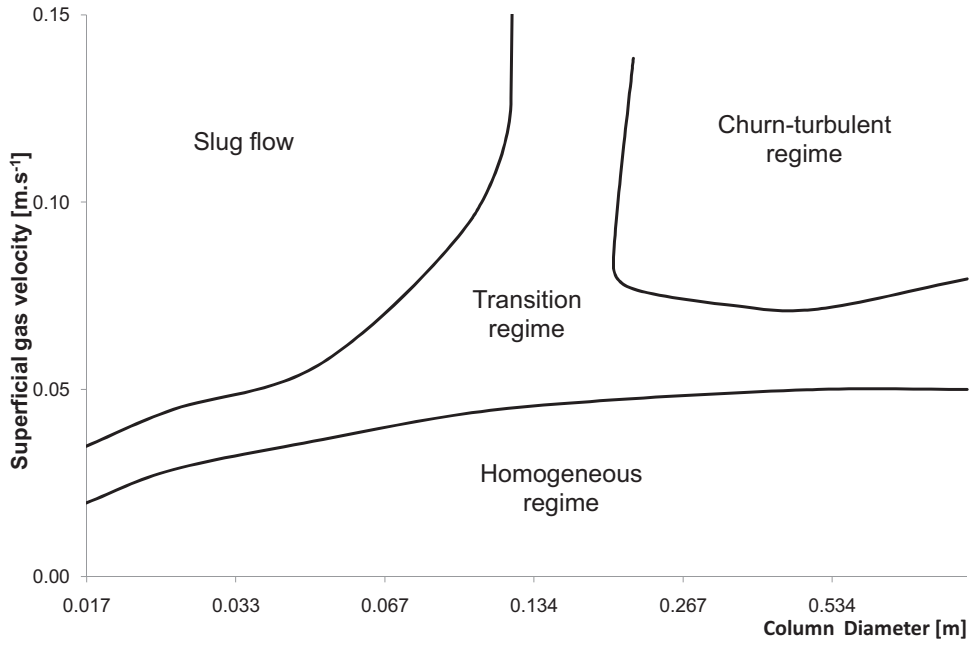

Fig. 2 – Flow regime diagram at ambient pressure and temperature. Air/water system. Adapted from (Kantarci et al., 2005).

that results on an increase of 10% of the transition velocity. These results have also been reported by Vial et al. (2001) and Thorat and Joshi (2004). They also found that regime transition depends on the H_c/D_c ratio: an increase of this ratio leads to a decrease of the gas holdup at transition. Ruzicka et al. (2001) show the same tendencies for H_c at constant diameter and also show that transition depends on D_c at constant height: increasing the diameter results on an increase of the transition point. They study the influence of the H_c/D_c ratio on the transition and found that above 5 critical gas flowrate and critical gas holdup are nearly constant. This is related to the effect of the H_c/D_c ratio on gas holdup (Section 3.1.7.3).

Cui (2005), Reilly et al. (1994) and Chilekar (2007) report higher transition velocities for low surface tension liquids (Norpar 15, Isopar-M, Isopar-G, Varsol) compared to water. Cui (2005) attributed this effect to a decrease of the bubble size when working with lower surface tension fluids (Section 3.1.4). An increase of the transition velocity is also observed for aqueous solutions of ethanol by Krishna et al. (2000) which is related to the surface tension effect of alcohols in aqueous solutions (see Section 3.1.4). Passos et al. (2015) obtained higher transition velocities by adding surfactants in Newtonian and Non-Newtonian liquids. The transition velocity is higher for lower solution surface tension. Jin et al. (2007b) report a slight increase (5.8%) of the transition velocity while increasing superficial liquid velocity (from 0 to 0.011 m s^{-1}) in a co-current bubble column at ambient pressure and temperature. This is attributed to an increased stability of the flow in co-current mode.

At high pressures and temperatures and for pressures over 10 MPa, temperature, physical properties of the liquid phase, superficial liquid velocity and sparger properties are the main parameters governing the transition.

2.3. Description of bubble column mechanisms

2.3.1. Bubble formation at the gas distributor

Among the different correlation available for estimation of bubble size at the gas sparger, correlation of Davidson et al. (1960) does not predict the effect of pressure. However, it shows that the primary bubble size increases when the diameter of the orifice of the sparger and the surface tension increase and the difference of density decreases. A more representative equation is the one of Bhavaraju et al. (1978) which takes more parameters into account and depends on two adimensionnal numbers. Given the expression of these two numbers (Appendix), it shows that primary bubble size increases with an increase of surface tension, viscosity, orifice diameter and superficial gas velocity. However, it does not predict any effect of pressure. It is given by Eq. (2).

$$\frac{d_{b,0}}{d_0} = 3.23 Re_{OL}^{-0.1} Fr_0^{0.21} \quad (2)$$

Those parameters are not the only ones that influence primary bubble size: an increase in the open area (or orifice number at constant diameter or the opposite) increases primary bubble size. This is frequently attributed to coalescence between two bubbles that are formed at two adjacent holes (Miyahara and Hayashino, 1983). A review dealing with the formation of bubbles at the sparger and their rise velocities is available elsewhere (Kulkarni and Joshi, 2005).

2.3.2. Bubble coalescence

Coalescence between two bubbles can be divided in three steps: collision between two bubbles with formation of a liquid film, decrease of the thickness of this film and then disappearance of the film with coalescence. This coalescence can only happen if the contact time of the two coalescing bubbles (t_B) is higher than the time needed to completely drain the film. Contact between two bubbles can be well represented by a collision frequency which increases when the number of bubbles is high and turbulence high. Among different authors, Lin et al. (1998) proposed the Eq. (3) for the speed of film drainage at pressures up to 15 MPa and temperature up to 353 K.

$$v_h \propto \frac{8\gamma_L^3}{3\mu_L r_h^2} \frac{4\sigma_L}{d_b} \quad (3)$$

This equation shows that film drainage speed increases (so coalescence rate increases) when viscosity and bubble size decrease and surface tension increases. Contact time for coalescence (t_B) depends mainly on the turbulence and physical and chemical properties of the liquid. An increase in viscosity contributes to reduce turbulence in the system and so to increase t_B and coalescence (Mouza et al., 2005). In fact, Eq. (3) predicts that viscosity has two possible way of influence: an increase can be favourable because of the influence of contact time (t_B) but can be negative via its influence on film drainage film and collision frequency.

2.3.3. Bubble breakage

An approach frequently used in literature (Lin et al., 1998) is to suppose that bubbles move without interaction in a stagnant liquid without external constraints. Rayleigh–Taylor theory of instability becomes the mechanism responsible for breakage. If the gas above the horizontal interface is denser than the liquid, this theory demonstrates that the interface is unstable, respect to perturbations with wavelengths superior to a critical value. Lin et al. (1998) affirm that it does not predict well the effect of pressure because they demonstrate that an increase of gas density stabilised the bubble. Another approach relies on Kelvin–Helmholtz theory of instability (Wilkinson and Van Dierendonck, 1990). This theory suggests that when a velocity difference exists at an interface thermally stable, a wavy movement is formed at the interface. Lin et al. (1998) demonstrate that this approach results in a better estimation than the Rayleigh–Taylor theory but it is not yet satisfactory. Hinze (1955) have shown that breakage happens if hydrodynamic forces become higher than surface tension forces. They assume that turbulent eddies generate velocity fluctuations which are responsible for breakage. They linked breakage to the Weber number and propose Eq. (4) to calculate a critical Weber number. At higher Weber number breakage happens, Weber number being calculated by Eq. (5).

$$We_C = \rho_L u^2 d_{b,max}/\sigma_L \quad (4)$$

$$We = \frac{\rho_L u_{G^2} d_b}{\sigma_L} \quad (5)$$

The critical Weber number must be determined experimentally measuring $d_{b,\,max}$ and depends on the operating conditions of the system. Several authors then proposed empirical or semi-empirical correlation to estimate $d_{b,max}$. Lin et al. (1998) show that classical theory that use this concept underestimate maximal bubble size and does not take into

account the viscosity and pressure effects. These authors proposed the correlation given by Eqs. (6) and (7) to estimate maximum bubble size by using an approach similar to Hinze and by correcting the critical Weber number by incorporating a term that takes into account the densities of gas and liquid and a viscosity term.

$$d_{b,max} = We_C'^{0.6}[\sigma_L^{0.5}/(g^{0.4}\rho_L^{0.4}\rho_G^{0.2}u_G^{0.4})](\mu_L/\mu_G)^{0.1} \quad (6)$$

$$\text{with } We_C' = We_C(\rho_L/\rho_G)^{1/3} \quad (7)$$

This indicates that maximum bubble size decreases with an increase in gas density and viscosity and a decrease in liquid viscosity and surface tension. According to Eqs. (6) and (7) the critical diameter increases when gas velocity decreases. In fact, the critical Weber number increases when the gas velocity increases which explains that the effect of the superficial gas velocity does not appear clearly in the equation. Lin et al. (1998) show that the results obtained with their equations are in good agreement at pressures up to 15 MPa and for a highly viscous fluid.

2.4. *Effect of chemical reaction*

As a chemical reaction occurs gas are produced and liquid are consumed (or the opposite). This can alter the physical and chemical properties of the phases and then affect the properties of the bubble column such as bubble size, gas holdup and mass transfer coefficient. This influence has almost never been studied in the literature. As an illustration, Ishibashi et al. (2001) report that their gas holdup changes significantly between the inlet and the outlet of the reactor in the case of coal liquefaction reaction which can be directly related to the gas produced (hydrogen and carbon dioxide). Their values of gas holdup are higher than those reported in literature at atmospheric conditions ((Zahradník et al., 1997) for example).

Choi and Wiesmann (2004) have studied the influence of chemical reaction in an ozonation bubble column. They propose a method to calculate the mass transfer coefficient without reaction, in the case when reactive gases are used. Knowing the mass transfer coefficient of a reactive gas in presence of a reaction by direct measurement, they estimate the increase of mass transfer due to chemical reaction from the measurement of the mass transfer of an inert gas. For ozonation processes, O_3 is the reactive gas, O_2 the inert gas and the mass transfer of one compound can be directly related to the other by Eq. (8).

$$(k_La)_{O_3} = (k_La)_{O_2}D_{m,O_3,solvent}/D_{m,O_2,solvent} \quad (8)$$

In this case, Eq. (8) is used to calculate the mass transfer of O_3 without reaction. The effect of the chemical reaction is then deduced from the measurement of the mass transfer of O_3 in the presence of the reaction. This equation is directly related to the double film theory assuming that the film thickness is the same for the two compounds. It also supposes that the interfacial area between the two compounds is the same (so the holdup and bubble size must be the same). The effect of density on interfacial area is not taken into account in this equation (Section 3.2.3.2).

3. Parametric study of bubble columns

3.1. *Study of gas holdup*

3.1.1. *Definition*

Gas holdup depends predominantly on the diameter of the gas bubbles and on their rising velocity. It is well accepted that gas holdup will be high when the number of bubbles is high and their diameter small. At the transition between homogeneous and heterogeneous regime, many authors observe a decrease in gas holdup for the air/water system at ambient temperature and pressure (Zahradník et al., 1997). This is supposed to be an effect of the apparition of large bubbles and the disappearance of small bubbles in the transition regime. Fig. 3 adapted from Zahradník et al. (1997) shows this phenomenon and the gas holdup profile versus superficial gas velocity for different sparger orifice diameters.

For the sparger orifice diameter of 0.5 mm the three regimes are observed. However for the other, the bubble column only works in the heterogeneous regime. In the homogeneous regime, gas holdup increases faster than in the heterogeneous regime, mostly because bubbles remain small and their number increases. In the case of an organic liquid, the profile may not show a maximum (Chaumat et al., 2005; De Swart and Krishna, 1995; Fan et al., 1999; Krishna and Ellenberger, 1996; Krishna et al., 1991; Lin et al., 2001; Öztürk et al., 1987; Reilly et al., 1986; Reilly et al., 1994; Urseanu et al., 2003) probably due to viscosity and/or interfacial tension effects. In this case, it becomes difficult to determine the regime without determining the bubble size distribution or the drift-flux.

Table 1 gives the different correlations available in literature to estimate gas holdup. As can be seen in this table, these correlations are mainly system dependant and their applicability range is limited to the range of the different parameters studied.

3.1.2. *Measurement*

Among the different method available to measure gas holdup, the easiest and usual way is the measurement of the differential pressure between two points in the column. It has been frequently used in the literature (Chaumat et al., 2005; Cui, 2005; De Bruijn et al., 1988; Forret et al., 2003; Hashemi et al., 2009; Hikita et al., 1980; Hikita and Kikukawa, 1974; Jin et al., 2007b; Kang et al., 1999; Kantarci et al., 2005; Letzel et al., 1999; Lin et al., 2001; Pjontek et al., 2014; Reilly et al., 1986; Shah et al., 2012; Therning and Rasmuson, 2001; Yang and Fan, 2003). The relation frequently used to calculate the gas holdup is given by Eq. (9).

$$\varepsilon_G = (\rho_L/(\rho_L - \rho_G))(1 - \Delta P/(\rho_L g \Delta z)) \quad (9)$$

This relation requires validation of several hypotheses. In particular, acceleration and friction pressure losses must be negligible (Shah et al., 2012; Tang and Heindel, 2006; Zahradník et al., 1997). A negligible acceleration pressure loss requires that the superficial gas and liquid velocity and their densities should be constant between the two points of measurement, the section of the column should be the same and the gas holdup is supposed to be constant between the two points of measurement. These assumptions could be difficult to fulfil at high pressures and temperatures because of the high solubility of gases. Moreover, the mass transfer from the gas to the liquid may not be neglected. Tang and Heindel (2006) show that

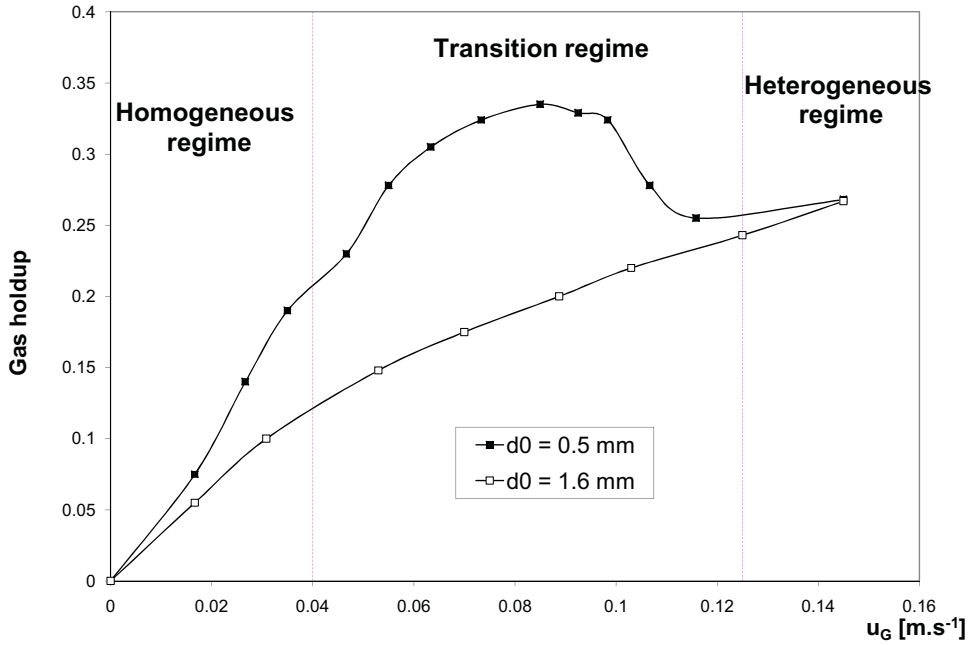

Fig. 3 – Gas holdup profile versus superficial gas velocity, D_c = 14 cm. Air/water system. (Zahradník et al., 1997).

generally the friction pressure drop is negligible when superficial velocities are low ($u_L < 1$ cm s^{-1}, $u_G \sim$ 0–30 cm s^{-1}) and for low viscous fluids (water for example). For highly viscous fluids Tang and Heindel (2006) developed a method to take into account the friction effect (Kumar et al., 2012a,b; Tang and Heindel, 2006).

Many others method could be used to measure gas holdup. A review on this subject is already available in the literature (Boyer et al., 2002), so the other methods will be briefly discussed. Dynamic gas disengagement and the measurement of dispersion height (batch for liquid mode) are extensively used in the literature but could not be used in continuous mode (Boyer et al., 2002; De Swart and Krishna, 1995; García-Abuín et al., 2010; Ishiyama et al., 2001; Kantarci et al., 2005; Krishna and Ellenberger, 1996; Krishna et al., 1991; Ohki and Inoue, 1970; Öztürk et al., 1987; Pohorecki et al., 2001; Zahradník et al., 1997). Probes are also commonly used in the literature. We can distinguish between ultrasonic probes, heat transfer probes and needle probes (Boyer et al., 2002; Ojima et al., 2014; Soong et al., 1997; Xue et al., 2008). The first ones should not be used for high gas holdups (over 0.20) and high column diameter. The heat transfer probes require high flow rate of liquid and low solid concentrations (Boyer et al., 2002). The needle probes require a large column diameter and work well only in the homogeneous regime (Boyer et al., 2002; Ojima et al., 2014). The resistance of these probes at high pressure and temperature should be carefully studied. Other methods repose on tomography of gamma ray (Kemoun et al., 2001; Parasu Veera and Joshi, 2000; Shaikh and Al-Dahhan, 2005), X-ray, electric (Jin et al., 2007a; Jin et al., 2007b) or ultrasonic wave. X-ray tomography should not be used for high column diameter (Boyer et al., 2002). Gamma-ray tomography is only valid for stationary flows (Boyer et al., 2002). Ultrasonic tomography presents the same drawbacks than ultrasonic probes (Boyer et al., 2002). Electric tomography is not well precise (Boyer et al., 2002). Other methods like Residence Time Distribution (RTD) measurements, RMN or conductimetry (Boyer et al., 2002) are seldom used in literature.

3.1.3. *Pressure influence on gas holdup*

Pressure increase results on an increase on gas holdup (Behkish et al., 2006; Behkish et al., 2007; Chilekar, 2007, 2010; Clark, 1990; Cui, 2005; De Bruijn et al., 1988; Dewes and Schumpe, 1997; Fan et al., 1999; Han and Al-Dahhan, 2007; Hashemi et al., 2009; Idogawa et al., 1985, 1986; Ishiyama et al., 2001; Jiang et al., 1995; Jordan and Schumpe, 2001; Kang et al., 1999; Kemoun et al., 2001; Krishna and Sie, 2000; Krishna et al., 1991; Kumar et al., 2012b; Letzel et al., 1998; Lin et al., 2001, 1998; Luo et al., 1999; Maalej et al., 2003; Pjontek et al., 2014; Reilly et al., 1994; Schäfer et al., 2002; Shaikh and Al-Dahhan, 2005; Tarmy et al., 1984; Therning and Rasmuson, 2001; Urseanu et al., 2003; Wilkinson et al., 1992; Wilkinson and Van Dierendonck, 1990). As an illustration of the different tendencies observed in the literature, the results of Lin et al. (1998) are shown on Fig. 4.

At the superficial gas velocity of 2 cm s^{-1}, the flow is homogeneous. At the gas velocity of 8 cm s^{-1}, the flow is heterogeneous. About Fig. 4, the authors said that the influence of pressure seems to be higher on the heterogeneous regime than in the homogeneous regime. However the gas holdup is doubled for the two superficial gas velocities at any temperature. This tendency could be linked to a decrease of the bubble size (Section 3.1.1). Lin et al. (1998) proved that in fact the bubble diameter decreases when pressure increases by their measurement of bubble size distribution at pressures up to 16 MPa. They used a photographic method to measure their bubble diameter. Their results at u_G = 8 cm s^{-1} show that the proportion of small bubbles increases when pressure increases: from a mean diameter of 2.7 mm at 0.1 MPa it becomes 2 mm at 3.5 MPa, 1 mm at 7 MPa and 0.8 mm at 15.2 MPa. This decrease is also observed at u_G = 2 cm s^{-1}.

In heterogeneous regime this positive effect of pressure on gas holdup is commonly observed in the literature (Behkish et al., 2007; Chilekar, 2007; Dewes and Schumpe, 1997; Fan et al., 1999; Han and Al-Dahhan, 2007; Ishiyama et al., 2001; Kang et al., 2000, 1999; Krishna et al., 1991; Letzel et al., 1999, 1997, 1998; Lin et al., 2001; Pjontek et al., 2014; Reilly et al., 1994; Shaikh and Al-Dahhan, 2005; Urseanu et al., 2003; Wilkinson and Van Dierendonck, 1990). However, in the homogeneous

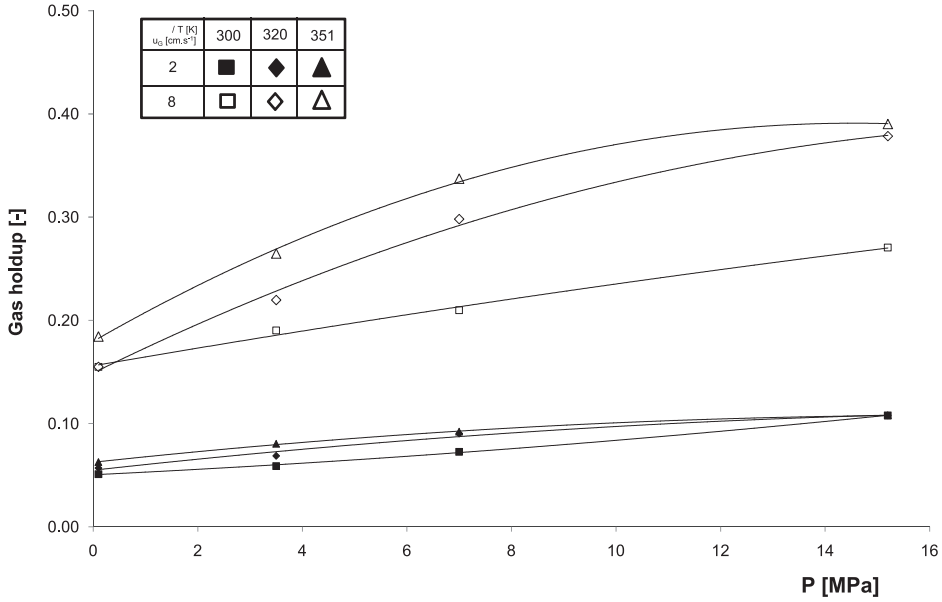

Fig. 4 – Effect of pressure on gas holdup for different temperatures and superficial gas velocity. (Lin et al., 1998).

regime and/or for low superficial gas velocity (typically below 5 cm s^{-1}), some authors observe an appreciable increase (De Bruijn et al., 1988; Idogawa et al., 1986; Lin et al., 2001, 1998; Schäfer et al., 2002; Shaikh and Al-Dahhan, 2005; Tarmy et al., 1984; Therning and Rasmuson, 2001; Wilkinson et al., 1992; Wilkinson and Van Dierendonck, 1990), some an increase less than in the heterogeneous regime (Clark, 1990; Dewes and Schumpe, 1997; Hashemi et al., 2009; Jiang et al., 1995; Kang et al., 2000, 1999; Krishna et al., 1991; Oyevaar et al., 1991; Pjontek et al., 2014; Reilly et al., 1994) and some observe no effect at all (Chilekar, 2007; Chilekar et al., 2010; Ishibashi et al., 2001; Kemoun et al., 2001; Krishna and Sie, 2000; Kumar et al., 2012b; Letzel et al., 1999, 1997, 1998; Pohorecki et al., 2001; Sangnimnuan et al., 1984).

For an air–water system, Schäfer et al. (2002) observe a notable decrease of bubble size while increasing pressure with different types of sparger and a pressure up to 5 MPa at ambient temperature in the homogeneous regime. This influence seems to depend on gas sparger. Maalej et al. (2003) have reported that the pressure effect is less important for porous plates than for perforated spargers. This effect is mainly due to the size of the bubbles that are formed on the different spargers, smaller for porous plates. Oyevaar et al. (1991) also observe higher effects on gas holdup for perforated plate sparger than for porous plates. However, they observe a plateau and no significant effect of pressure on the gas holdup for pressures over 6 MPa in the homogeneous regime. This phenomenon is also observed on Fig. 4 (Lin et al., 1998) where the effect of pressure decreases for pressure over 7 MPa and depends on temperature. In addition, Idogawa et al. (1986) report that the effect of gas sparger vanishes under pressure. A plateau for the effect of pressure is observed above 10 MPa for the air/water system. Behkish et al. (2007) also observed this plateau at pressures depending on operating conditions. The existence of this plateau and the observed minor effect of pressure in the homogeneous regime for some authors (see above) seem to indicate that the effect of pressure decreases when the bubble diameter decreases. The plateau is observed in the experiments of many authors (Chilekar, 2007; Chilekar et al., 2010; Hashemi et al., 2009; Idogawa et al., 1986; Jiang et al., 1995; Kemoun et al., 2001; Krishna and Sie, 2000; Krishna et al., 1991; Kumar et al., 2012b; Letzel et al., 1999, 1997, 1998; Lin and Fan, 1999; Neubauer, 1977; Pjontek et al., 2014; Therning and Rasmuson, 2001; Wilkinson et al., 1992; Wilkinson and Van Dierendonck, 1990). Chilekar (2007) also observe a plateau for the effect of pressure on bubble size: the average larger bubble diameter does not change significantly for pressures over 0.5 MPa in their conditions. However, pressure has still an effect at pressures over 0.5 MPa. This could be linked to a pressure effect on primary bubble and/or on bubble density. This tendency is also observed by Jiang et al. (1995) who observe a plateau for gas holdup around 10 MPa but a plateau for bubble diameter at 1.5 MPa; suggesting pressure has another effect that decreasing bubble diameter. In fact, Kang et al. (2000), Wilkinson and Van Dierendonck (1990) and Lin and Fan (1999) report an increased number of bubbles and a decreased bubble rising speed while increasing pressure, which may also results on an increase of gas holdup. Urseanu et al. (2003) report a minor effect of pressure on gas holdup while working with viscous fluids ($\mu_L > 70$ mPa s) which is attributed to the opposite effect of pressure and viscosity on bubble size (Section 3.1.4).

Pohorecki et al. (1999, 2001) observe no effect of pressure up to 1.1 MPa for the systems air/cyclohexane and air/water at 303–433 K. For the air/cyclohexane system, they explained their results arguing that saturation of gas by evaporation of liquid increases their bubble size. For the air/water system they report no effect of temperature and pressure upon gas holdup and bubble size but a major effect of the saturated superficial gas velocity. A possible explanation would be that the lower the saturation (high pressure and low temperature), the lower the difference between dry and saturated superficial gas velocity. By using the dry superficial gas velocity, gas holdup would increase when temperature increases and pressure decreases, suggesting an effect of water evaporation. Wilkinson et al. (1992) report such effects of evaporation. For the bubble size trends, it seems that the measurement is not well precise as bubble size varies between 4.5 and 8 mm and is given constant. This lack of precision and evaporation may have hidden some effects. Ishibashi et al. (2001) observe no effect of pressure between 16.8 and 18.6 MPa, in presence of a chemical reaction. (Letzel et al., 1999, 1997, 1998) report that

only larger bubbles are affected by pressure, which explains that no effect is observed in the homogeneous regime. Under coal liquefaction conditions, Sangnimnuan et al. (1984) report no effect of pressure in the range 4.5–15 MPa in conditions representative of the homogeneous regime, which is in agreement with the remarks above. Similar results are obtained by Soong et al. (1997) at pressures in the range 0.1–1.36 MPa at 538 K. However, they observe a decrease of the bubble size and velocity while increasing pressure which is contradictory with their gas holdup trends. Temperature may have hidden the effect of pressure on gas holdup (Section 3.1.4). Kölbel et al. (1971) report no effect of pressure in the range 0.1–0.6 MPa in either homogeneous or heterogeneous regime which is attributed to the performance of the sparger giving narrow bubble distribution. Ishiyama et al. (2001) report a negative effect of pressure on gas holdup at pressures above 0.8 MPa for the CO_2/water system in heterogeneous regime. They explain this trend by an increase of liquid viscosity with dissolved CO_2.

The effect of pressure can be related to several parameters. First it increases faintly liquid viscosity and liquid density. This effect remains small as reported by Lin et al. (1998). The effect of pressure is mainly due to the increase of the gas density. It has been shown in Section 2.3.3 that an increase in gas density could lead to breakage, which seems to be validated by the results shown of Fig. 4. Dewes and Schumpe (1997) studied the effect of gas density on gas holdup and showed that an increase in the gas density can lead to a higher gas holdup: the gas holdup is higher for denser gases. Increasing pressure for the same gas also increases gas holdup. Gas density effect seems again to be low at the lowest superficial gas velocities which can be the conditions for the homogeneous regime (under 4 cm s^{-1} for N_2 at 0.1 MPa/298 K, Section 2.2). Jordan and Schumpe (2001) Krishna and Ellenberger (1996), Reilly et al. (1994), Wilkinson and Van Dierendonck (1990) and Krishna et al. (1991) also reported such an effect of gas density. Letzel et al. (1998) also reported that increasing gas density by increasing pressure leads to a decrease of the bubble rise velocity, which results in an increase of gas holdup. Moreover, Hashemi et al. (2009) found a higher gas holdup for CO_2 compared to air and they showed that this increase is higher at higher pressures (they do not explain this trend). This effect of gas density on gas holdup is also reported at ambient pressure and temperature by Hikita et al. (1980) and Reilly et al. (1986, 1994), in xylene by Öztürk et al. (1987) and at pressures up to 0.3 MPa by Ishiyama et al. (2001).

3.1.4. *Temperature influence on gas holdup*

Authors observe generally an increase of gas holdup and/or decrease of bubble diameter while increasing temperature (Behkish et al., 2007; Hashemi et al., 2009; Ishiyama et al., 2001; Lau et al., 2004; Lin et al., 1998; Lorenz et al., 2005; Luo et al., 1999; Pohorecki et al., 2001; Sangnimnuan et al., 1984; Schäfer et al., 2002; Soong et al., 1997; Wilkinson et al., 1992). Lin et al. (1998) observed an increase of the gas holdup with temperature at a pressure of 15.2 MPa, which can be related to their bubble size distribution: it becomes narrower when temperature is increased. A temperature increase leads to a decrease in surface tension and thus leads to a decrease of the film drainage speed (Eq. (3)); a decrease of primary bubble size and a decrease of maximum stable bubble size (Eq. (6)). A temperature increase also leads to a decrease of viscosity which, as said in Section 2.3, can lead to a decrease of the primary bubble diameter (Eq. (2)), a decrease of maximum stable bubble size (Eq. (6)) but has two effect on bubble coalescence. On the one hand, it increases film drainage speed (Eq. (9)) and collision frequency and thus promotes coalescence. On the other hand, it decreases contact time t_B. It is likely that the increase of gas holdup with the increase of temperature is linked to the concomitant decrease of viscosity and surface tension. Viscosity and surface tension can have contradictory effects on bubble size via the effect on coalescence. The increase of gas holdup is then linked to the effect on primary bubble size, maximum bubble size and contact time for coalescence.

Pohorecki et al. (1999) observe no effect of temperature on gas holdup which might be due to evaporation (Section 3.1.3). Other authors observe a decrease of gas holdup while increasing temperature (Deckwer et al., 1980; Grover et al., 1986; Kölbel et al., 1971; Yang et al., 2001). Yang et al. (2001) observe a decrease on interfacial area (also on gas holdup which is closely linked to interfacial area as it will be shown in Section 3.2.1) in a homogeneous system in the presence of solid (5% by volume, system H_2/CO—viscous paraffin) and at different pressures (1–3 MPa) as shown on Fig. 5.

The effect is mainly attributed to the decrease in liquid viscosity, which will increase the coalescence (Section 2.3.2: the collision frequency and the rate of liquid film drainage are increased). As the liquid remains relatively viscous at those high temperatures, it is likely that the contact time t_B does not decrease considerably (Section 2.3.2). In the publication of Grover et al. (1986), the authors observed a negative effect of temperature at atmospheric pressure and temperatures between 303 and 353 K in the air/water system. They also measured gas holdup in an air/water solution with dissolved salts, and observed an increase of gas holdup while increasing temperature for these solution. The salts are inhibitors of coalescence so it is likely that the negative effect of temperature is mainly due to the promotion of coalescence. In the publication of Deckwer et al. (1980), a decrease of gas holdup until a plateau is observed, for the same range of superficial gas velocity (up to 3.5 cm s^{-1}) and for a N_2/Paraffin system. They attributed this decrease to wall effect as their column diameter was small (4.1 cm). This decrease is also observed by Kölbel et al. (1971) in homogeneous regime (same u_G range and D_c as Deckwer et al. (1980)) while no effect is observed in the heterogeneous regime (great performance of the sparger, see Section 3.1.3). These four publications have similarities as they operate at low superficial gas velocity in the homogeneous regime. As reported by Yang et al. (2001) for these conditions, turbulence is low: an increase in temperature (thereby reducing the viscosity) weakly promotes turbulence. The main effect of decreasing viscosity by increasing temperature is then to promote collision and to increase film drainage speed (Section 2.3.2).

Olivieri et al. (2011) study the effect of viscosity on gas holdup. They used aqueous solutions of alginate to increase the viscosity and air as the gas phase. Their results are presented on Fig. 6.

The viscosity of the solution of alginate increases when concentration increases, the surface tension being nearly constant. Fig. 6 shows that when viscosity increases the transition is delayed up to a certain concentration (0.1%wt). At the same time gas holdup increases. Further increase of viscosity leads to a destabilization of the homogeneous regime and a decrease of the gas holdup at transition. The stability range of the homogeneous regime spans from 1 to 4.25 mPa in their conditions. At low superficial gas velocity (below 4 cm s^{-1}) gas holdup is higher for the highest viscous solutions: the column work in the transition regime for the highest viscous solutions

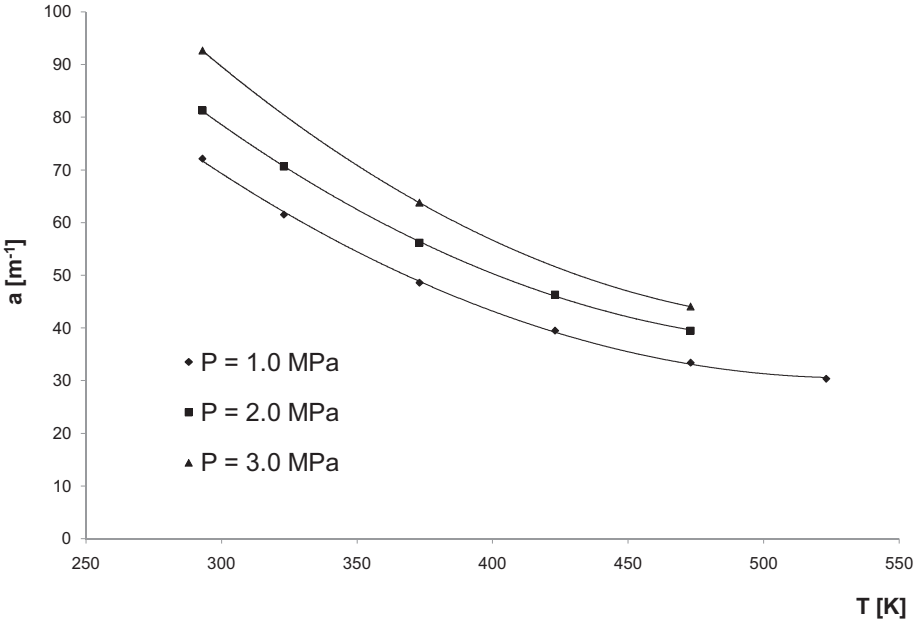

Fig. 5 – Effect of temperature on interfacial area for different pressures. $u_G = 1.6\,cm\,s^{-1}$; $C_v = 5\%$. System: H_2-CO/Paraffin. (Yang et al., 2001).

and in the homogeneous regime at lower concentration. In the homogeneous regime and for the lowest viscous solutions, viscosity has no effect on gas holdup: its influence is limited to the transition and heterogeneous regime and on the stabilisation of the homogeneous regime. Zahradník et al. (1997) observed no stabilizing effect of viscosity in the case of aqueous solutions of saccharose. Their viscosity range spans from 1 to 110 mPa s. They also shown that homogeneous regime never appear in the case of highly viscous solutions. This effect was suppressed by addition of a surface active agent (ethanol). Same trends are reported by Parasu Veera and Joshi (2000) in the case of aqueous solutions of carboxymethyl cellulose (CMC) and butanol. Gourich et al. (2006) obtained a stabilizing effect with propanol. Shah et al. (2012) found no stabilizing effect in the range 1–50 mPa s for polyethylene glycol aqueous solutions. García-Abuín et al. (2012) report that in fact increasing viscosity by adding a polymer lead to a decrease of gas holdup and interfacial until a certain concentration. Further increase of the viscosity results in an increase of the gas holdup and interfacial area. Furthermore they observe that increasing viscosity results on a slight increase of the bubble mean diameter while bubble size distribution becomes larger: small and large bubbles are produced. The heterogeneous regime appears. The increasing effect of concentration observed on gas holdup and interfacial area is attributed to a decrease of the bubble rise velocity. By adding a surfactant in their polymer solutions, they observe that the negative effect of the polymer is neutralised–their mean bubble size remains constant while increasing polymer concentration – except at high polymer concentration where gas holdup and interfacial area start to decrease: the heterogeneous regime is delayed while adding the surfactant. In definitive, it is likely that the

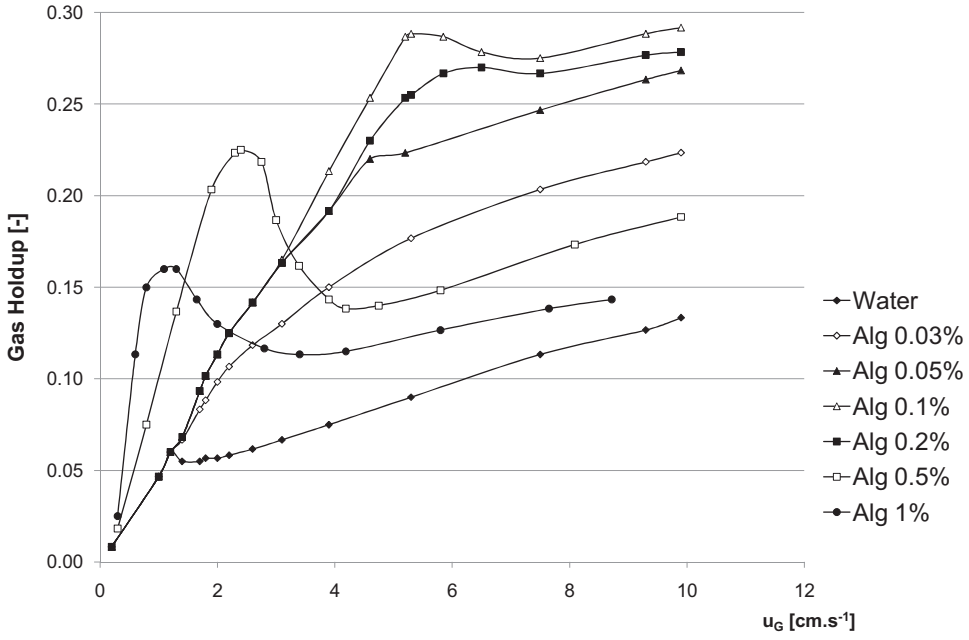

Fig. 6 – Influence of u_G on gas holdup for different solutions. P = 0.1 MPa; T = 303 K. (Olivieri et al., 2011).

stabilizing effect of viscosity on the homogeneous regime, observed in Fig. 6, is linked to a surface tension effect of the alginate. Moreover adding a surfactant results on a decrease of the bubble size and an increase of gas holdup (García-Abuín et al., 2012; Hikita et al., 1980; Hikita and Kikukawa, 1974; La Rubia et al., 2010; Parasu Veera and Joshi, 2000; Passos et al., 2015; Reilly et al., 1986; Wilkinson et al., 1992; Zahradník et al., 1997). Hikita et al. (1980) report coalescence inhibiting effects of alcohols in aqueous solutions, which is in agreement with the stabilizing effects described above.

As for the effect of pure fluids surface tension, Cui (2005) and Chilekar (2007) report smaller bubble size and higher gas holdup for low surface tension fluids compared to water, which can be due to a decrease of maximum stable bubble size and/or primary bubble size. Simonnet et al. (2007) also report a decrease of bubble size for a butanol aqueous solution compared to water. An increase is also observed by Krishna and Ellenberger (1996) and Öztürk et al. (1987) for gas holdup. Passos et al. (2015) obtained a decrease of bubble size and an increase of gas holdup while adding non-ionic surfactants in Non-Newtonian fluids.

3.1.5. *Superficial liquid velocity effect on gas holdup*

Lau et al. (2004) studied the effect of superficial liquid velocity in the case of the N_2/Paratherm NF system at two pressures (0.1 MPa and 4.24 MPa) and at 298 K. They found that, at 0.1 MPa, u_L has an effect only at high superficial gas velocity and for low u_L values. Their gas holdup is decreased by 7% at $u_G = 30\,cm\,s^{-1}$ by changing u_L from 0.08 to $0.20\,cm\,s^{-1}$. At 4.24 MPa the superficial liquid velocity seems to have no influence. The influence of this parameter is then limited to the pressure near the atmospheric pressure and it results in a marginal decrease of the gas holdup by increasing the proportion of liquid. These results are consistent with other publications (Chaumat et al., 2005; Jin et al., 2007b; Kumar et al., 2012a,b; Pjontek et al., 2014; Shah et al., 2012; Simonnet et al., 2007) where a decrease of gas holdup is observed while increasing superficial liquid velocity. Indeed, Chaumat et al. (2005) observe, in the case of cyclohexane/N_2-CO_2 system, a decrease of the gas holdup by increasing the superficial velocity of the liquid. Their superficial liquid velocity is an order of magnitude higher than Lau et al. (2004) (Table 1). A higher influence of the superficial liquid velocity is observed: by changing superficial liquid velocity from 4 to $8\,cm\,s^{-1}$ at $u_G = 12\,cm\,s^{-1}$, gas holdup is decreased by 28.6%. Pjontek et al. (2014), Simonnet et al. (2007) and Kumar et al. (2012a, 2012b) report a decrease of the gas holdup while increasing superficial liquid velocity in the same range than Chaumat et al. (2005). The effect is attributed to an increase of the bubble rise velocity while increasing superficial liquid velocity. Indeed, Simonnet et al. (2007) found that the relative velocity of bubbles (difference between superficial velocities) and their diameters do not change while increasing superficial liquid velocity. This means that bubble diameter does not increase while bubble velocity does. Shah et al. (2012) observed the decrease in the same range that Lau et al. (2004) with a liquid which have nearly the same viscosity (25 mPa s) but the effect is lower than for the other authors (Chaumat et al., 2005; Kumar et al., 2012a; Kumar et al., 2012b; Pjontek et al., 2014; Simonnet et al., 2007). This is attributed, in counter-current mode, to an increase of friction forces between gas bubbles and liquid that results on bigger bubbles formation. At ambient conditions, Jin et al. (2007b) report a decrease of the gas holdup with superficial liquid velocity only in the heterogeneous regime, not in the homogeneous regime. This is consistent with Lau et al. (2004). The decrease is lower than for the other authors, which may be due to a narrower range of u_L tested (up to $1.1\,cm\,s^{-1}$). At atmospheric pressure and for the air/water system, Pjontek et al. (2014) report a shearing effect of the liquid as it passes through the gas sparger which results on an increase of the gas holdup while increasing liquid velocity. This is not observed at pressures over 1.0 MPa.

On the contrary, under coal liquefaction conditions in the homogeneous regime, Sangnimnuan et al. (1984) and De Bruijn et al. (1988) do not observe any effect of the superficial liquid velocity on gas holdup in a limited range of u_L (an order of magnitude below) which is in agreement with Lau et al. (2004) for the homogeneous regime. Yang and Fan (2003) did not observe any effect of the liquid superficial velocity at atmospheric pressure, in the case of an air/water system. The superficial liquid velocity varied between 0 (semi-batch) and $2.15\,cm\,s^{-1}$ and the superficial gas velocity varied between 2 and $20\,cm\,s^{-1}$. The difference between Yang and Fan (2003) and Lau et al. (2004) could be linked to the system studied: the liquid phase is less viscous for Yang and Fan (2003), the rising velocity of bubbles is then higher and less impacted by liquid velocity. In the slug flow regime, Shawaqfeh (2003) did not observe any effect of superficial liquid velocity on gas holdup.

The influence of the superficial liquid velocity seems to be system and pressure dependant. It seems to be higher at high superficial gas velocity and at high liquid velocity.

3.1.6. *Working mode effect on gas holdup*

Biń et al., 2001 studied the effect of the working mode on gas holdup. They measured gas holdup in counter, co-current and semi-batch mode for a small superficial gas velocity range (up to $1.6\,cm\,s^{-1}$). They showed that the gas holdup increases with superficial liquid velocity in counter-current mode and decreases or remains constant in co-current mode. The effect is more pronounced at high gas velocity. The difference in gas holdup between co-current and counter-current mode is around 10%. These tendencies are also reported by Jin et al. (2010). For an air–water system at ambient temperature and pressure, they observed the same trends but their gas holdup is an order of magnitude higher. They observed difference of maximum of 2% between counter and co-current working operation. It can be inferred that the differences between the two working mode can be related to the movement of bubbles which are slowed down in counter-current mode and accelerated in co-current mode. The influence of woking mode is lower at high gas holdup.

Jin et al. (2010) report that the transition between homogeneous and heterogeneous regime is the same for the two working mode in continuous mode. It implies that the holdup at transition is higher for counter-current operation. For high superficial liquid velocity (higher than $4\,cm\,s^{-1}$), the authors observe that the transition velocity decreases when the superficial liquid velocity increases, which is not explained. Baawain et al. (2007) developed artificial neural network models and calculate the weight percent of contributions on the gas holdup. The operating mode (counter or co-current mode) influenced the holdup for around 5% in weight, and less than 1% on bubble size. This shows that the effect observed is not entirely linked to the bubble size but also depends on bubble rise velocity, which is in agreement with the experimental results and remarks above. Nevertheless, the working mode effect on gas holdup is weak.

3.1.7. *Effect of other parameters on gas holdup: superficial gas velocity, column and distributor design.*

3.1.7.1. *Effect of superficial gas velocity on gas holdup.* As already seen before, the superficial gas velocity increases the gas holdup because of the increase of the bubble density, except in the case where the maximum is observed at the transition (Fig. 3). A discussion can be made about the evolution of the bubble size with superficial gas velocity. Few authors have studied this effect, but it appears that in the homogeneous regime, the mean diameter increases slightly with the superficial gas velocity (until transition regime) (Kluytmans et al., 2003). At the transition it increases and, thereafter, in the heterogeneous regime, the proportion of large bubbles grows and that of the small ones is almost constant. As an example, for an air/water system, Fukuma et al. (1987) reported an increase of the bubble size with superficial gas velocity in the homogeneous and in the heterogeneous regime. Other authors also found an increase of the bubble mean diameter while increasing superficial gas velocity, whatever is the flow regime (Chilekar, 2007; Chilekar et al., 2010; Cui, 2005; Ferreira et al., 2013; García-Abuín et al., 2012; García-Abuín et al., 2010; Kang et al., 2000; Lau et al., 2012; Majumder et al., 2006; Muroyama et al., 2013; Passos et al., 2015; Schäfer et al., 2002; Simonnet et al., 2007; Smith et al., 1996; Xue et al., 2008). An end effect is reported by Muroyama et al. (2013) who observe a decrease of gas holdup while increasing superficial gas velocity for very low u_G (<1 mm/s), which is linked to the increase of the bubble size. However, Idogawa et al. (1985) reported a very small effect of u_G on the bubble size, in conditions representative of the homogeneous regime ($u_G < 5\,cm\,s^{-1}$, Section 2.4), which is not explained. Soong et al. (1997) report no effect of superficial gas velocity on bubble size in the homogeneous regime at 538 K and at pressures between 0.1–1.36 MPa. The high temperature applied may have hidden the small effect of superficial gas velocity on bubble size in the homogeneous regime. La Rubia et al. (2010) report a slight decrease (between 4.6 and 4.2 mm) of the bubble diameter while increasing superficial gas velocity in the presence of a highly viscous compound (Table 1), which is not explained. However, Lau et al. (2012) report an increase of shearing while increasing superficial gas velocity for single nozzle tubes that are used in those two studies: this shearing effect lead to a decrease of the bubble diameter. Pohorecki et al. (1999) report no effect of saturated superficial gas velocity on bubble size (Section 3.1.3).

3.1.7.2. *Effect of gas sparger on gas holdup.* Zahradník et al. (1997) show that the distributor has an influence at the limit between the homogeneous and the transition regime, but has no effect in well established homogeneous and heterogeneous regime, whatever distributor is used. This is effectively observed by Ohki and Inoue (1970) and Reilly et al. (1986) in the heterogeneous regime. However, Bouaifi et al. (2001), Jin et al. (2007a), Şal et al. (2013) and Parasu Veera and Joshi (2000) report an influence of the sparger in the heterogeneous regime and/or in the homogeneous regime. These differences may be explained by Wilkinson et al. (1992). For perforated plates, Wilkinson et al. (1992) report that, below 1 mm, d_0 has not more influence on gas holdup. This is effectively validated by the publications cited above in well established homogeneous and heterogeneous regime but not at the transition which can be delayed by a further decrease of d_0 (down to 0.4 mm). Table 1 show that, in fact, the authors observing an effect in well established homogeneous or heterogeneous regime used a sieve sparger with $d_0 > 1$ mm or changed the type of sparger. Zahradník et al. (1997) also reported that using a certain type of distributor has a positive influence on the stability of the homogeneous regime (Section 2.2). The nature of the distributor plays an important role. Generally, the porous and membrane diffusers lead to narrower size distributions and thus higher gas holdup than perforated plates (Bouaifi et al., 2001; Kantarci et al., 2005; Krishna and Ellenberger, 1996; Zahradník et al., 1997). The comparative performance of porous and membrane distributors shows that different tendencies can be obtained. They can be almost identical in an air/water system at atmospheric conditions (Bouaifi et al., 2001) or largely different (Zahradník et al., 1997) in favour of membrane diffusers when the pore diameter of the porous plates is high (200 μm). For higher pore diameter (600 μm) perforated plates ($d_0 = 3$ mm) have the same performances than porous plate (Lau et al., 2012). When working with the same kind of sparger, the diameter of the orifice is the main parameter influencing the gas holdup: decreasing d_0 leads to an increase of gas holdup (Jin et al., 2007a; Ohki and Inoue, 1970; Parasu Veera and Joshi, 2000; Şal et al., 2013).

Idogawa et al. (1986) do not observe these trends. At pressures up to 15 MPa, they report that the effect of gas sparger on gas holdup is no longer significant which is attributed to a lower primary bubble size. For single nozzle spargers, Ishiyama et al. (2001) report another effect: for high diameter nozzles (above 4.0 mm), the bubbling is mainly bubble by bubble. As the diameter of the nozzle decreases, the bubbling becomes a jet. For single bubble formation, pressure has been shown to have no effect on gas holdup.

It is interesting to note that the diameter of the holes is not the only parameter that influences the bubble size distribution. The open area (φ_0) of the distributor can be calculated, assuming round holes, by E. (10).

$$\varphi_0 = N_0 \left(\frac{d_o}{D_0} \right)^2 \tag{10}$$

Increasing number of holes (N_0) at constant d_0 (which increases the open area) has an effect on the formation of bubbles when the holes are close enough to allow coalescence between two bubbles that form at the orifices. Miyahara and Hayashino (1983) showed that the number of holes had no effect when the ratio between the average distance between each hole and the orifice diameter is higher than 8, for a small amount of holes (80) and for a perforated plate. In the other cases, a promotion of coalescence is observed when the number of holes increases and then increasing open area leads to an increase of the bubble size. For membrane sparger, Hasanen et al. (2006) still observe an influence on the number of holes for ratios higher than eight with membranes having a large number of holes (>1000). Ohki and Inoue find that for perforated plates of d_0 in the range 0.4–0.7 mm, decreasing the number of holes (from 91 to 19) results on a decrease of the gas holdup, suggesting limited coalescence for these conditions at the sparger. Polli et al. (2002) and Zahradník et al. (1997) increased the open area (for holes and distributor diameters constant) by increasing the number of holes: they decreased the gas flowrate through an orifice, which reduced the size of the bubbles formed. In those two publications, no coalescence is reported. Note that the general correlations of Lemoine et al. (2008) predict an influence of the type of the distributor in heterogeneous regime although this influence is weak. In particular, they generalize the notion of

homogeneous/heterogeneous systems to coalescing or non-coalescing systems and suggested that the distributor has an influence only in non-coalescing regime.

3.1.7.3. *Effect of column design on gas holdup.* The influence of the dispersion height at constant column diameter has been studied by Zahradník et al. (1997). They observed that the lower the height of dispersion, the higher the gas holdup in the case of the homogeneous regime. In the heterogeneous regime, it has no influence. The decrease in the height of dispersion extends the homogeneous regime. They observed that the height of dispersion has no more influence for a ratio H_c/D_c higher than 5. These tendencies are also reported elsewhere in literature (Kantarci et al., 2005; Kumar et al., 2012a; Lau et al., 2012; Luo et al., 1999; Parasu Veera and Joshi, 2000; Ruzicka et al., 2001; Wilkinson et al., 1992). An interesting point is that Xue et al. (2008), who made local gas holdup measurements, found a strong influence of the sparger properties in the sparger region of the bubble column. However, this influence is no longer visible for a ratio z/D_c greater than 5 where equilibrium is reached. This indicates again that the height has no more influence for ratio over 5 even at the scale of the column at constant height and that in fact, for small column, sparger region has a strong influence.

If the column diameter is small, side effects alter maximum stable bubble size, bubble rising velocity and liquid recirculation. Ohki and Inoue (1970), Krishna and Sie (2000) and Krishna and Ellenberger (1996) report a decrease of gas holdup while increasing column diameter: this effect is due to wall effects at low column diameter which decrease the bubble rise velocity. In homogeneous regime, Krishna et al. (2001) report the same trend and an increase of the liquid recirculation while increasing column diameter. In the heterogeneous system, the presence of large diameter spherical caps subjected to wall effect, especially at atmospheric pressure is reported (Krishna et al., 1999b). Behkish et al. (2007) noticed that the effect of column diameter for viscous fluid is higher. Most authors (Kantarci et al., 2005; Shah et al., 1982; Wilkinson and Van Dierendonck, 1990) propose a rule for the design: the column diameter has no longer influence for diameters higher than 0.15 m in either well established homogeneous or heterogeneous system. This is validated by many experimental results (Chilekar, 2007; Forret et al., 2003; Ruzicka et al., 2001; Zahradník et al., 1997). However, Urseanu et al. (2003) observed the decrease of gas holdup for a D_c range 0.15–0.23 m ($H_c/D_c > 5$) while working with viscous fluids. This is in agreement with the remark of Behkish et al. (2007) above. Lemoine et al. (2008), through their global correlation, propose a model where the column diameter has an influence up to 0.70 m in either homogeneous or heterogeneous regime. Krishna et al. (2001) report a decrease of gas holdup while increasing column diameter up to 0.38 m in the homogeneous regime. However, by increasing the column diameter while fixing the column height (1 m) they reduced the H_c/D_c ratio below 5, other effects may then appear. Same results are obtained by Ruzicka et al. (2001) in the heterogeneous regime.

3.2. *Study of interfacial area, mass transfer coefficient and volumetric mass transfer coefficient*

3.2.1. *General considerations*

In this section, the behaviour of k_La, a and k_L in relation to the different operating parameters is studied in order to find the dominant parameters, if existing. k_L is seldom studied in publications (Baz-Rodríguez et al., 2014; Bouaifi et al., 2001; Chaumat et al., 2005; Chilekar, 2007; Dewes et al., 1995; García-Abuín et al., 2010; Gopal and Sharma, 1983; Han and Al-Dahhan, 2007; Jin et al., 2014; Kluytmans et al., 2003; Kulkarni, 2007; Lau et al., 2012; Lemoine et al., 2004; Maalej et al., 2003; Voyer and Miller, 1968; Yang et al., 2001) and the parametric study for k_L is more complex than for the gas holdup and the overall coefficient k_La. As for gas holdup; Table 1 gives the available correlations for estimating k_L, a or k_La.

Higbie's penetration theory is frequently used in the literature for the interpretation of the results obtained for k_L. This theory expresses that the fluid elements are transported by convection at the interface. They stay for a time t_c at the interface during which they are likely to share matter with gas by molecular diffusion. By convection they move away from the interface and transmit the matter accumulated in the surrounding fluid. In this theory the coefficient k_L is expressed by Eq. (11).

$$k_L = 2\sqrt{(D_{mi,j}/(\prod t_c))} \tag{11}$$

In Higbie's theory the fluid elements have the same contact time. According to Nedeltchev et al. (2007), the Higbie equation has not been tested in a sufficiently large diffusion coefficient and viscosity range and is valid only for potential flows with high Reynolds number. They also state that the theory predicts higher k_L than experimental ones because it does not take into account the form of bubbles, usually ellipsoidal in industrial conditions (Zieminski and Raymond, 1968). The contact time of the penetration theory t_c was assessed by different authors. It can be expressed as the ratio of the bubble size on the sliding velocity of bubbles (Calderbank, 1967), which implies that for low viscosity fluids, k_L decreases as the bubble size increases (Kulkarni, 2007). The contact time was also evaluated using the Kolmogorov theory of isotropic turbulence as the ratio of the kinematic viscosity over the energy dissipation rate (Kulkarni, 2007). However, this approach assumes that the flow regime is turbulent, which is not the case at small gas and liquid velocities and the turbulence should be isotropic, which is rarely the case, and one must take into account a correction factor for the energy dissipation. More recently, it has been calculated as the ratio of the bubble surface (considering the bubble ellipsoidal) over the rate of surface formation, which is a function of the rise velocity and the dimensions of the bubbles. A correction factor has been successfully developed to estimate k_L in slurry bubble columns at low pressures, up to 4 MPa (Nedeltchev et al., 2007, 2014).

3.2.2. *Measurement*

In this section, the methods focus on the determination of a global k_La, k_L or a in the column, although it can be applied locally on a part of the bubble column.

The first methods are based on the measurement of the dissolved concentration of a gas in a liquid (Akita and Yoshida, 1974; Baz-Rodríguez et al., 2014; Behkish et al., 2002; Bouaifi et al., 2001; Chaumat et al., 2005; Chilekar, 2007; Ferreira et al., 2013; Han and Al-Dahhan, 2007; Hashemi et al., 2009; Hikita et al., 1981; Jin et al., 2004, 2014; Jordan and Schumpe, 2001; Kang et al., 1999; Kluytmans et al., 2003; Kojima et al., 1997; Lau et al., 2012, 2004; Lemoine et al., 2004; Mena et al., 2011; Muroyama et al., 2013; Öztürk and Schumpe, 1987; Öztürk et al., 1987; Shah et al., 2012; Vandu et al., 2004; Zahradník et al., 1997). The method can be made by desorption or by

absorption. The gas is initially completely desorbed in the case of absorption or completely saturated in the case of desorption. An inert gas is used to desorbed the gas when using the desorption method. The dissolved concentration is measured most of the time by oxygen probes, recording oxygen concentration (Baz-Rodríguez et al., 2014; Bouaifi et al., 2001; Chilekar, 2007, 2010; Elgozali et al., 2002; Ferreira et al., 2013; Han and Al-Dahhan, 2007; Hashemi et al., 2009; Jordan and Schumpe, 2001; Kang et al., 1999; Kluytmans et al., 2003; Kojima et al., 1997; Lau et al., 2012, 2004; Mena et al., 2011; Muroyama et al., 2013; Öztürk and Schumpe, 1987; Öztürk et al., 1987; Shah et al., 2012; Vandu et al., 2004; Zahradník et al., 1997) although some authors used gas chromatography or other external analysers (IR, oxygen) for samples analyses (Chaumat et al., 2005; Hikita et al., 1981; Jin et al., 2014) or by linking the column and the chromatograph in line (Jin et al., 2004). At high pressures and temperatures the main problem for sampling and measuring dissolved gas concentration is the change in solubility of gases that can lead to a mass transfer from the samples to the environment. It implies that the liquid samples must be hermetic and both phases after decompression must be analysed (apparatus of Japas and Franck, 1985). For transient regime, the time of sampling and residence time must be inferior to the characteristic time of mass transfer ($1/k_La$) (Charpentier et al., 1997). In the case of a not perfectly mixed flow, which may be the case in bubble columns, non-ideal flow model can be applied. The axial dispersion model (Section 3.3) is frequently used to model bubble columns (Bouaifi et al., 2001; Gourich et al., 2008; Han and Al-Dahhan, 2007; Hikita et al., 1981; Kang et al., 1999; Kantak et al., 1994; Lau et al., 2004; Shah et al., 2012). Some authors model the bubble column with a cascade of perfectly stirred reactors (Chaumat et al., 2005; Han and Al-Dahhan, 2007). However, many authors made the assumption that the liquid is perfectly mixed (Baz-Rodríguez et al., 2014; Behkish et al., 2002; Elgozali et al., 2002; Ferreira et al., 2013; Hashemi et al., 2009; Hikita et al., 1981; Jin et al., 2004, 2014; Jordan and Schumpe, 2001; Kluytmans et al., 2003; Kojima et al., 1997; Lau et al., 2012, 2004; Lemoine et al., 2004; Letzel et al., 1999; Mena et al., 2011; Muroyama et al., 2013; Öztürk et al., 1987; Vandu et al., 2004) which seems to be justified at least in the heterogeneous regime (Behkish et al., 2002). However, Gourich et al. (2008) show that using the assumption of the perfectly mixed reactor should be avoided when using water and coalescence-inhibiting mixtures, except at low superficial gas velocities in the homogeneous regime. They show that the axial dispersion model and the liquid perfectly mixed model lead to similar results when the characteristic time of mass transfer (t_c) is five times superior to the mixing time of gas phase ($\varepsilon_G h_P/u_G$). In their work, for a high H_c/D_c ratio, the axial dispersion model shows the best results. Their estimation of k_La is highly dependent on the axial dispersion coefficient.

Chemical methods are based on the absorption of a gas A into the liquid where a chemical reaction takes place with a compound B. They can be applied when the expression of the absorption flux of the gas studied is known. This absorption flux is measured experimentally by determining the evolution of the concentration of one reactive in the column. This absorption flux is given by different equations depending on operating conditions. Those conditions are given by the value of specific adimensionnal numbers: Hatta number, 'R' number and Damköhler number (equations are given in Appendix). The regime of slow reaction rate in the film but fast in the liquid requires the following conditions: $Ha < 0.3$ and $R + 1/Da \gg 1$. In those conditions, the expression of the flux is given by Eq. (12) (Charpentier et al., 1997).

$$\varphi = k_L a C_A^* \tag{12}$$

The knowledge of the solubility and the absorption flux gives the k_La. Three kinds of reactions are typically used with this technique: sulphite oxidation by oxygen catalysed by cobalt sulphate (Charpentier et al., 1997; Dewes and Schumpe, 1997; Wilkinson et al., 1994), carbonatation of some carbonate and hydrogen-carbonate compounds catalysed by hypochlorite ions and carbamation of some amino compounds (Charpentier et al., 1997).

Another method to measure k_La is the Danckwerts method, applied in intermediate conditions of Hatta number ($1 < Ha < 3$). The absorption flux expression is given by Eq. (13).

$$\begin{aligned}(\varphi/C_A^*)^2 &= (k_La)^2 + a^2((2/(m+1))D_{mA,B}C_A^{*(m-1)}C_B^n) \\ &= (k_La)^2 + \alpha a^2\end{aligned} \tag{13}$$

With this method it is possible to obtain k_L, a and k_La simultaneously by measuring the absorption flux and drawing $\varphi^2/C_A{}^{*2}$ versus α. α is typically varied by using different concentration of a catalyst. This method is commonly used with sulphite oxidation by oxygen (Charpentier et al., 1997; Kulkarni, 2007) but different systems have been used in literature: CO_2/carbonate-bicarbonate (Cents et al., 2005; Maalej et al., 2005; Vázquez et al., 2000a, b), CO_2/TEA (La Rubia et al., 2010) and CO_2/glucosamine (García-Abuín et al., 2010). Kulkarni (2007) shows that in bubble columns the non ideal distribution of bubble sizes can lead to a variation of conditions and Hatta number which results in errors on the determination of k_La.

With Eq. (12), the mass transfer coefficient k_L cannot be directly determined and one needs to know the interfacial area and k_La to estimate this parameter. The interfacial area can be determined by a chemical method. With $Ha > 3$, the chemical regime is obtained and the interfacial area is given by Eq. (14) (Charpentier et al., 1997).

$$\varphi = a\sqrt{((2/(m+1))k_r D_{m.A,B}C_A^{*(m-1)}C_B^n)} \tag{14}$$

This method can be applied by using sulphite oxidation (Charpentier et al., 1997; Vázquez et al., 2000b), dithionite oxidation by oxygen (Vázquez et al., 2000b) and chemical reaction of CO_2 with bases (Charpentier et al., 1997; Oyevaar et al., 1991; Stegeman et al., 1996).

The chemical systems using CO_2 have shown some drawbacks, especially at high pressures and temperatures. The limitation comes from the exhaustion of the gas phase or of the liquid phase because of the high reaction rate and the high solubility of the gas phase (CO_2). This method is valid when the molar fraction of CO_2 in the bubbles at the outlet of the reactor is homogeneous (Charpentier et al., 1997). This implies that the residence time of the bubbles in the reactor should be the same, so the regime must be homogeneous (Charpentier et al., 1997). For the sulphite oxidation, the main drawback is that the reaction is catalysed by traces of transition metals in water: the kinetic rate is highly dependent on water purity (Charpentier et al., 1997). The salts used in the dithionite and sulphite method are coalescence inhibitors:

the tendencies measured may be different compared to pure water (Charpentier et al., 1997).

3.2.3. Pressure influence on mass transfer properties

3.2.3.1. Pressure effect on k_La. The k_La_L increases while increasing pressure (Behkish et al., 2002; Chilekar, 2007; Dewes et al., 1995; Han and Al-Dahhan, 2007; Hashemi et al., 2009; Jin et al., 2004, 2014; Jordan and Schumpe, 2001; Kang et al., 1999; Kantarci et al., 2005; Kojima et al., 1997; Lau et al., 2004; Lemoine et al., 2004; Letzel et al., 1999; Wilkinson et al., 1994). As for the gas holdup, some authors have reported the effect of the increase of k_La_L with the gas density by either increasing pressure or changing the gas phase (Dewes et al., 1995; Dewes and Schumpe, 1997; Hashemi et al., 2009; Jordan and Schumpe, 2001; Öztürk et al., 1987). For many publications, the effect of pressure exhibits a plateau at the highest pressures (Behkish et al., 2002; Han and Al-Dahhan, 2007; Hashemi et al., 2009; Jin et al., 2004; Kojima et al., 1997; Lemoine et al., 2004; Letzel et al., 1999; Wilkinson et al., 1994). However, in the case of an air/Paratherm NF system at room temperature and in continuous mode, Lau et al. (2004), do not observe a plateau (which is present for pressures lower than 2.86 MPa). They also showed that the influence of pressure is higher at high superficial gas velocity. This trend is also observed by Kang et al. (1999), Jin et al. (2014) and Behkish et al. (2002) for other viscous liquids ($\mu_L > 2$ mPa s). A plateau for the effect of pressure at 8 MPa is observed by Behkish et al. (2002) for the less viscous fluid, indicating that the effect of pressure is higher for the highest viscous fluids and superficial gas velocities.

Wilkinson et al. (1994) show that at low superficial velocity ($u_G < 3$ cm s^{-1}) no effect of pressure is observed for pressure between 0.1 and 0.8 MPa. They explained it by considering that their regime is homogeneous. In this regime, pressure would have a negligible effect as breakage and coalescence are not the governing mechanisms of the bubble column, which is instead the formation of the primary bubble. Maalej et al. (2003) report a decrease of the k_La with pressure at constant mass flow rate. In fact, fixing a mass flow rate and increasing pressure result in a decrease of the superficial gas velocity because of the increase of the gas density. It results in a decrease of the k_La (Section 3.2.7). Hikita et al. (1981) do not observe any effect of gas density on k_La_L while observing an effect on gas holdup, which is not explained.

3.2.3.2. Pressure effect on interfacial area. The variations of interfacial area with pressure are expected to be the same than gas holdup: $a = 6\varepsilon_G/d_B$. Indeed, a pressure increase leads to an increase of the interfacial area (Han and Al-Dahhan, 2007; Jin et al., 2014; Lemoine et al., 2004; Oyevaar et al., 1991; Yang et al., 2001). A plateau is observed for the effect of pressure, except for Jin et al. (2014) (Section 3.2.3.1).

3.2.3.3. Pressure effect on k_L. Han and Al-Dahhan (2007) observed the decrease of k_L while increasing the pressure until a plateau. k_L decreases by 20% between 0.1 and 0.4 MPa but remains constant between 0.4 and 1 MPa. The authors explain this trend with the theory of Higbie: the effect of an increase in pressure reduces the size of bubbles. Indeed, they observe that their bubble size decreases between 0.1 and 0.4 MPa but this decrease is marginal between 0.4 and 1 MPa. The authors argue that the small bubbles have a slower slip velocity, so the contact time would decrease (Section 3.2.1). This would mean that the k_L decreases when the bubble size decreases. This is in disagreement with Kulkarni (2007) and his interpretation of the theory of Calderbank, which affirms exactly the opposite. In fact, if the slip velocity decreases when the diameter decreases, it is difficult to assess the evolution of the ratio d_b/u_s when both terms decrease in the absence of correlation. Among the available correlations for the estimation of bubble terminal rise velocity under pressure in literature (Fan et al., 1999; Mendelson, 1967; Rollbusch et al., 2015; Tomiyama et al., 2002), the Fan-Tsuchiya equation can be used to calculate the bubble rising velocity in the conditions of Han and Al-Dahhan, as suggested by Rollbusch et al. (2015). This correlation is given by Eqs. (15) and (16).

$$u_{b\infty}(\rho_L/(g\sigma_L))^{1/4} = \left[\left((\mathrm{Mo}^{-1/4}/K_b)(1-\rho_G/\rho_L)^{5/4} d_b^2 \rho_L g/\sigma_L\right)^{-p} + \left(2c\sigma_L^{0.5}/(d_b\rho_L^{0.5}g^{0.5}) + (1-\rho_G/\rho_L)(d_b/2)(\rho_L g/\sigma_L)^{0.5}\right)^{-p/2}\right]^{-1/p} \quad (15)$$

$$K_b = \max(K_{b0}\mathrm{Mo}^{-0.038},\ 12) \quad (16)$$

Parameters p, c and K_b depend on the system. For p, the authors propose the value of 0.8 for non pure liquids and the value of 1.6 for pure liquids. For c, the authors propose the value of 1.2 for a single component liquid and the value of 1.4 for a multi-component system. The parameter K_b is calculated by Eq. (16) where K_{b0} is a parameter equal to 14.7 for aqueous solutions and equal to 10.2 for solvents or organic mixtures.

Calculations of the contact time (t_c) have been performed assuming that the bubble rising velocity is equal to the terminal rising velocity calculated by Eqs. (15) and (16) (Fan et al., 1999). The contact time is defined as $d_b/u_s = d_b/(u_{b\infty}-u_L)$. Calculations have been performed in the conditions of Han and Al-Dahhan (2007). Fig. 7 shows the variation of the contact time with the bubble diameter and pressure.

Fig. 7 shows that an increase in pressure increases slightly the contact time of the fluid elements and therefore reduces the k_L. As for the evolution of the contact time versus bubble diameter, it goes through a minimum around 1–2 mm and then increases. This would imply that k_L would increase when the bubble diameter decreases down to 2 mm, remain almost constant for bubble diameter between 1 and 2 mm and then decreases below 1 mm. However, this does not correspond to the observations of Han and Al-Dahhan (2007) as their bubble diameter is around 10 mm. Lemoine et al. (2004) also report a decrease of the k_L coefficient for two systems (N_2-Toluene and Air-Toluene) at a temperature of 300 K and $u_G = 10$ cm s^{-1}. They also attributed this decrease to the decrease of the bubble size and they report that k_L is proportional to $d_b^{1/2}$. Baz-Rodríguez et al. (2014) also report a decrease of k_L when bubble diameter decreases (by adding coalescence inhibiting salts) while k_La and a increase in the homogeneous regime. Hashemi et al. (2009) report a decrease of the ratio k_L/d_B while increasing pressure. As bubble diameter is reduced when increasing pressure, k_L effectively decreases. Chilekar (2007) used the same approach and found that the ratio k_L/d_B remains constant while increasing pressure, which implies that k_L follow the same trend as bubble diameter: a decrease until a plateau around 0.5 MPa, which is consistent with Han and Al-Dahhan (2007). This trend is also observed by Letzel et al. (1999).

Yang et al. (2001) observed no influence of pressure on the mass transfer coefficient k_L, at different temperatures (from 293 to 473 K) in the case of a quite viscous liquid

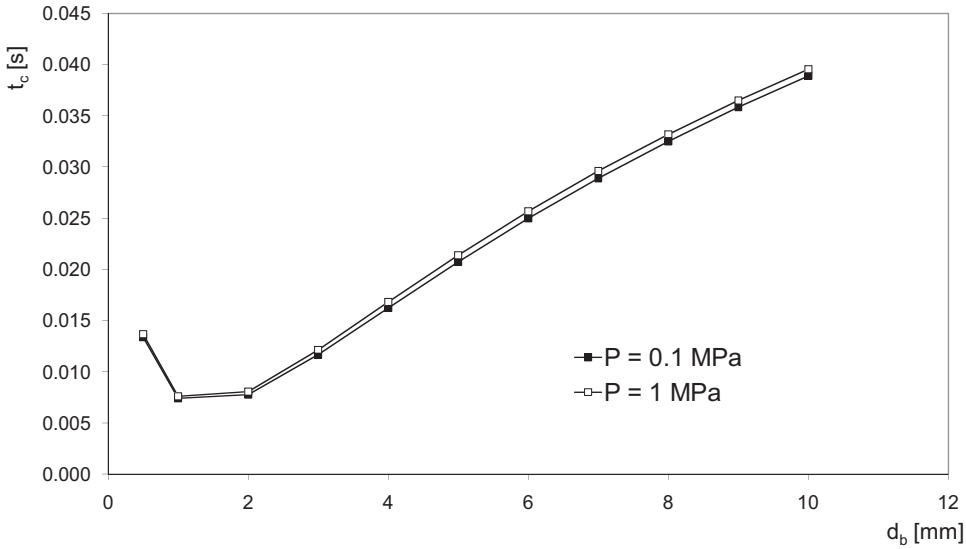

Fig. 7 – Contact time of Higbie theory versus bubble diameter for two pressures (P = 0.1 and 1 MPa; T = 298 K; u_G = 0–0.6 m s^{-1}; u_L = 0 m s^{-1}).

paraffin (μ_L = 0.26–3 Pa s). The authors report that the bubble size decreases with pressure. Furthermore, they explain that the gas solubility increases with pressure. This increasing solubility results in more gas dissolved in the liquid, which leads to a decrease in viscosity. They therefore conclude that the k_L decreases when the bubble size decreases, but in parallel, it is favoured by the decrease in viscosity reduction that would increase the molecular diffusivity. Ultimately the two effects cancel each other out and k_L appears constant in this pressure range. These trends and explanations are also reported by Jin et al. (2014) with another paraffin (μ_L = 4 mPa s). Dewes et al. (1995) also observe no effect of pressure on the k_L. Maalej et al. (2003) observed two effect of pressure on k_L at constant mass flowrate. At low mass flowrate they observed that an increase of pressure (up to 2 MPa) increases the k_L but at higher mass flowrate it decreases with pressure. In every case they observed a decrease of bubble size and superficial gas velocity while increasing pressure. They explained their results by an increase of bubble detachment at the sparger at low mass flowrate which promotes turbulence. At higher mass flowrate this effect is still present but the decrease of the superficial gas velocity seems to be the main effect on turbulence. The differences between the different results and the predictions of the Higbie theory could come from the position of the minima (Fig. 7) that shifts to larger diameters of bubbles in more viscous fluid and/or with lower surface tension. Another point is that Nedeltchev et al. (2007) reported that the Higbie theory poorly predicts mass transfer coefficient in the presence of turbulence induced by the bubbles. The turbulence decreases as the diameter of bubbles decreases and consequently the k_L is negatively affected.

Literature results show that the effect of pressure on k_L is not predominant because, even when k_L decreases or remain constant, k_La still increases (Chilekar, 2007; Dewes et al., 1995; Han and Al-Dahhan, 2007; Hashemi et al., 2009; Lemoine et al., 2004; Yang et al., 2001). It can be assumed that the increase in k_La is mainly due to the interfacial area in the conditions studied, which cover homogeneous (Dewes et al., 1995; Hashemi et al., 2009) and heterogeneous (Chilekar, 2007; Dewes et al., 1995; Han and Al-Dahhan, 2007; Hashemi et al., 2009; Lemoine et al., 2004) flow regimes.

3.2.4. *Temperature effect on mass transfer properties*

3.2.4.1. Temperature effect on k_La. Literature show that k_La increases with temperature (Hashemi et al., 2009; Jin et al., 2004, 2014; Jordan and Schumpe, 2001; Lau et al., 2004; Yang et al., 2001). As an illustration, Jin et al. (2004) studied the effect of temperature on k_La_L in a wide temperature range (from 298 to 473 K) and for three pressures (1, 2 and 3 MPa). They showed that k_La_L increases with temperature for the three pressures. Their hydrodynamic regime is not specified but, as the superficial gas velocity is low, the homogeneous regime could be assumed. The tendency is also observed in the heterogeneous regime (Lau et al., 2004).

Viscosity effects are linked to temperature as liquid viscosity decreases when temperature increases. Viscosity effects are reported by Shah et al. (2012) who observe a decrease of k_La by 67% while increasing liquid viscosity from 1 to 50 mPa s. This is attributed to a decrease of k_L (Section 3.2.4.3). Kang et al. (1999) report a decrease of k_La when increasing viscosity which is attributed to a decrease of gas holdup and interfacial area. Öztürk et al. (1987) found lower k_La values for organic solvents and mixtures compared to water which is attributed to the higher viscosity of the organic solvents. Hashemi et al. (2009) also report a predominant effect of viscosity and surface tension when changing temperature. Adding surface active compounds results on an increase of k_La_L, as shown by Hikita et al. (1981).

3.2.4.2. Temperature effect on interfacial area. The evolution of interfacial area with temperature has been partially studied in the section dedicated to the gas holdup (Section 3.1.4). The interfacial area seems to increase with temperature in the large majority of the publications ((Jin et al., 2014; Pohorecki et al., 2001) and Section 3.1.4) except for three publications (Grover et al., 1986; Pohorecki et al., 1999; Yang et al., 2001). The differences have been discussed before.

3.2.4.3. Temperature effect on k_L. Few studies deal with this effect. Lau et al. (2004), Jin et al. (2014) and Yang et al. (2001) studied the effect of temperature on the coefficient k_L. Yang et al. (2001) observed that the k_L coefficient increases significantly with temperature. Authors explain their results by reporting that an increase in temperature decreases the

viscosity and therefore promotes the molecular diffusion. In the same conditions, they also observe a decrease of the interfacial area (Fig. 5) and they suppose that their bubble size increases. It may also affect positively the k_L (Section 3.2.3.3 for the effect of bubble size on k_L). Jin et al. (2014) observe an increase of both k_L and a. They also stated that a decrease of viscosity promotes molecular diffusion but they report that this decrease may also reduce t_c because of the slightly higher bubble velocities, both resulting on an increase of k_L (Eq. (11)). It is likely that the differences for a between those two publications rely on the viscosity of the liquid phase. Lau et al. (2004) only study qualitatively the difference between their measurement of k_La and gas holdup. They conclude that the rate of increase of k_La with temperature is faster than that of gas holdup: in their conclusion k_L also increases with temperature. They explain it by the promotion of molecular diffusion. In fact, if gas holdup increases it is likely that the bubble diameter decreases with temperature. Calculations have been made for this review by considering their values of k_La and ε_G and calculating the ratio k_L/d_b using interfacial area definition: $k_L/d_b = k_La/(6\varepsilon_G)$. While temperature increases, the bubble diameter decreases and calculations show that k_L increases with temperature if the bubble diameter is divided by less than 4 when the temperature increases. As they do not specify their bubble diameters, it is then difficult to conclude.

One may wonder what would be the evolution of k_La in the case where the interfacial area or gas holdup decreases with temperature (Deckwer et al., 1980; Grover et al., 1986; Yang et al., 2001). Only Yang et al. (2001) studied the evolution of k_L and a with temperature (Fig. 5). Their results show that for most experiments k_La_L still increases with temperature, in the case where the interfacial area decreases, which indicates a predominant effect of k_L. A plateau at high temperatures is clearly observed for the experiments made with CO in gas phase. What is not studied in Yang et al. (2001) is the effect of temperature on k_La (k_La can be obtained by multiplying k_La_L by ε_L). Gas holdup is not measured but ε_L increases with temperature (Fig. 5 and explanations reported in Section 3.1.4). When the plateau is observed for k_La_L, an increase of k_La with temperature may be observed. Other experiments are needed to clarify this effect.

As for temperature influence on liquid properties, some authors (García-Abuín et al., 2010; La Rubia et al., 2010) have reported a negative effect of viscosity on k_L, which decreases when viscosity increases. This is attributed to a decrease of the diffusion coefficient. Chilekar (2007) found that k_L is lower for a low surface tension and a slightly viscous fluid (Isopar-M) than water. As gas holdup is higher and bubble size lower for Isopar-M, it can be deduced that viscosity has no effect and that surface tension has a decreasing effect on k_L. Öztürk et al. (1987) found lower k_La for organic solvents than for water but higher gas holdups. This can be attributed again to a decrease of k_L while increasing viscosity.

3.2.5. *Superficial liquid velocity effect on mass transfer properties*

Chaumat et al. (2005) observe an increase of the k_La while increasing superficial liquid velocity. At the same time they observe a decrease of the gas holdup (Section 3.1.5). As gas holdup and interfacial area decrease when increasing superficial liquid velocity, it is easy to conclude that k_L increases. Lau et al. (2004) observed an increase of the k_La with the superficial liquid velocity. This effect is observed at low superficial liquid velocity at ambient pressure and at the highest pressure (2.86 MPa) for higher u_L. The effect is higher at high superficial gas velocity. The gas holdup (and interfacial area) remains constant at the 2.86 MPa but is slightly decreased at ambient pressure. This indicates again a positive effect on k_L. Shah et al. (2012) observed the same tendencies. The authors explained this result by the promotion of turbulence induced by the liquid, which has a positive effect on k_L. The higher effect at 2.86 MPa has to be linked with the decreasing effect of pressure on k_L as reported on Section 3.2.3.3. At high pressures, turbulence induced by the increase of u_L compensates the negative effect of the pressure. Chaumat et al. (2005) found that the ratio k_L/a increases with the superficial liquid velocity. In their conditions, the product k_La is measured over the entire reactor but the interfacial area of the denominator is obtained by local measurements in the middle of the column: k_L cannot be calculated. The authors note that the local interfacial area decreases with u_L in their conditions and that the k_La increases. Their measure of overall gas holdup shows that it decreases with u_L and by extension it is also the case for the interfacial area. It is therefore likely that the k_L increases with u_L. At ambient pressure and temperature in the heterogeneous regime, Hikita et al. (1981) do not observe any effect of superficial liquid velocity on k_La_L. However, the range of u_L applied is not specified.

3.2.6. *Working mode effect on mass transfer properties*

As for the working mode no publications showing experimental results are available. The contribution for the influence of working mode on k_La is 2.5% in weight in the publication of Baawain et al. (2007) which is less than the effect of working mode on gas holdup (Section 3.1.6). This result is obtained by comparing different publications with different working modes. Singh and Majumder (2011) simulate co and counter-current bubble columns working in the homogeneous regime and report better mass transfer efficiency in the case of counter-current operation while k_La is not affected by working mode. They report an effect of backmixing on mass transfer. Mixing is better in counter-current operation due to higher relative velocity between the two phases. Better mass transfer efficiency is obtained with higher backmixing. In fact, Bouaifi et al. (2001) observe that k_L depends on the liquid axial dispersion coefficient and report an increase of k_L while increasing $D_{ax,L}$. This is also attributed to an increase of the relative velocity and a lower contact time. However, the two publications seem to disagree as the model predicts constant k_La and a, while relative velocity increases.

3.2.7. *Effect of other parameters on mass transfer properties: superficial gas velocity, column and distributor design.*

3.2.7.1. Effect of superficial gas velocity on mass transfer properties. Superficial gas velocity has an increasing effect on k_La (Akita and Yoshida, 1973, 1974; Behkish et al., 2002; Chaumat et al., 2005; Ferreira et al., 2013; Han and Al-Dahhan, 2007; Hashemi et al., 2009; Hikita et al., 1981; Jin et al., 2014; Kang et al., 1999; Lau et al., 2004; Letzel et al., 1999; Muroyama et al., 2013; Shah et al., 2012). This is observed in literature whatever the operating conditions in the homogeneous and heterogeneous regime. However, as for the gas holdup (Fig. 3) some authors report a maximum in the transition regime (Lau et al., 2004; Letzel et al., 1999; Zahradník et al., 1997) for ambient conditions or pressures up to 0.4 MPa. It is not observed at higher pressure (Lau et al., 2004) and temperature. The interfacial area increases with an increase

of the superficial gas velocity (Baz-Rodríguez et al., 2014; Bouaifi et al., 2001; Ferreira et al., 2013; García-Abuín et al., 2012, 2010; Gopal and Sharma, 1983; Han and Al-Dahhan, 2007; Jin et al., 2014; La Rubia et al., 2010; Lau et al., 2012; Lemoine et al., 2004; Maalej et al., 2003; Maceiras et al., 2010; Majumder et al., 2006; Oyevaar et al., 1991; Pohorecki et al., 1999, 2001; Smith et al., 1996; Vázquez et al., 2000b; Xue et al., 2008) in every cases even when the small effect of superficial gas velocity on bubble size described in Section 3.1.7 is observed (Bouaifi et al., 2001; Ferreira et al., 2013; García-Abuín et al., 2012, 2010; Lau et al., 2012; Lemoine et al., 2004; Majumder et al., 2006; Pohorecki et al., 1999; Smith et al., 1996; Xue et al., 2008). As gas holdup, a maximum is observed in the transition regime for some authors (Han and Al-Dahhan, 2007).

As for the evolution of k_L with superficial gas velocity, opposite trends are observed in literature. Some authors report an increase in their whole range of u_G with a plateau (Han and Al-Dahhan, 2007; La Rubia et al., 2010), other only observe the increase at high superficial gas velocity (Kluytmans et al., 2003), other do not observe the plateau (Chaumat et al., 2005; Chilekar, 2007; Ferreira et al., 2013; Gopal and Sharma, 1983; Jin et al., 2014; Lemoine et al., 2004), others observe no effects at all (Dewes et al., 1995; García-Abuín et al., 2010; Lau et al., 2012; Vandu et al., 2004; Voyer and Miller, 1968; Yang et al., 2001) and some observe a decrease (Baz-Rodríguez et al., 2014). Chaumat et al. (2005) studied the evolution of the ratio k_La/a. They conclude that the increase of k_L with superficial gas velocity is in disagreement with Higbie's theory of penetration. They assume that there is a promotion of the turbulence induced by the bubbles. This is consistent with Nedeltchev et al. (2007) who argue that Higbie's theory actually does not take into account the effect of the drag of bubbles on k_L. Han and Al-Dahhan (2007) also conclude that the increase of k_L with u_G is linked to the turbulence induces by the bubbles. Lemoine et al. (2004) report that the increase of the bubble size (Section 3.2.3.3) results in an increase of k_L, which is validated by Chilekar (2007) who observes a constant k_L/d_B ratio while d_B increases. However, this seems to be invalidated by La Rubia et al. (2010) as they observe the increase of k_L while d_b decreases. They report a decreasing effect of u_G on k_L while increasing viscosity (0.8–1.22 mPa s). This effect is attributed to the decrease of the turbulence induced by the bubbles while increasing viscosity, which is consistent with the remarks above. At high viscosity no effect is observed. However, this is in contradiction with Jin et al. (2014) who observe a strong effect of u_G at higher liquid viscosity (4 mPa s) but under pressure (1.0 MPa). Some authors do not observe any effect of u_G on k_L because of the small u_G range studied (García-Abuín et al., 2010; Yang et al., 2001). However, Vandu et al. (2004) and Hashemi et al. (2009), who did not observe any effect of u_G on k_L, observe that the ratio k_L/d_b remains almost constant while the gas velocity increases (up to 40 cm s^{-1}). No information is given for d_B. However, these two publications work with a highly viscous fluid: this is consistent with the remarks of La Rubia et al. (2010) who observe no effect of u_G at high viscosity. Their k_L is nearly independent of u_G but an increase can be seen depending on operating conditions, especially at the highest pressure for Hashemi et al. (2009) which would be in agreement with Jin et al. (2014). At high viscosity, working under pressure may have a positive effect on the turbulence induced by the bubbles: their number would be higher while d_B remains nearly constant (Section 3.1.3 for the concomitant effect of viscosity and pressure).

Baz-Rodríguez et al. (2014) observe a decrease of k_L while increasing u_G (in a small range and for low u_G) and report another effect: k_L is higher for isolated bubbles than for bubble swarms due to lower rise velocity for bubble swarms. Another effect is reported by De Swart and Krishna (1995) who found an increasing effect of k_L in presence of frequent bubble coalescence and breakage which is the case in the heterogeneous flow at high gas velocity.

3.2.7.2. *Effect of gas sparger on mass transfer properties*. As reported in the section dedicated to gas holdup (Section 3.1.7) gas sparger properties may have no influence in well established homogeneous and heterogeneous regime. This is also observed for k_La in literature (Han and Al-Dahhan, 2007; Hikita et al., 1981; Zahradník et al., 1997). In other cases, as for the gas holdup, porous and membrane diffusers lead to higher k_La than perforated plates (Bouaifi et al., 2001; Lau et al., 2012). Decreasing the orifice diameter for perforated plates leads to an increase of k_La (Chaumat et al., 2005; Han and Al-Dahhan, 2007; Jordan and Schumpe, 2001).

These tendencies are also observed for the interfacial area (Bouaifi et al., 2001; Lau et al., 2012; Smith et al., 1996; Xue et al., 2008). As for k_L, in the heterogeneous regime, Han and Al-Dahhan (2007) observed no effect of the distributor orifice diameter on k_L. It should be noticed that in the same conditions, gas holdup, k_La and interfacial area are also not affected by sparger orifice diameter. Bouaifi et al. (2001) show that k_L depends on the type of sparger used. In their larger column (D_c = 20 cm) the porous plate and the membrane sparger give higher k_L than the perforated plate (see Table 1 for the properties of the spargers). At the same time, the porous and the membrane spargers lead to similar bubble diameter (between 3.7–5 mm), smaller than the ones obtained with the perforated plate (between 4.5 and 7.5 mm). They conclude that their tendencies are in good agreement with Higbie's theory. In fact, this is also in agreement with Fig. 7. Lau et al. (2012) observe higher k_L for spargers that give larger bubbles, which is also in agreement with Higbie's theory (Section 3.2.3.3).

Kang et al. (1999) report that an even distribution of bubbles at the sparger leads to a higher mass transfer coefficient which is linked to interfacial area and gas holdup and less coalescence.

3.2.7.3. *Effect of column design on mass transfer properties*. Lau et al. (2012) report a decrease of k_La and interfacial area while increasing the H_c/D_c ratio, as for the gas holdup (Section 3.1.7). However, in the same conditions, k_L seems to be independent of H_c/D_c. Muroyama et al. (2013) also observe a decrease of k_La while increasing H_c, gas holdup remaining constant (their bubble size distribution does not depend on z). This is attributed to an increase of the gas residence time, leading to a decrease of the bubble size, down to their complete disappearance, when residence time is high. Fewer bubbles contribute to mass transfer near the outlet of tall bubble columns: the decrease is observed because k_La is measured globally. Xue et al. (2008) found that for z/D_c ratios over 5, the effect of the sparger region on interfacial area can be neglected. This indicates again that H_c/D_c has no more influence for ratios over 5 (explanations in Section 3.1.7). This is in agreement with Hikita et al. (1981) who do no observe any effect of H_c for H_c/D_c ratios over 7.

Bouaifi et al. (2001) observe an increase of k_La with the column diameter. At the same time, they observe an increase of

interfacial area with the column diameter (from 15 to 20 cm), which is not in agreement with the tendencies observed in Section 3.1.7 for gas holdup. However as they do not measure their bubble diameter and gas holdup in both columns, it is difficult to conclude on the interfacial area. They observe that k_L increases with the column diameter for two types of sparger (porous and membrane) but decreases for the perforated plate. The tendencies are not explained. Lau et al. (2004), however, observe a decrease of k_La (and gas holdup) while increasing column diameter (from 5 to 10 cm). They attributed this effect to wall effects, as already reported for gas holdup in Section 3.1.7. Chilekar (2007) observe no effect of column diameter on k_La in well established homogeneous and heterogeneous regime for column diameters over 0.15 m, which is in agreement with the tendencies observed for gas holdup (Section 3.1.7). In well established heterogeneous regime, Hikita et al. (1981) do not observe any effect of D_c in the range 0.1–0.19 m. This may be due to reduced wall effects in the sparger region for single-nozzle spargers.

3.3. *Study of liquid axial dispersion coefficient*

3.3.1. *Definition*

The degree of mixing in the column is quantified by the measurement of the axial dispersion through the axial dispersion coefficient $D_{ax,L}$. Many authors show that, generally, there is a good mixing in bubble column and the dispersion cannot be ignored. Some correlations are given in Table 1 for the estimation of the axial dispersion coefficient. Mixing mechanisms have already been reported in Section 2.1.

3.3.2. *Measurement*

The liquid axial dispersion coefficient is measured by determining the Residence Time Distribution (RTD). The measurement can be made in liquid or in gas phase. For measurement of the liquid RTD the tracer is typically saline (concentration followed by conductimetry, Biń et al., 2001; Bouaifi et al., 2001; Forret et al., 2003; Hikita and Kikukawa, 1974; Krishna et al., 1999a; Ohki and Inoue, 1970; Shah et al., 2012; Therning and Rasmuson, 2001), coloured (Shawaqfeh, 2003; Smith et al., 1996; Zahradník et al., 1997) or radioactive. A variant of the technique is the use of a non-radioactive tracer that interacts with neutrons (requires a neutron source) (Boyer et al., 2002). Major drawbacks at high pressures and temperatures are corrosion problems due to the use of salts (chloride for instance) and degradation of coloured tracer at high temperatures (for example BBT is degraded under 473 K). The radioactive and neutron techniques have been reported as efficient techniques to avoid those problems (Boyer et al., 2002; Onozaki et al., 2000). The calculation of $D_{ax,L}$ must be made by the use of a model (as the axial dispersion model), the simple ones being largely discussed in literature (Smith et al., 1996; Villermaux, 1994). For bubble columns, more complex models have been reported, taking into account the possible transfer in stagnant zones. The analysis then becomes more complicated and requires the fitting of other parameters. There may be problems with the sensitivity of the results with respect to various parameters (Boyer et al., 2002). For complex models, some authors propose an algorithm to perform calculations (Dudukovic et al., 2000). Another drawback for bubble columns is that accuracy can be low if the concentrations do not correspond to a perfectly mixed fluid locally (strong interactions between elements of fluids) (Boyer et al., 2002). This is typically the case when tracer concentration is followed by the use of probes giving concentration near the wall which can differ from the true concentration. Bubbles have also been reported to disturb the measurement from probes: signals must be filtered (Boyer et al., 2002). For gas RTD measurement, calculations are more complicated because of the mass transfer, especially at high pressure and temperature. Mass transfer has to be taken into account (Boyer et al., 2002). The use of two balances on gas and liquid phase allow the determination of gas and liquid axial dispersion coefficient simultaneously if holdup, concentrations and mass transfer properties are known (Boyer et al., 2002).

Another measuring technique has also been reported: the thermal dispersion technique (Holcombe et al., 1983; Lorenz et al., 2005; Yang and Fan, 2003). It is based on the analogy between mass and heat transfer under nonreactive conditions. The equation used for the calculations is similar to a mass balance replacing concentration by temperature, the mass transfer term by a heat loss term taking into account the heat from the liquid phase to the environment (through the wall and the gas phase and due to evaporation) and defining the thermal dispersion coefficient as $\lambda_L/(\rho_L C_{pL})$. Calculations are made by measuring the temperature profile inside the bubble column.

3.3.3. *Pressure influence on liquid axial dispersion coefficient*

Yang and Fan (2003) observed a decrease of the liquid axial dispersion coefficient with an increase of pressure in a wide range of superficial gas and liquid velocity (Table 1). Their experimental results are shown on Fig. 8.

Fig. 8 shows that the $D_{ax,L}$ decreases when increasing pressure (up to 4.2 MPa). It also shows that the effect is higher at high superficial gas velocity and that the effect of pressure decrease when increasing pressure. The authors explain their results using the correlation of Joshi (Eq. (17)) which is used to estimate the velocity of fluid recirculation (V_c) in the case where only the turbulence associated with liquid circulation is considered (case of heterogeneous regime).

$$V_c = 1.31\left[gD_c\left(u_G - \frac{\varepsilon_G}{1-\varepsilon_G}u_L - \varepsilon_G u_{b\infty}\right)\right]^{1/3} \quad (17)$$

According to Eq. (17) the effect of pressure would be linked to several contradictory effects on V_c. The increase of gas holdup causes an increase of the term $\varepsilon_G u_{b\alpha}$. The decrease of the bubble size with pressure (Section 3.1.3) and thus the decrease of the bubble rising velocity leads to a decrease of the term $\varepsilon_G u_{b\alpha}$. Therefore both effects damped each other and V_c does not vary too much. At the same time, reducing the size of the bubbles leads to a reduction of turbulence and thus the overall effect is a decrease. Tarmy et al. (1984) compared their measurement to correlations developed at ambient pressure and temperature and found that their measured axial coefficients were lower than predictions, concluding on a decrease of the axial coefficient with pressure.

This decrease of the liquid axial dispersion coefficient with pressure disagrees with other publications (Chilekar et al., 2010; Holcombe et al., 1983; Houzelot et al., 1983; Sangnimnuan et al., 1984; Therning and Rasmuson, 2001; Wilkinson et al., 1993). Sangnimnuan et al. (1984) do not observe any effect of pressure in the range 4.5–15 MPa in the homogeneous regime, as for their gas holdup. Houzelot et al. (1983) observed no effect of pressure on the liquid axial

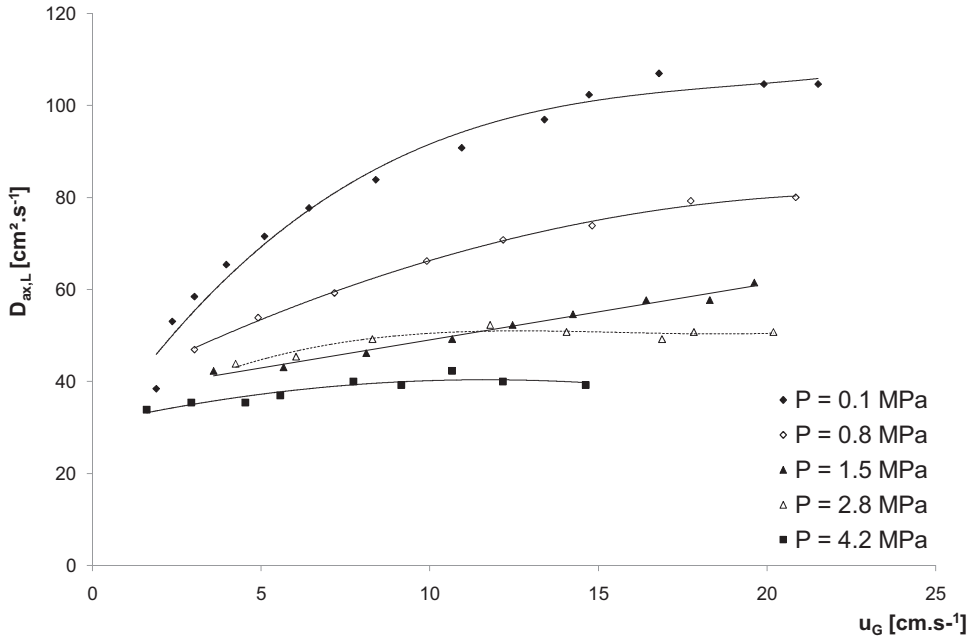

Fig. 8 – Evolution of liquid axial dispersion coefficient with superficial gas velocity for different pressures. $T = 300$ K; $D_c = 10.16$ cm; $u_L = 0.17$ cm s^{-1}. System: N_2/Paratherm-NF. (Yang and Fan, 2003).

dispersion coefficient for pressures between 0.1 and 0.3 MPa in the homogeneous regime. Their experiments could be consistent with the observation of Yang and Fan (2003) since in the homogeneous regime the influence of pressure on the bubble size is limited and bubble size does not vary too much. Holcombe et al. (1983) observe no effect of pressure in continuous mode at higher superficial gas velocities and for a limited range of pressure (0.3–0.71 MPa). It disagrees with Wilkinson et al. (1993) who observed an increase of the liquid axial dispersion coefficient with pressure between 0.1 and 1.5 MPa for the same nitrogen/water system but with a higher column diameter. Effect of pressure is more pronounced for high gas velocities (which correspond to the heterogeneous regime) as on Fig. 8. However, they observe an increase of the liquid axial dispersion coefficient with pressure despite the decrease of bubble size. This is also the case for Chilekar et al. (2010) who observed that, in fact, liquid recirculation increases when increasing pressure. Therning and Rasmuson (2001) also observed the increase of axial dispersion coefficient with a packed column. This increase is attributed to a decrease of radial dispersion while bubble size decreases as for Wilkinson et al. (1993). It can be noted that for studies where pressure has no influence (Holcombe et al., 1983; Houzelot et al., 1983; Sangnimnuan et al., 1984) the column diameters are the lowest and typically below 10 cm. D_C influence on axial dispersion coefficient may be another possible explanation for these trends (Section 3.3.7.3).

The decrease is effectively observed for Yang and Fan (2003) who used a viscous fluid ($\mu_L > 7$ mPa s). It can then be stated that the influence of pressure on liquid axial dispersion coefficient depends on liquid phase properties. For the more viscous fluids, mixing may be dramatically affected by pressure as liquid recirculation turbulence is lower for these systems and mixing is more dependent on bubble induced turbulence. Eq. (17) and Sangnimnuan et al. (1984) results also suggest that pressure effect depends on its influence on gas holdup. Lorenz et al. (2005) proposed a CFD model based on the equations of mass balances and force balance to calculate the liquid axial dispersion coefficient and the velocity profile of the liquid. Their results are in agreement with Yang and Fan (2003), Wilkinson et al. (1993) and Houzelot et al. (1983). The authors observe that the effect of pressure leads to a decrease of the liquid velocity and the eddy viscosity. They show that an increase of the liquid velocity results in an increase of the liquid axial dispersion coefficient. As the eddy viscosity increases, the profile of the axial dispersion coefficient presents a maximum. The evolution of the axial dispersion coefficient depends on the intensity of those two effects. They depend in turn on the gas holdup and the superficial gas velocity. The authors use the experimental conditions from Wilkinson et al. (1993) and conducted CFD simulations at higher pressure and changing superficial gas velocity. They show that the dispersion coefficient follows the profile shown on Fig. 9.

Fig. 9 shows that in the pressure conditions of Yang and Fan (2003), liquid axial dispersion coefficient decreases when gas holdup increases up to 0.26 and then increases. Thus they attributed the observed effects to the influence of the gas superficial velocity and gas holdup, the effects of liquid properties being included in the gas holdup. As gas holdup stays at low values, a decrease is effectively observed. These results must be discussed. On the one hand, Lorenz et al. (2005) give no indication about the superficial liquid velocity used and its effect (Section 3.3.4) on the axial dispersion coefficient. The effect of this parameter on the results of the CFD results cannot be extrapolated easily because Yang and Fan (2003) show that, at constant superficial gas velocity, the superficial liquid velocity influences the axial dispersion coefficient, but not gas holdup. The couple of parameters (u_G, ε_G) is then not perfectly adapted to the study of the axial dispersion coefficient.

3.3.4. *Temperature influence on liquid axial dispersion coefficient*

No publications to date investigate this effect. However, Onozaki et al. (2000), in the homogeneous regime, found a lower axial dispersion coefficient at the lowest temperature (313 K versus 730 K) in the case of an industrial plant. This can be attributed to the increase of the liquid viscosity by reducing

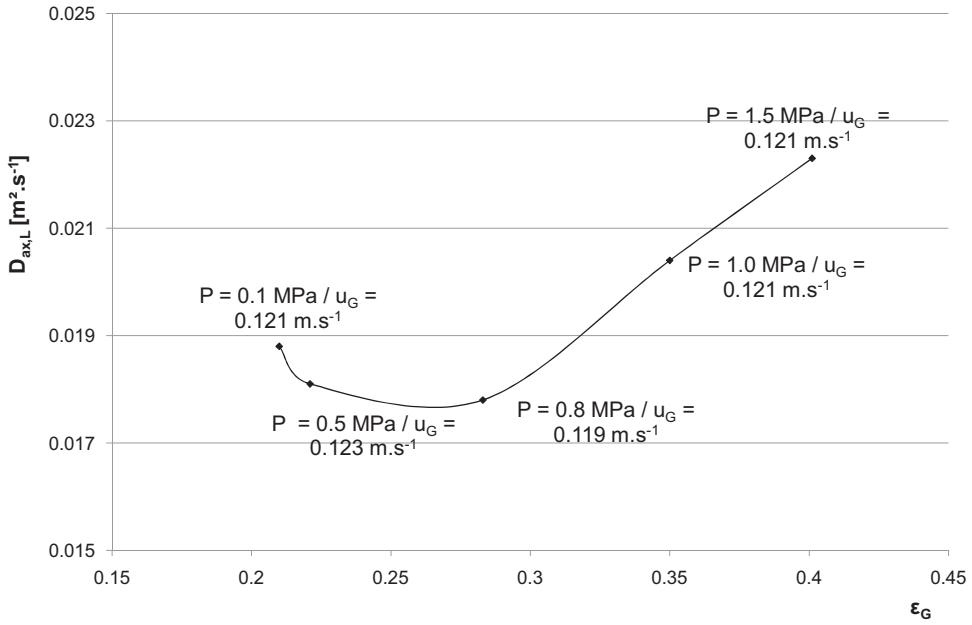

Fig. 9 – Liquid axial dispersion coefficient versus gas holdup for different pressures. D_c = 0.15 m. Wilkinson et al. (1993) (Wilkinson et al., 1993) operating conditions. Adapted from (Lorenz et al., 2005).

temperature. As for other publications, a decrease of the liquid axial dispersion coefficient while increasing viscosity is commonly observed (Hikita and Kikukawa, 1974; Shah et al., 2012) which is attributed to a decrease of liquid recirculation in conditions representative of the heterogeneous regime. Hikita and Kikukawa (1974) found that axial dispersion coefficient do not depend on liquid surface tension. This may the case in heterogeneous regime where the turbulence induced by the bubbles is limited.

3.3.5. *Superficial liquid velocity effect on liquid axial dispersion coefficient*

Yang and Fan (2003) observed an increase of the axial dispersion coefficient while increasing superficial liquid velocity. No effect on gas holdup is observed. The observed effect is higher in the case of the Paratherm NF than in water. The authors explain this effect by the increase of the liquid turbulence. Liquid velocity range being limited, the authors suggest that this increase is not due to the movement of bubbles, but rather linked to the increased energy exchange between liquid vortexes. The difference between water and Paratherm NF is mainly due to the effect of solvent on bubble size: smaller in the case of Paratherm, which has a much lower surface tension despite a higher viscosity. These bubbles contribute less to the turbulence which explains the difference. This tendency is also observed in other publications (Biń et al., 2001; Zahradník et al., 1997). The increase has been observed in the homogeneous and heterogeneous regime (Zahradník et al., 1997).

In the slug flow regime, Shawaqfeh (2003) observe a decrease of the axial dispersion coefficient while increasing superficial liquid velocity, which is attributed to a predominant effect of convection compared to dispersion in this regime. However, in counter-current mode, Shah et al. (2012) observed the decrease of the liquid axial dispersion coefficient while increasing superficial liquid velocity, which is attributed to a promotion of the liquid plug-flow behaviour by reducing the residence time of the liquid. Holcombe et al. (1983) and Sangnimnuan et al. (1984) observe no effect of superficial liquid velocity on liquid axial dispersion coefficient for low column diameters. As for pressure, the effect of liquid velocity may be neglected for low column diameters.

3.3.6. *Working mode effect on liquid axial dispersion coefficient*

Biń et al., 2001 observed no significant influence of the working mode on the liquid axial dispersion coefficient for liquid velocities (up to 6 mm s^{-1}) for an air-ozone/water system at ambient conditions. This is the only publication that studied this parameter influence on liquid axial dispersion coefficient.

3.3.7. *Effect of other parameters on liquid axial dispersion coefficient: superficial gas velocity, column and distributor design.*

3.3.7.1. Effect of superficial gas velocity on liquid axial dispersion coefficient. Increasing the superficial gas velocity leads to an increase of liquid axial dispersion coefficient (Biń et al., 2001; Chilekar et al., 2010; Forret et al., 2003; Hikita and Kikukawa, 1974; Holcombe et al., 1983; Krishna et al., 1999a; Lorenz et al., 2005; Ohki and Inoue, 1970; Sangnimnuan et al., 1984; Shah et al., 2012; Shawaqfeh, 2003; Smith et al., 1996; Wilkinson et al., 1993; Yang and Fan, 2003). Yang and Fan (2003) found that the increase is faster in homogeneous regime than in the heterogeneous regime. The authors explain this phenomenon by promoting liquid recirculation velocity in heterogeneous regime and the turbulence induced by the bubbles in the homogeneous regime. The increase of the liquid recirculation speed in heterogeneous regime does not cause as much turbulence as the one induced by the bubbles in homogeneous regime which implies that the increase is less important in the heterogeneous regime. Ohki and Inoue (1970) found that the axial dispersion coefficient shows a maximum at the transition point between homogeneous and heterogeneous regime and follows the trend of the gas holdup for D_c > 4 cm. This is in agreement with the remark made above. Zahradník et al. (1997) studied the influence of the superficial gas velocity on the liquid Peclet. Their results show that the liquid Peclet in the homogeneous regime

increases with the superficial gas velocity and decreases in the heterogeneous regime, indicating that the axial dispersion coefficient decreases in homogeneous regime and increases in heterogeneous regime. The authors conclude that in the homogeneous regime, the behaviour of the liquid is close to plug-flow in their conditions. This is in contradiction with the results of other authors who conclude that the superficial gas velocity promotes the axial dispersion coefficient even in the homogeneous regime (Biń et al., 2001; Ohki and Inoue, 1970; Shah et al., 2012; Smith et al., 1996; Yang and Fan, 2003).

3.3.7.2. *Effect of gas sparger on liquid axial dispersion coefficient.* Hikita and Kikukawa (1974) and Ohki and Inoue (1970) observe no influence of gas sparger in heterogeneous regime. Zahradník et al. (1997) showed that the liquid axial dispersion coefficient is affected by the type of sparger only in the homogeneous regime for an air/water system in atmospheric conditions: the axial dispersion coefficient is lower for lower orifice diameters (the bubble size is lower). In the homogeneous regime, Ohki and Inoue (1970) found higher axial coefficients for higher open areas (high number of holes at constant hole diameter) and higher hole diameter (at constant number of holes), which suggests again that the higher the gas holdup and bubble size, the higher the axial coefficient. Bouaifi et al. (2001) obtained, in their homogeneous system, similar results: axial dispersions coefficients are lower in the case of membranes than for perforated or porous plates which present nearly similar dispersions in the same conditions and for their two column diameters. In the column of smaller diameter, however, it can be noted that the dispersions are larger for the perforated distributor. This can be attributed to the turbulence induced by the bubbles since their diameters are slightly larger for the perforated distributor than for the porous or the membranes. This suggests that the larger the bubbles, the higher the axial dispersion. However, Yang and Fan (2003) found no significant influence of the type of distributor (porous or perforated plates) on the axial dispersion coefficient in the case of Paratherm NF, whether the regime is homogeneous or heterogeneous. This may be related with the publication of Bouaifi et al. (2001) who observed that the axial coefficients obtained with the use of perforated and porous plates are almost identical in the larger column. Smith et al. (1996) also observed that the axial dispersion coefficients do not seem to depend on the type of sparger. They work with an inclined column and they conclude that their scale of turbulence does not seem to be equal to the ones of other authors. This could explain the differences.

3.3.7.3. *Effect of column design on liquid axial dispersion coefficient.* As far as it has been tested, axial dispersion coefficient increases when column diameter increases (Bouaifi et al., 2001; Forret et al., 2003; Hikita and Kikukawa, 1974; Holcombe et al., 1983; Krishna and Sie, 2000; Krishna et al., 1999a; Ohki and Inoue, 1970; Yang and Fan, 2003). Forret et al. (2003) show that this dependency may not be linked to gas holdup (their gas holdup does not depend on column diameter) but is linked to liquid recirculation velocity at high superficial gas velocity. For the experiments of Yang and Fan (2003), the increase is observed at low and high pressures but the effect of column diameter is lower at high pressures. At the same time, gas holdup decreases when column diameter increases, which indicate that overall effect would be related to the larger bubbles in large columns that contribute more to the turbulence. At high pressures their proportion is reduced. On the contrary, Bouaifi et al. (2001) observed an increase of gas holdup when increasing column diameter, which is not explained (Section 3.1.7.3). Yang and Fan (2003) finally propose Eqs. (18) and (19) to link the dispersion coefficient and the column diameter.

$$D_{ax,L} \alpha D_c^w \tag{18}$$

$$\text{With } 1 - w/w_0 = 0.11 \ln(\rho_G/\rho_{G0}) \tag{19}$$

The index 0 indicates that the density and the coefficient w are measured at atmospheric pressure.

Hikita and Kikukawa (1974) show that axial dispersion coefficient do not depend on column height in heterogeneous regime, for H_c/D_c ratios over 7.

4. Conclusion

This article has shown the complexity of the study of the hydrodynamics in bubble columns reactors: many parameters have been reported to be relevant for the design.

Gas holdup has been shown to be strongly dependent of operating conditions such as pressure, temperature, system studied and superficial gas velocity but also on design parameters such as gas sparger and column design. Column design has no more influence for H_c/D_c ratios over 5 and D_c over 0.70 m. Working mode has minor effect on gas holdup but superficial liquid velocity has been reported to be a relevant parameter, although its effects are not yet clear. Mass transfer properties (interfacial area, k_L and k_La) have also been shown to be dependent of these operating and design parameters. Superficial liquid velocity has been reported as a relevant parameter and its influence on mass transfer is validated. Working mode has no effect, as for gas holdup. However, pressure influence on k_L is not yet clear and further investigations have to be carried out. Some negative influence of temperature on interfacial area has been reported and this tendency seems to depend on the system studied: it has to be checked in the desired operating conditions. Axial dispersion coefficient also depends on pressure, superficial liquid and gas velocities and sparger and column design. However, pressure influence is contradictory and some clues have been reported for the understanding of its effect: it seems to depend on the extent of its effect on gas holdup. Temperature effect is poorly known. Working mode, as for the other parameters, is not a relevant parameter. This article shows that, in fact, the correlations given in Table 1 are not reliable for the estimation of gas holdup, a, k_L, k_La and $D_{ax,L}$ at high pressure and/or high temperature conditions as only one or two operating parameters are studied in each publication.

For the design of high pressure processes, operating parameters such as pressure, temperature, superficial gas and liquid velocities and the liquid system studied have to be taken into account. As for the sparger, porous plate spargers are shown to provide better mass transfer properties. Column design has to be taken into account. Generally, this article shows that the operating conditions of the WAO process (pressures up to 30 MPa, temperatures up to 573 K, water as the solvent) allow increasing mass transfer efficiency. However, a plateau is observed for some effects (pressure, superficial gas and liquid velocities) and better understanding of these effects would be necessary to optimise mass transfer. In particular, pressure effect has been tested up to 19 MPa in literature and only up to 10 MPa for the water system. As a plateau may be observed, its effect has to be checked

at higher pressures (up to 30 MPa) in WAO conditions in order to find the optimal conditions for mass transfer while reducing the cost of operation. The lack of correlations of the different parameters studied here at higher pressure and higher temperature conditions is then penalizing.

Appendix A.

Roman letters

A	parameter in the Krishna et al. (1991) correlation [dimensionless]
a	interfacial area (per volume of dispersion) [m^{-1}]
a_L	interfacial area (per volume of liquid) [m^{-1}]
B	parameter in the Krishna et al. (1991) correlation [dimensionless]
B_1, B_2	parameter in the Jordan and Schumpe (2001) correlations [dimensionless]
d_b	bubble diameter [m]
d_{32}	Sauter bubble diameter [m]
$d_{b,0}$	primary bubble diameter [m]
d_0	gas sparger orifice diameter [m]
C, C'	constants in the Bouaifi et al. (2001) correlations [dimensionless]
C_1	parameter in the Jin et al. (2004) correlation [s^{-1}]
c	Eq. (15) parameter [dimensionless]
C_v	volume concentration of solid [%]
C_A^*	solubility of gas A [mol m^{-3}]
C_B	concentration of B in liquid [mol m^{-3}]
C_{pL}	liquid heat capacity [J kg^{-1} K^{-1}]
D_i	coefficients in the Mena et al. (2011) correlation [dimensionless]
$D_{ax,L}$	liquid axial dispersion coefficient [m^2 s^{-1}]
D_0	diameter of the distributor [m]
D_c	column diameter [m]
$D_{m,I,j}$	coefficient of molecular diffusivity (of compound i in solvent j) [m^2 s^{-1}]
E_R	energy dissipation rate [J s^{-1}]
g	gravity constant [m s^{-2}]
H_i	parameters in the Yang et al. (2001) correlations [dimensionless]
H_c	column height/Dispersion height [m]
h_P	probe position above the sparger [m]
I_i	parameters in the Kojima et al. (1997) correlations [dimensionless]
K_i	Parameters in the Öztürk and Schumpe (1987) correlations [dimensionless]
K_B	Eq. (15) parameter [dimensionless]
K_{B0}	Eq. (15) parameter [dimensionless]
k_L	liquid mass transfer coefficient [m s^{-1}]
k_La	volumetric liquid mass transfer coefficient [s^{-1}]
k_r	kinetic constant [(mol m^{-3})$^{1-m-n}$ s^{-1}]
M	gas phase momentum in Reilly et al. (1994) correlations [dimensionless]
M_i	molar mass of compound i [kg mol^{-1}]
m	partial order of reaction [dimensionless]
n	partial order of reaction [dimensionless]
N_0	number of holes in the sparger [dimensionless]
p	Eq. (15) parameter [dimensionless]
P	pressure [MPa]
q_D	drift-flux [m s^{-1}]
r_h	radius of the liquid film between two coalescing bubbles [m]
t_c	Higbie's theory contact time [s]
t_B	contact time between two coalescing bubbles [s]
t	time [s]
T	temperature [K]
u	velocity fluctuation [m s^{-1}]
u_b	bubble rising speed [m s^{-1}]
u_{BS}	small bubble rising speed [m s^{-1}]
u_{BL}	large bubble rising speed [m s^{-1}]
$u_{b,0}$	primary bubble rising speed [m s^{-1}]
$u_{b\infty}$	bubble terminal rising speed [m s^{-1}]
u_0	superficial gas velocity at sparger [m s^{-1}]
u_G	superficial gas velocity [m s^{-1}]
$u_{G,trans}$	superficial gas velocity at the end of the homogeneous regime [m s^{-1}]
u_L	superficial liquid velocity [m s^{-1}]
u_S	slip velocity [m s^{-1}]
$v_{m,i}$	molar volume of solute i [m^3/mol]
V_c	liquid recirculation velocity [m s^{-1}]
V_R	dispersion volume [m^3]
w	Eqs. (18) and (19) parameter [dimensionless]
z	axial position in the column [m]
z_i	parameters in the Parasu Veera and Joshi (2000) correlation [dimensionless]
Z_i	parameters in the Reilly et al. (1994) correlations [dimensionless]

Greek letters

ΔP	differential pressure [Pa]
ΔP_0	pressure drop at sparger [Pa]
Δz	height difference [m]
ε_G	gas holdup [dimensionless]
$\varepsilon_{G,trans}$	gas holdup at the end of the homogeneous regime [dimensionless]
ε_L	liquid holdup [dimensionless]
σ_L	liquid surface tension [N m^{-1}]
ρ_G	gas density [kg m^{-3}]
ρ_L	liquid density [kg m^{-3}]
μ_L	liquid viscosity [Pa s]
μ_{SL}	slurry viscosity [Pa s]
μ_G	gas viscosity [Pa s]
v_h	film drainage speed [m s^{-1}]
υ_L	liquid kinematic viscosity [m^2 s^{-1}]
υ_{SL}	slurry kinematic viscosity [m^2 s^{-1}]
γ_L	thickness of the liquid film between two coalescing bubbles [m]
φ	absorption flux [mol m^{-3} s^{-1}]
Φ_0	open area [dimensionless]
τ_L	liquid residence time [s]
α	parameter of the Danckwerts equation [m^2 s^{-2}]
β	parameter of the Akita et al. (1974) correlation [dimensionless]
λ_L	liquid thermal conductivity [W m^{-1} K^{-1}]

Adimensionnal numbers

$Re_{0L} = \rho_L u_0 d_0/\mu_L$ liquid Reynolds number at sparger

$Fr_0 = {u_0}^2/(g d_0)$ Froude number at sparger

$R = [2k_r {C_A}^{*(m-1)} {C_B}^n \varepsilon_L]/[k_L a\,(m+1)]$ 'R' number

$Da = k_L a \tau_L$ Damköhler number

$Ha = ([2k_r {C_A}^{*(m-1)} {C_B}^n D_m]/[{k_L}^2\,(m+1)])^{1/2}$ Hatta criterion

$Mo = g{\mu_L}^4(\rho_L - \rho_G)/({\rho_L}^2{\sigma_L}^3)$ Morton number

$Pe_L = u_L D_c/D_{ax,L}$ liquid axial Peclet number

Abbreviations

SB	semi-batch
Co-C	co-current
Coun-C	counter-current

References

Akita, K., Yoshida, F., 1973. Gas holdup and volumetric mass transfer coefficient in bubble columns. Effects of liquid properties. Ind. Eng. Chem. Process Design Dev. 12, 76–80.

Akita, K., Yoshida, F., 1974. Bubble size, interfacial area, and liquid-phase mass transfer coefficient in bubble columns. Ind. Eng. Chem. Process Design Dev. 13, 84–91.

Baawain, M.S., El-Din, M.G., Smith, D.W., 2007. Artificial neural networks modeling of ozone bubble columns: mass transfer coefficient, gas hold-up, and bubble size. Ozone: Sci. and Eng 29, 343–352.

Baz-Rodríguez, S.A., Botello-Alvarez, J.E., Estrada-Baltazar, A., Vilchiz-Bravo, L.E., Padilla-Medina, J.A., Miranda-López, R., 2014. Effect of electrolytes in aqueous solutions on oxygen transfer in gas–liquid bubble columns. Chem. Eng. Res. Design.

Behkish, A., Lemoine, R., Oukaci, R., Morsi, B.I., 2006. Novel correlations for gas holdup in large-scale slurry bubble column reactors operating under elevated pressures and temperatures. Chem. Eng. J. 115, 157–171.

Behkish, A., Lemoine, R., Sehabiague, L., Oukaci, R., Morsi, B.I., 2007. Gas holdup and bubble size behavior in a large-scale slurry bubble column reactor operating with an organic liquid under elevated pressures and temperatures. Chem. Eng. J. 128, 69–84.

Behkish, A., Men, Z., Inga, J.R., Morsi, B.I., 2002. Mass transfer characteristics in a large-scale slurry bubble column reactor with organic liquid mixtures. Chem. Eng. Sci. 57, 3307–3324.

Bhavaraju, S.M., Russell, T.W.F., Blanch, H.W., 1978. The design of gas sparged devices for viscous liquid systems. AIChE J. 24, 454–466.

Biń, A.K., Duczmal, B., Machniewski, P., 2001. Hydrodynamics and ozone mass transfer in a tall bubble column. Chem. Eng. Sci. 56, 6233–6240.

Bouaifi, M., Hebrard, G., Bastoul, D., Roustan, M., 2001. A comparative study of gas hold-up, bubble size, interfacial area and mass transfer coefficients in stirred gas–liquid reactors and bubble columns. Chem. Eng. Process.: Process Intensif. 40, 97–111.

Boutin, O., Ferrasse, J.-H., Lefèvre, S., 2011. Procédés d'oxydation en voie humide. Techniques de l'ingénieur Chimie verte et nouvelle gestion des déchets base documentaire: TIB495DUO.

Boyer, C., Duquenne, A.-M., Wild, G., 2002. Measuring techniques in gas–liquid and gas–liquid–solid reactors. Chem. Eng. Sci. 57, 3185–3215.

Calderbank, P.H., 1967. Gas Absorption from Bubbles. The Institution of Chemical Engineers, London.

Cents, A.H.G., Brilman, D.W.F., Versteeg, G.F., 2005. CO_2 absorption in carbonate/bicarbonate solutions: the Danckwerts-criterion revisited. Chem. Eng. Sci. 60, 5830–5835.

Charpentier, J.-C., Roizard, C., Wild, G., 1997. Absorption avec réaction chimique. Techniques de l'ingénieur Opérations unitaires: techniques séparatives sur membranes base documentaire: TIB331DUO.

Chaumat, H., Billet-Duquenne, A.-M., Augier, F., Mathieu, C., Delmas, H., 2005. Mass transfer in bubble column for industrial conditions—effects of organic medium, gas and liquid flow rates and column design. Chem. Eng. Sci. 60, 5930–5936.

Chilekar, V.P., 2007. Hydrodynamics and mass transfer in slurry bubble columns: Scale and pressure effects.

Chilekar, V.P., Van der Schaaf, J., Kuster, B.F.M., Tinge, J.T., Schouten, J.C., 2010. Influence of elevated pressure and particle lyophobicity on hydrodynamics and gas–liquid mass transfer in slurry bubble columns. AIChE J. 56, 584–596.

Choi, I.S., Wiesmann, U., 2004. Effect of chemical reaction and mass transfer on ozonation of the azo dyes reactive black 5 and reactive orange 96. Ozone: Sci. Eng. 26, 539–549.

Clark, K.N., 1990. The effect of high pressure and temperature on phase distributions in a bubble column. Chem. Eng. Sci. 45, 2301–2307.

Cui, Z., 2005. Hydrodynamics in a Bubble Column at Elevated Pressures and Turbulence Energy Distribution in Bubbling Gas–Liquid and Gas–Liquid–Solid Flow Systems. The Ohio State University, Columbus.

Davidson, J.F., Mech, A.M.I., Schüler, B.O.G., 1960. Bubble formation at an orifice in an inviscid liquid. Trans. Inst. Chem. Eng. 38, 335.

De Bruijn, T.J.W., Chase, J.D., Dawson, W.H., 1988. Gas holdup in a two-phase vertical tubular reactor at high pressure. Can. J. Chem. Eng. 66, 330–333.

De Swart, J.W.A., Krishna, R., 1995. Influence of particles concentration on the hydrodynamics of bubble column slurry reactors. Chem. Eng. Res. Design 73, 308–313.

Debellefontaine, H., Chakchouk, M., Foussard, J.N., Tissot, D., Striolo, P., 1996. Treatment of organic aqueous wastes: wet air oxidation and wet peroxide oxidation®. Environ. Pollut. 92, 155–164.

Deckwer, W.-D., Louisi, L., Zaidi, A., Ralek, M., 1980. Hydrodynamic properties of the Fischer-Tropsch slurry process. Ind. Eng. Chem. Process Design Dev 19, 699–708.

Dewes, I., Kueksal, A., Schumpe, A., 1995. Gas density effect on mass transfer in three-phase sparged reactors. Chem. Eng. Res. Design 73, 697–700.

Dewes, I., Schumpe, A., 1997. Gas density effect on mass transfer in the slurry bubble column. Chem. Eng. Sci. 52, 4105–4109.

Dudukovic, M.P., Antoine, B., Leclerc, J.P., Claudel, S., Lintz, H.G., Potier, O., 2000. Distribution des temps de séjour dans les procédés industriels: interprétation théorique. Oil Gas Sci. Technol.—Rev. IFP 55, 159–169.

Elgozali, A., Linek, V., Fialová, M., Wein, O., Zahradnıík, J., 2002. Influence of viscosity and surface tension on performance of gas–liquid contactors with ejector type gas distributor. Chem. Eng. Sci. 57, 2987–2994.

Fan, L.-S., Yang, G.Q., Lee, D.J., Tsuchiya, K., Luo, X., 1999. Some aspects of high-pressure phenomena of bubbles in liquids and liquid–solid suspensions. Chem. Eng. Sci. 54, 4681–4709.

Ferreira, A., Cardoso, P., Teixeira, J.A., Rocha, F., 2013. pH influence on oxygen mass transfer coefficient in a bubble column. Individual characterization of kL and a. Chem. Eng. Sci. 100, 145–152.

Forret, A., Schweitzer, J.M., Gauthier, T., Krishna, R., Schweich, D., 2003. Influence of scale on the hydrodynamics of bubble column reactors: an experimental study in columns of 0.1, 0.4 and 1 m diameters. Chem. Eng. Sci. 58, 719–724.

Fukuma, M., Muroyama, K., Yasunishi, A., 1987. Properties of bubbles swarm in a slurry bubble column. J. Chem. Eng. Jpn. 20, 28–33.

Gandhi, B., Prakash, A., Bergougnou, M.A., 1999. Hydrodynamic behavior of slurry bubble column at high solids concentrations. Powder Technol. 103, 80–94.

García-Abuín, A., Gómez-Díaz, D., Losada, M., Navaza, J.M., 2012. Bubble column gas–liquid interfacial area in a polymer + surfactant + water system. Chem. Eng. Sci. 75, 334–341.

García-Abuín, A., Gómez-Díaz, D., Navaza, J.M., Vidal-Tato, I., 2010. CO_2 capture by aqueous solutions of glucosamine in a bubble column reactor. Chem. Eng. J. 162, 37–42.

García-Molina, V., Kallas, J., Esplugas, S., 2007. Wet oxidation of 4-chlorophenol: kinetic study. Chem. Eng. J. 126, 59–65.

Gopal, J.S., Sharma, M.M., 1983. Mass transfer characteristics of low H/D bubble columns. Can. J. Chem. Eng. 61, 517–526.

Gourich, B., Vial, C., El Azher, N., Belhaj Soulami, M., Ziyad, M., 2008. Influence of hydrodynamics and probe response on oxygen mass transfer measurements in a high aspect ratio bubble column reactor: effect of the coalescence behaviour of the liquid phase. Biochem. Eng. J. 39, 1–14.

Gourich, B., Vial, C., Essadki, A.H., Allam, F., Belhaj, S.M., Ziyad, M., 2006. Identification of flow regimes and transition points in a bubble column through analysis of differential pressure signal—influence of the coalescence behavior of the liquid phase. Chem. Eng. Process.: Process Intensif. 45, 214–223.

Grover, G.S., Rode, C.V., Chaudhari, R.V., 1986. Effect of temperature on flow regimes and gas hold-up in a bubble column. Can. J. Chem. Eng. 64, 501–504.
Han, L., Al-Dahhan, M.H., 2007. Gas–liquid mass transfer in a high pressure bubble column reactor with different sparger designs. Chem. Eng. Sci. 62, 131–139.
Hasanen, A., Orivuori, P., Aittamaa, J., 2006. Measurements of local bubble size distributions from various flexible membrane diffusers. Chem. Eng. Process.: Process Intensif. 45, 291–302.
Hashemi, S., Macchi, A., Servio, P., 2009. Gas–liquid mass transfer in a slurry bubble column operated at gas hydrate forming conditions. Chem. Eng. Sci. 64, 3709–3716.
Hikita, H., Asai, S., Tanigawa, K., Segawa, K., Kitao, M., 1980. Gas hold-up in bubble columns. Chem. Eng. J. 20, 59–67.
Hikita, H., Asai, S., Tanigawa, K., Segawa, K., Kitao, M., 1981. The volumetric liquid-phase mass transfer coefficient in bubble columns. Chem. Eng. J. 22, 61–69.
Hikita, H., Kikukawa, H., 1974. Liquid-phase mixing in bubble columns: effect of liquid properties. Chem. Eng. J. 8, 191–197.
Hinze, J.O., 1955. Fundamentals of the hydrodynamic mechanism of splitting in dispersion processes. AIChE J. 1, 289–295.
Holcombe, N.T., Smith, D.N., Knickle, H.N., O'Dowd, W., 1983. Thermal dispersion and heat transfer in nonisothermal bubble columns. Chem. Eng. Commun. 21, 135–150.
Houzelot, J.L., Thiebaut, M.F., Charpentier, J.C., Schiber, J., 1983. Contribution à l'étude hydrodynamique des colonnes à bulles. Entropie (Paris) 19, 121–126.
Hulet, C., Clement, P., Tochon, P., Schweich, D., Dromard, N., Anfray, J., 2009. Literature review on heat transfer in two- and three-phase bubble columns. Int. J. Chem. Reactor Eng., 7.
Idogawa, K., Ikeda, K., Fukuda, T., Morooka, S., 1985. Effects of gas and liquid properties on the behavior of bubbles in a bubble column under high pressure. Kagaku Kogaku Ronbunshu 11, 432–437.
Idogawa, K., Ikeda, K., Fukuda, T., Morooka, S., 1986. Behavior of bubbles of the air–water system in a column under high pressure. Int. Chem. Eng. 26, 468–474.
Ishibashi, H., Onozaki, M., Kobayashi, M., Hayashi J. i. Itoh, H., Chiba, T., 2001. Gas holdup in slurry bubble column reactors of a 150 t/d coal liquefaction pilot plant process. Fuel 80, 655–664.
Ishiyama, H., Isokawa, Y., Sawai, J., Kojima, H., 2001. Hydrodynamics in a small size pressurized bubble column. Chem. Eng. Sci. 56, 6273–6278.
Japas, M.L., Franck, E.U., 1985. High pressure phase equilibria and PVT-Data of the water-nitrogen system to 673 K and 250 MPa. Berichte der Bunsengesellschaft für physikalische Chemie. 89, 793–800.
Jhawar, A.K., Prakash, A., 2011. Heat transfer in a slurry bubble column reactor: a critical overview. Ind. Eng. Chem. Res. 51, 1464–1473.
Jiang, P., Lin, T.J., Luo, X., Fan, L.-S., 1995. Flow visualization of high pressure (21 MPa) bubble column: bubble characteristics. Chem. Eng. Res. Design 73, 269–274.
Jin, H., Liu, D., Yang, S., He, G., Guo, Z., Tong, Z., 2004. Experimental Study of Oxygen Mass Transfer Coefficient in Bubble Column with High Temperature and High Pressure. Chemical Engineering & Technology 27, 1267–1272.
Jin, H., Wang, M., Williams, R.A., 2007a. Analysis of bubble behaviors in bubble columns using electrical resistance tomography. Chem. Eng. J. 130, 179–185.
Jin, H., Yang, S., He, G., Liu, D., Tong, Z., Zhu, J., 2014. Gas–Liquid Mass Transfer Characteristics in a Gas–Liquid–Solid Bubble Column under Elevated Pressure and Temperature. Chinese Journal of Chemical Engineering 22, 955–961.
Jin, H., Yang, S., He, G., Wang, M., Williams, R.A., 2010. The effect of gas-liquid counter-current operation on gas hold-up in bubble columns using electrical resistance tomography. Journal of Chemical Technology & Biotechnology 85, 1278–1283.
Jin, H., Yang, S., Wang, M., Williams, R.A., 2007b. Measurement of gas holdup profiles in a gas liquid cocurrent bubble column using electrical resistance tomography. Flow Meas. Instrum. 18, 191–196.
Jordan, U., Schumpe, A., 2001. The gas density effect on mass transfer in bubble columns with organic liquids. Chem. Eng. Sci. 56, 6267–6272.
Joshi, J.B., Veera, U.P., Prasad, C.V., Phanikumar, D.V., Deshphande, N.S., Thakre, S.S., Thorat, B.N., 1998. Gas hold-up structure in bubble column reactors. Proc. Indian Ntl. Sci. Acad 64, 441–567.
Kang, Y., Cho, Y.J., Woo, K.J., Kim, K.I., Kim, S.D., 2000. Bubble properties and pressure fluctuations in pressurized bubble columns. Chem. Eng. Sci. 55, 411–419.
Kang, Y., Cho, Y.J., Woo, K.J., Kim, S.D., 1999. Diagnosis of bubble distribution and mass transfer in pressurized bubble columns with viscous liquid medium. Chemical Engineering Science 54, 4887–4893.
Kantak, M.V., Shetty, S.A., Kelkar, B.G., 1994. Liquid phase backmixing in bubble column reactors—a new correlation. Chem. Eng. Commun. 127, 23–34.
Kantarci, N., Borak, F., Ulgen, K.O., 2005. Bubble column reactors. Process Biochemistry 40, 2263–2283.
Kemoun, A., Cheng Ong, B., Gupta, P., Al-Dahhan, M.H., Dudukovic, M.P., 2001. Gas holdup in bubble columns at elevated pressure via computed tomography. Int. J. Multiph. Flow 27, 929–946.
Kluytmans, J.H.J., Van Wachem, B.G.M., Kuster, B.F.M., Schouten, J.C., 2003. Mass transfer in sparged and stirred reactors: influence of carbon particles and electrolyte. Chem. Eng. Sci. 58, 4719–4728.
Kojima, H., Sawai, J., Suzuki, H., 1997. Effect of pressure on volumetric mass transfer coefficient and gas holdup in bubble column. Chem. Eng. Sci. 52, 4111–4116.
Kolaczkowski, S.T., Plucinski, P., Beltran, F.J., Rivas, F.J., McLurgh, D.B., 1999. Wet air oxidation: a review of process technologies and aspects in reactor design. Chem. Eng. J. 73, 143–160.
Kölbel, H., Klötzer, D., Hammer, H., 1971. Zur Reaktionstechnik von Blasensäulen-Reaktoren mit suspendiertem Katalysator bei erhöhtem Druck. Chemie Ingenieur Technik 43, 103–111.
Krishna, R., De Swart, J.W.A., Hennephof, D.E., Ellenberger, J., Hoefsloot, H.C.J., 1994. Influence of increased gas density on hydrodynamics of bubble-column reactors. AIChE Journal 40, 112–119.
Krishna, R., Ellenberger, J., 1996. Gas holdup in bubble column reactors operating in the churn-turbulent flow regime. AIChE Journal 42, 2627–2634.
Krishna, R., Sie, S.T., 2000. Design and scale-up of the Fischer–Tropsch bubble column slurry reactor. Fuel Processing Technology 64, 73–105.
Krishna, R., Van Baten, J.M., Urseanu, M.I., 2001. Scale effects on the hydrodynamics of bubble columns operating in the homogeneous flow regime. Chem. Eng. Technol. 24, 451–458.
Krishna, R., Urseanu, M.I., Dreher, A.J., 2000. Gas hold-up in bubble columns: influence of alcohol addition versus operation at elevated pressures. Chem. Eng. Process.: Process Intensif. 39, 371–378.
Krishna, R., Urseanu, M.I., Van Baten, J.M., Ellenberger, J., 1999a. Influence of scale on the hydrodynamics of bubble columns operating in the churn-turbulent regime: experiments vs. Eulerian simulations. Chem. Eng. Sci. 54, 4903–4911.
Krishna, R., Urseanu, M.I., Van Baten, J.M., Ellenberger, J., 1999b. Rise velocity of a swarm of large gas bubbles in liquids. Chem. Eng. Sci. 54, 171–183.
Krishna, R., Wilkinson, P.M., Van Dierendonck, L.L., 1991. A model for gas holdup in bubble columns incorporating the influence of gas density on flow regime transitions. Chem. Eng. Sci. 46, 2491–2496.
Kulkarni, A.A., 2007. Mass Transfer in Bubble Column Reactors: Effect of Bubble Size Distribution. Ind. Eng. Chem. Res. 46, 2205–2211.
Kulkarni, A.A., Joshi, J.B., 2005. Bubble formation and bubble rise velocity in gas–liquid systems: a review. Ind. Eng. Chem. Res. 44, 5873–5931.
Kumar, S., Kumar, R.A., Munshi, P., Khanna, A., 2012a. Gas hold-up in three phase co-current bubble columns. Proc. Eng. 42, 782–794.

Kumar, S., Munshi, P., Khanna, A., 2012b. High pressure experiments and simulations in cocurrent bubble columns. Proc. Eng. 42, 842–853.
La Rubia, M.D., García-Abuín, A., Gómez-Díaz, D., Navaza, J.M., 2010. Interfacial area and mass transfer in carbon dioxide absorption in TEA aqueous solutions in a bubble column reactor. Chem. Eng. Process. 49, 852–858.
Lau, R., Lee, P.H.V., Chen, T., 2012. Mass transfer studies in shallow bubble column reactors. Chem. Eng. Process.: Process Intensif. 62, 18–25.
Lau, R., Peng, W., Velazquez-Vargas, L.G., Yang, G.Q., Fan, L.-S., 2004. Gas–liquid mass transfer in high-pressure bubble columns. Ind. Eng. Chem. Res. 43, 1302–1311.
Lefèvre, S., 2010. Dégradation et valorisation d'effluents aqueux par oxydation en voie humide, PhD Thesis, Aix-Marseille University.
Lefèvre, S., Boutin, O., Ferrasse, J.-H., Malleret, L., Faucherand, R., Viand, A., 2011. Thermodynamic and kinetic study of phenol degradation by a non-catalytic wet air oxidation process. Chemosphere 84, 1208–1215.
Lemoine, R., Behkish, A., Morsi, B.I., 2004. Hydrodynamic and mass-transfer characteristics in organic liquid mixtures in a large-scale bubble column reactor for the toluene oxidation process. Ind. Eng. Chem. Res. 43, 6195–6212.
Lemoine, R., Behkish, A., Sehabiague, L., Heintz, Y.J., Oukaci, R., Morsi, B.I., 2008. An algorithm for predicting the hydrodynamic and mass transfer parameters in bubble column and slurry bubble column reactors. Fuel Process. Technol. 89, 322–343.
Letzel, H.M., Schouten, J.C., Krishna, R., Van den Bleek, C.M., 1999. Gas holdup and mass transfer in bubble column reactors operated at elevated pressure. Chem. Eng. Sci. 54, 2237–2246.
Letzel, H.M., Schouten, J.C., Van den Bleek, C.M., Krishna, R., 1997. Influence of elevated pressure on the stability of bubbly flows. Chem. Eng. Sci. 52, 3733–3739.
Letzel, M.H., Schouten, J.C., Van den Bleek, C.M., Krishna, R., 1998. Effect of gas density on large-bubble holdup in bubble column reactors. AIChE J. 44, 2333–2336.
Lin, T.-J., Fan, L.-S., 1999. Heat transfer and bubble characteristics from a nozzle in high-pressure bubble columns. Chem. Eng. Sci. 54, 4853–4859.
Lin, T.J., Juang, R.C., Chen, C.C., 2001. Characterizations of flow regime transitions in a high-pressure bubble column by chaotic time series analysis of pressure fluctuation signals. Chem. Eng. Sci. 56, 6241–6247.
Lin, T.J., Tsuchiya, K., Fan, L.-S., 1998. Bubble flow characteristics in bubble columns at elevated pressure and temperature. AIChE J. 44, 545–560.
Lorenz, O., Schumpe, A., Ekambara, K., Joshi, J.B., 2005. Liquid phase axial mixing in bubble columns operated at high pressures. Chem. Eng. Sci. 60, 3573–3586.
Luo, X., Lee, D.J., Lau, R., Yang, G., Fan, L.-S., 1999. Maximum stable bubble size and gas holdup in high-pressure slurry bubble columns. AIChE J. 45, 665–680.
Maalej, S., Benadda, B., Otterbein, M., 2003. Interfacial area and volumetric mass transfer coefficient in a bubble reactor at elevated pressures. Chem. Eng. Sci. 58, 2365–2376.
Maceiras, R., Alvarez, E., Cancela, M.A., 2010. Experimental interfacial area measurements in a bubble column. Chem. Eng. J. 163, 331–336.
Majumder, S.K., Kundu, G., Mukherjee, D., 2006. Bubble size distribution and gas–liquid interfacial area in a modified downflow bubble column. Chem. Eng. J. 122, 1–10.
Mena, P., Ferreira, A., Teixeira, J.A., Rocha, F., 2011. Effect of some solid properties on gas-liquid mass transfer in a bubble column. Chem. Eng. Process. 50, 181–188.
Mendelson, H.D., 1967. The prediction of bubble terminal velocities from wave theory. AIChE J. 13, 250–253.
Miyahara, T., Hayashino, T., 1983. The size of bubbles generated from perforated plates. Int. Chem. Eng. 23, 517–523.
Mouza, A.A., Dalakoglou, G.K., Paras, S.V., 2005. Effect of liquid properties on the performance of bubble column reactors with fine pore spargers. Chem. Eng. Sci. 60, 1465–1475.
Muroyama, K., Imai, K., Oka, Y., Hayashi, J.i., 2013. Mass transfer properties in a bubble column associated with micro-bubble dispersions. Chem. Eng. Sci. 100, 464–473.
Nedeltchev, S., Jordan, U., Schumpe, A., 2007. Correction of the penetration theory based on mass-transfer data from bubble columns operated in the homogeneous regime under high pressure. Chem. Eng. Sci. 62, 6263–6273.
Nedeltchev, S., Nigam, K.D.P., Schumpe, A., 2014. Prediction of mass transfer coefficients in a slurry bubble column based on the geometrical characteristics of bubbles. Chem. Eng. Sci. 106, 119–125.
Neubauer, G., 1977. Beitrag zur Auslegung von Lochböden für die Flüssigkeitsbegasung in Blasensäulen unter Hochdruck.
Ohki, Y., Inoue, H., 1970. Longitudinal mixing of the liquid phase in bubble columns. Chem. Eng. Sci. 25, 1–16.
Ojima, S., Hayashi, K., Tomiyama, A., 2014. Effects of hydrophilic particles on bubbly flow in slurry bubble column. Int. J. Multiph. Flow 58, 154–167.
Olivieri, G., Elena Russo, M., Simeone, M., Marzocchella, A., Salatino, P., 2011. Effects of viscosity and relaxation time on the hydrodynamics of gas–liquid systems. Chem. Eng. Sci. 66, 3392–3399.
Onozaki, M., Namiki, Y., Sakai, N., Kobayashi, M., Nakayama, Y., Yamada, T., Morooka, S., 2000. Dynamic simulation of gas–liquid dispersion behavior in coal liquefaction reactors. Chem. Eng. Sci. 55, 5099–5113.
Oyevaar, M.H., Bos, R., Westerterp, K.R., 1991. Interfacial areas and gas hold-ups in gas-liquid contactors at elevated pressures from 0.1 to 8.0 MPa. Chem. Eng. Sci. 46, 1217–1231.
Öztürk, S.S., Schumpe, A., 1987. The influence of suspended solids on oxygen transfer to organic liquids in a bubble column. Chem. Eng. Sci. 42, 1781–1785.
Öztürk, S.S., Schumpe, A., Deckwer, W.D., 1987. Organic liquids in a bubble column: holdups and mass transfer coefficients. AIChE J. 33, 1473–1480.
Parasu Veera, U., Joshi, J.B., 2000. Measurement of gas hold-up profiles in bubble column by gamma ray tomography: effect of liquid phase properties. Chem. Eng. Res. Design 78, 425–434.
Passos, A.D., Voulgaropoulos, V.P., Paras, S.V., Mouza, A.A., 2015. The effect of surfactant addition on the performance of a bubble column containing a non-Newtonian liquid. Chem. Eng. Res. Design 95, 93–104.
Pjontek, D., Parisien, V., Macchi, A., 2014. Bubble characteristics measured using a monofibre optical probe in a bubble column and freeboard region under high gas holdup conditions. Chem. Eng. Sci. 111, 153–169.
Pohorecki, R., Moniuk, W., Zdrójkowski, A., 1999. Hydrodynamics of a bubble column under elevated pressure. Chem. Eng. Sci. 54, 5187–5193.
Pohorecki, R., Moniuk, W., Zdrójkowski, A., Bielski, P., 2001. Hydrodynamics of a pilot plant bubble column under elevated temperature and pressure. Chem. Eng. Sci. 56, 1167–1174.
Polli, M., Stanislao, M.D., Bagatin, R., Bakr, E.A., Masi, M., 2002. Bubble size distribution in the sparger region of bubble columns. Chem. Eng. Sci. 57, 197–205.
Reilly, I.G., Scott, D.S., De Bruijn, T., Jain, A., Piskorz, J., 1986. A correlation for gas holdup in turbulent coalescing bubble columns. Can. J. Chem. Eng. 64, 705–717.
Reilly, I.G., Scott, D.S., Debruijn, T.J.W., Macintyre, D., 1994. The role of gas phase momentum in determining gas holdup and hydrodynamic flow regimes in bubble column operations. Can. J. Chem. Eng. 72, 3–12.
Rollbusch, P., Bothe, M., Becker, M., Ludwig, M., Grünewald, M., Schlüter, M., Franke, R., 2015. Bubble columns operated under industrially relevant conditions—current understanding of design parameters. Chem. Eng. Sci. 126, 660–678.
Ruzicka, M.C., Drahoš, J., Fialová, M., Thomas, N.H., 2001. Effect of bubble column dimensions on flow regime transition. Chem. Eng. Sci. 56, 6117–6124.

Şal, S., Gül, Ö.F., Özdemir, M., 2013. The effect of sparger geometry on gas holdup and regime transition points in a bubble column equipped with perforated plate spargers. Chem. Eng. Process.: Process Intensif. 70, 259–266.

Sangnimnuan, A., Prasad, G.N., Agnew, J.B., 1984. Gas hold-up and backmixing in a bubble-column reactor under coal-hydroliquefaction conditions. Chem. Eng. Commun. 25, 193–212.

Schäfer, R., Merten, C., Eigenberger, G., 2002. Bubble size distributions in a bubble column reactor under industrial conditions. Exp. Thermal Fluid Sci. 26, 595–604.

Shah, M., Kiss, A.A., Zondervan, E., Van der Schaaf, J., De Haan, A.B., 2012. Gas holdup, axial dispersion, and mass transfer studies in bubble columns. Ind. Eng. Chem. Res. 51, 14268–14278.

Shah, Y.T., Kelkar, B.G., Godbole, S.P., Deckwer, W.D., 1982. Design parameters estimations for bubble column reactors. AIChE J. 28, 353–379.

Shaikh, A., Al-Dahhan, M., 2005. Characterization of the hydrodynamic flow regime in bubble columns via computed tomography. Flow Meas. Instrum. 16, 91–98.

Shaikh, A., Al-Dahhan, M.H., 2013. Scale-up of bubble column reactors: a review of current state-of-the-art. Ind. Eng. Chem. Res. 52, 8091–8108.

Shawaqfeh, A.T., 2003. Gas holdup and liquid axial dispersion under slug flow conditions in gas–liquid bubble column. Chem. Eng. Process.: Process Intensif. 42, 767–775.

Simonnet, M., Gentric, C., Olmos, E., Midoux, N., 2007. Experimental determination of the drag coefficient in a swarm of bubbles. Chem. Eng. Sci. 62, 858–866.

Singh, M.K., Majumder, S.K., 2011. Co- and counter-current mass transfer in bubble column. Int. J. Heat and Mass Transfer. 54, 2283–2293.

Smith, J.S., Burns, L.F., Valsaraj, K.T., Thibodeaux, L.J., 1996. Bubble column reactors for wastewater treatment. 2. The effect of sparger design on sublation column hydrodynamics in the homogeneous flow regime. Ind. Eng. Chem. Res. 35, 1700–1710.

Soong, Y., Harke, F.W., Gamwo, I.K., Schehl, R.R., Zarochak, M.F., 1997. Hydrodynamic study in a slurry-bubble-column reactor. Catal. Today 35, 427–434.

Stacy, C.J., Melick, C.A., Cairncross, R.A., 2014. Esterification of free fatty acids to fatty acid alkyl esters in a bubble column reactor for use as biodiesel. Fuel Process. Technol. 124, 70–77.

Stegeman, D., Knop, P.A., Wijnands, A.J.G., Westerterp, K.R., 1996. Interfacial area and gas holdup in a bubble column reactor at elevated pressures. Ind. Eng. Chem. Res. 35, 3842–3847.

Tang, C., Heindel, T.J., 2006. Estimating gas holdup via pressure difference measurements in a cocurrent bubble column. Int. J. Multiph. Flow 32, 850–863.

Tarmy, B., Chang, M., Coulaloglou, C., Ponzi, P., 1984. Hydrodynamic characteristics of three phase reactors. Chem. Eng., 18–23.

Therning, P., Rasmuson, A., 2001. Liquid dispersion, gas holdup and frictional pressure drop in a packed bubble column at elevated pressures. Chem. Eng. J. 81, 331–335.

Thorat, B.N., Joshi, J.B., 2004. Regime transition in bubble columns: experimental and predictions. Exp. Thermal Fluid Sci. 28, 423–430.

Tomiyama, A., Celata, G.P., Hosokawa, S., Yoshida, S., 2002. Terminal velocity of single bubbles in surface tension force dominant regime. Int. J. Multiph. Flow 28, 1497–1519.

Urseanu, M.I., Guit, R.P.M., Stankiewicz, A., van Kranenburg, G., Lommen, J.H.G.M., 2003. Influence of operating pressure on the gas hold-up in bubble columns for high viscous media. Chem. Eng. Sci. 58, 697–704.

Vandu, C.O., Koop, K., Krishna, R., 2004. Volumetric mass transfer coefficient in a slurry bubble column operating in the heterogeneous flow regime. Chem. Eng. Sci. 59, 5417–5423.

Vázquez, G., Cancela, M.A., Riverol, C., Alvarez, E., Navaza, J.M., 2000a. Application of the Danckwerts method in a bubble column: effects of surfactants on mass transfer coefficient and interfacial area. Chem. Eng. J. 78, 13–19.

Vázquez, G., Cancela, M.A., Riverol, C., Alvarez, E., Navaza, J.M., 2000b. Determination of interfacial areas in a bubble column by different chemical methods. Ind. Eng. Chem. Res. 39, 2541–2547.

Vial, C., Poncin, S., Wild, G., Midoux, N., 2001. A simple method for regime identification and flow characterisation in bubble columns and airlift reactors. Chem. Eng. Process.: Process Intensif. 40, 135–151.

Villermaux, J., 1994. Réacteurs chimiques Principes. Techniques de l'ingénieur Réacteurs chimiques base documentaire: TIB330DUO.

Voyer, R.D., Miller, A.I., 1968. Improved gas–liquid contacting in co-current flow. Can. J. Chem. Eng. 46, 335–341.

Wilkinson, P.M., Haringa, H., Stokman, F.P.A., Van Dierendonck, L.L., 1993. Liquid mixing in a bubble column under pressure. Chem. Eng. Sci. 48, 1785–1791.

Wilkinson, P.M., Haringa, H., Van Dierendonck, L.L., 1994. Mass transfer and bubble size in a bubble column under pressure. Chem. Eng. Sci. 49, 1417–1427.

Wilkinson, P.M., Spek, A.P., Van Dierendonck, L.L., 1992. Design parameters estimation for scale-up of high-pressure bubble columns. AIChE J. 38, 544–554.

Wilkinson, P.M., Van Dierendonck, L.L., 1990. Pressure and gas density effects on bubble break-up and gas hold-up in bubble columns. Chem. Eng. Sci. 45, 2309–2315.

Xue, J., Al-Dahhan, M.H., Dudukovic, M.P., Mudde, R.F., 2008. Bubble velocity, size, and interfacial area measurements in a bubble column by four-point optical probe. AIChE J. 54, 350–363.

Yang, G.Q., Fan, L.-S., 2003. Axial liquid mixing in high-pressure bubble columns. AIChE J. 49, 1995–2008.

Yang, W., Wang, J., Jin, Y., 2001. Mass transfer characteristics of syngas components in slurry system at industrial conditions. Chem. Eng. Technol. 24, 651–657.

Zahradník, J., Fialová, M., Růžička, M., Drahoš, J., Kaštánek, F., Thomas, N.H., 1997. Duality of the gas-liquid flow regimes in bubble column reactors. Chem. Eng. Sci. 52, 3811–3826.

Zieminski, S.A., Raymond, D.R., 1968. Experimental study of the behavior of single bubbles. Chem. Eng. Sci. 23, 17–28.